

REACTION FORMULATION FOR RADIATION AND SCATTERING
FROM PLATES, CORNER REFLECTORS AND
DIELECTRIC-COATED CYLINDERS

Nan N. Wang

(NASA-CR-138175) REACTION FORMULATION FOR
RADIATION AND SCATTERING FROM PLATES,
CORNER REFLECTORS AND DIELECTRIC-COATED
CYLINDERS (Ohio State Univ.) 135 p HC
\$9.75 136 CSCL 20N G3/23

N74-22318

Unclas
37538

TECHNICAL REPORT 2902-15

April 1974

Grant Number NGL 36-008-138



National Aeronautics and Space Administration
Langley Research Center
Hampton, Va. 23365

NOTICES

When Government drawings, specifications, or other data are used for any purpose other than in connection with a definitely related Government procurement operation, the United States Government thereby incurs no responsibility nor any obligation whatsoever, and the fact that the Government may have formulated, furnished, or in any way supplied the said drawings, specifications, or other data, is not to be regarded by implication or otherwise as in any manner licensing the holder or any other person or corporation, or conveying any rights or permission to manufacture, use, or sell any patented invention that may in any way be related thereto.

REACTION FORMULATION FOR RADIATION AND SCATTERING FROM PLATES,
CORNER REFLECTORS AND DIELECTRIC-COATED CYLINDERS

Nan N. Wang

TECHNICAL REPORT 2909-15

April 1974

Grant Number NGL 36-008-138

The material contained in this report is also used as a dissertation submitted to the Department of Electrical Engineering, The Ohio State University as partial fulfillment for the degree Doctor of Philosophy.

National Aeronautics and Space Administration
Langley Research Center
Hampton, Va. 23365

ABSTRACT

The reaction concept is employed to formulate an integral equation for radiation and scattering from plates, corner reflectors, and dielectric-coated conducting cylinders. The surface-current density on the conducting surface is expanded with subsectional bases. The dielectric layer is modeled with polarization currents radiating in free space. Maxwell's equation and the boundary conditions are employed to express the polarization-current distribution in terms of the surface-current density on the conducting surface. By enforcing reaction tests with an array of electric test sources, the moment method is employed to reduce the integral equation to a matrix equation. Inversion of the matrix equation yields the current distribution, and the scattered field is then obtained by integrating the current distribution.

This report presents the theory, computer program and numerical results for radiation and scattering from plates, corner reflectors, and dielectric-coated conducting cylinders.

CONTENTS

Chapter	Page
I INTRODUCTION	1
II THE REACTION INTEGRAL FORMULATION	3
III ELECTRIC TEST SOURCES AND EXPANSION MODES	9
A. Longitudinal Strip Sources	9
B. Transverse Strip Sources	10
C. Rectangular Surface Sources	13
IV THE IMPEDANCE MATRIX	18
V THE EXCITATION COLUMN	25
A. Plane Wave Illumination (Two-dimensional TM Case)	25
B. Plane Wave Illumination (Two-dimensional TE Case)	25
C. Plane Wave Illumination (Three-dimensional Case)	26
VI APPLICATIONS	29
A. Cylinders with Thin Dielectric Coating (TM Case)	29
B. Cylinders with Thin Dielectric Coating (TE Case)	32
C. Plates and Corner Reflectors with Perfect Conductivity	35
VII FAR-FIELD RADIATION AND SCATTERING	37
A. Longitudinal, Dielectric-coated Strip Source	37
B. Transverse, Dielectric-coated Strip Monopole	40
C. Rectangular Surface Dipole	42
VIII NUMERICAL RESULTS	45
A. TM Dielectric-coated Cylinders	45
B. TE Dielectric-coated Cylinders	45
C. Perfectly-conducting Plates and Corner Reflectors	45
IX SUMMARY AND DISCUSSIONS	73
REFERENCES	75

Chapter	Page
Appendix	
A. Electric Field Induced in the Thin Dielectric Layer Coated on a Perfectly-Conducting Polygon Cylinder Illuminated by an Incident Plane Wave	77
B. Computer Programs for Radiation and Scattering from TM Dielectric-Coated Cylinders.	79
C. Computer Programs for Radiation and Scattering from TE Dielectric-Coated Cylinders.	93
D. Computer Programs for Radiation and Scattering from Perfectly-Conducting Plates.	116

CHAPTER I INTRODUCTION

Low-frequency solutions for radiation and scattering from cylinders have been reported in several published papers [1-8]. Among them, Mei and Van Bladel [1] employed a point-matching procedure to solve the electric-field integral equation and the magnetic-field integral equation for transverse-magnetic and transverse-electric incident waves, respectively. In the point-matching procedure the surface current distribution was expanded into rectangular-pulse bases and the appropriate boundary conditions were enforced at discrete points on the conducting surface of the cylinder. Richmond [4] has developed a wire-grid array model for cylinders with transverse-magnetic incident wave and shown that if a sufficiently great number of wires is employed, the scattering pattern approaches that of a solid cylinder of the same contour. Richmond [9] has also developed a piecewise-sinusoidal reaction formulation for electromagnetic radiation and scattering problems involving cylinders with non-circular cross section for the transverse-electric incident wave. No solution, however, has been published for non-circular cylinders with a dielectric coating.

For three-dimensional problems, two methods are available for electromagnetic modeling of a continuous conducting surface with arbitrary shape: the wire-grid model [10] and the surface-current model [11,12] with rectangular-pulse bases. Both methods have similar limitations with the maximum cell width restricted to approximately one-tenth of a wavelength. Unless the conducting body is symmetric or is a figure of revolution, computer storage requirements have limited the conducting surface area to one or two square wavelengths.

In this dissertation, Rumsey's [13] reaction concept is employed to formulate an integral equation for scattering by plates, corner reflectors and dielectric-coated cylinders with noncircular cross section. In the reaction formulation, the surface-current density on the conducting surface is expanded with suitable bases. The dielectric layer is modeled with the equivalent polarization currents radiating in free space. Maxwell's equations and the boundary conditions are employed to express the polarization-current distribution in terms of the surface-current density on the conducting surface. By enforcing reaction tests with an array of electric test sources, the moment method is employed to reduce the integral equation to a matrix equation. Numerical solution of this system yields a stationary result for the samples of the current distribution. Finally, the quantities of interest such as the gain, far-field pattern, and the radar cross section are determined from the current distribution. With perfect conductivity, the analysis presented in this dissertation is valid for open as well as closed cylinders. With finite conductivity or with a thin dielectric coating, however, the analysis is restricted to closed cylinders.

The remaining text presents the general theory of the reaction formulation for radiation and scattering from conducting bodies. The time dependence $e^{j\omega t}$ is understood and suppressed. Chapter II presents the detailed theoretical outline of the reaction concept which forms the foundation of this dissertation. Relevant electric sources employed as the expansion functions and the test sources are discussed in Chapter III. Evaluation of the mutual impedances and excitation voltages are considered in Chapter IV and Chapter V. The electromagnetic modeling of the conducting body is an essential step in the reaction formulation. This is described in Chapter VI. The field scattered by a conducting body is the sum of the contributions from all the current modes which appear in the expansion for the surface-current distribution. In Chapter VII the far-field contributions of these sources are discussed. Numerical results for the radar cross section of rectangular plates, corner reflectors and dielectric-coated cylinders are presented in Chapter VIII.

CHAPTER II THE REACTION INTEGRAL FORMULATION

Two well known integral equations, the electric-field integral equation and the magnetic-field integral equation are usually employed to solve electromagnetic radiation and scattering problems. In this chapter, however, we develop the more general reaction integral equation of Rumsey [13]. It has been noted [14] that the reaction integral equation is more general in the sense that it can be reduced to either the electric-field integral equation or the magnetic-field integral equation if one enforces the reaction integral equation with a set of delta-function electric or magnetic test sources. In the following sections the reaction concept and its application in electromagnetic problems will be examined.

Consider the exterior scattering problem illustrated in Fig. 1a. In the presence of a conducting body, the impressed electric and magnetic currents ($\underline{J}_i, \underline{M}_i$) generate the electric and magnetic field intensities ($\underline{E}, \underline{H}$). For simplicity, let the exterior medium be free space.

From the surface-equivalence theorem of Schelkunoff [15], the interior field will vanish (without disturbing the exterior field) if we introduce the following surface-current densities

$$(1) \quad \underline{J}_S = \hat{n} \times \underline{H}$$

$$(2) \quad \underline{M}_S = \underline{E} \times \hat{n}$$

on the closed surface S of the scatterer. (The unit vector \hat{n} is directed outward on S .) In this situation, illustrated in Fig. 1b, we may replace the scatterer with free space without disturbing the field anywhere.

By definition, the incident field ($\underline{E}_i, \underline{H}_i$) is generated by ($\underline{J}_i, \underline{M}_i$) in free space, and the scattered field is:

$$(3) \quad \underline{E}_S = \underline{E} - \underline{E}_i$$

$$(4) \quad \underline{H}_S = \underline{H} - \underline{H}_i .$$

When the surface current ($\underline{J}_S, \underline{M}_S$) radiates in free space, it generates the field ($\underline{E}_S, \underline{H}_S$) in the exterior and ($-\underline{E}_i, -\underline{H}_i$) in the interior region. This result, illustrated in Fig. 1c, is deduced from Fig. 1b and the superposition theorem.

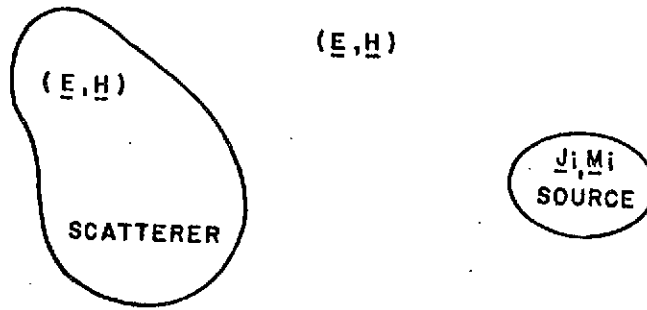


Fig. 1a--The source $(\underline{J}_i, \underline{M}_i)$ generates the field $(\underline{E}, \underline{H})$ with scatterer.

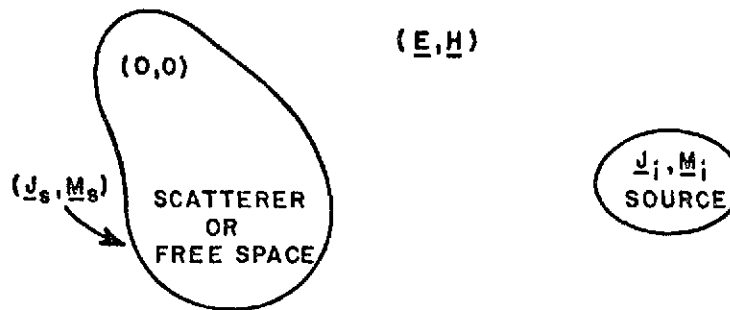


Fig. 1b--The interior field vanishes when the currents $(\underline{J}_s, \underline{M}_s)$ are introduced on the surface of the scatterer.

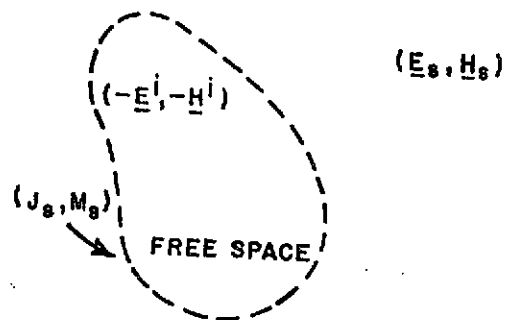


Fig. 1c--The exterior scattered field may be generated by $(\underline{J}_s, \underline{M}_s)$ in free space.

With the scatterer replaced by free space, we have noted in Fig. 1b that the interior region has a null field. As shown in Fig. 2, we place an electric test source \underline{J}_t in this region and find from the reciprocity theorem that

$$(5) \quad \oint_S (\underline{J}_s \cdot \underline{E}_t - \underline{M}_s \cdot \underline{H}_t) ds + \iiint (\underline{J}_i \cdot \underline{E}_t - \underline{M}_i \cdot \underline{H}_t) dv = 0$$

where $(\underline{E}_t, \underline{H}_t)$ is the free-space field of the test source. In words, Eq. (5) states that the interior test source has zero reaction with the other sources. This "zero-reaction theorem" was developed by Rumsey [13].

Equation (5) is the integral equation for the scattering problem, and our objective is to use this equation to determine the surface-current distributions \underline{J}_s and \underline{M}_s . To accomplish this, we expand these functions in finite series so there will be a finite number N of unknown expansion constants. Next we obtain N simultaneous linear equations to permit a solution for these constants. One such equation is obtained from Eq. (5) each time we set up a new test source.

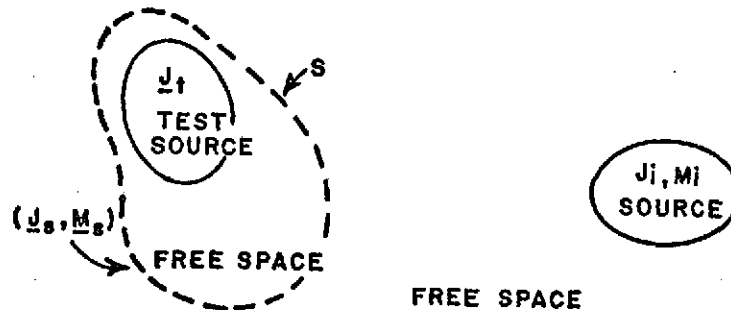


Fig. 2--An electric test source \underline{J}_t is positioned in the interior of the scattering region.

The magnetic current \underline{M}_s vanishes if the scatterer is a perfect conductor. We assume a finite conductivity and use the impedance boundary condition:

$$(6) \quad \underline{M}_s = Z_s \underline{J}_s \times \hat{n}$$

where Z_s denotes the surface impedance defined by $\hat{n} \times \underline{E} = z_s \hat{n} \times \underline{H}$.

For three-dimensional problems involving arbitrary scatterers, \underline{J}_S and \underline{M}_S are functions only of the position on the surface of the scatterer. Eqs. (5) and (6) yield

$$(7) \quad -\iint_S \underline{J}_S \cdot [\underline{E}_m - (\hat{n} \times \underline{H}_m) Z_S] ds = \iint \underline{J}_i \cdot \underline{E}_m ds - \iint \underline{M}_i \cdot \underline{H}_m ds$$

where $(\underline{E}_m, \underline{H}_m)$ denotes the free-space field of test-source m .

We represent the electric current distribution as follows:

$$(8) \quad \underline{J}_S = \sum_{n=1}^N I_n \underline{J}_n$$

where the complex constants I_n are samples of the function J_S . The vector functions \underline{J}_n are known as basis functions, subsectional bases, expansion functions or dipole modes. We employ expansion functions \underline{J}_n and test sources \underline{J}_m with unit current density at the terminals.

From Eqs. (7) and (8) we obtain the simultaneous linear equations

$$(9) \quad \sum_{n=1}^N I_n C_{mn} = A_m \quad \text{with} \quad m = 1, 2, 3, \dots, N$$

where

$$(10) \quad C_{mn} = -\iint_n \underline{J}_n \cdot [\underline{E}_m - (\hat{n} \times \underline{H}_m) Z_S] ds = -\iint_m \underline{J}_m \cdot \underline{E}_n ds$$

$$(11) \quad A_m = \iint_i \underline{J}_i \cdot \underline{E}_m ds - \iint_i \underline{M}_i \cdot \underline{H}_m ds = \iint_m \underline{J}_m \cdot \underline{E}_i ds$$

In Eqs. (10) and (11) the integrations extend over the region where the integrand is non-zero. For example, region n is that portion of the surface S covered by the expansion function \underline{J}_n . Region m covers the interior test source \underline{J}_m . The reciprocity theorem relates the first and second integrals in Eq. (10). In the second integral, \underline{E}_n is the free-space field generated by \underline{J}_n and the associated magnetic current \underline{M}_n .

For computational speed and storage, it will be advantageous to have a symmetric impedance matrix C_{mn} . Furthermore, the test sources should be selected to yield a well-conditioned set of simultaneous linear equations. For these reasons, we employ test sources \underline{J}_m of the same size, shape and functional form as the

expansion functions J_n . Finally, we position the interior test sources a small distance δ from surface S and take the limiting form of the integrals as δ tends to zero.

The effect of a dielectric coating on a conducting body will now be considered. For simplicity, let the dielectric layer have the same permeability as free space. From the volume equivalence theorem of Rhodes [16] the dielectric coating may be replaced with free space and an equivalent electric current density

$$(12) \quad \underline{J}_{eq} = j\omega(\epsilon - \epsilon_0) \underline{E}$$

where \underline{E} denotes the electric field intensity in the dielectric and $\epsilon = \epsilon_r \epsilon_0$ is the permittivity of the dielectric layer. From Eq. (12) the equivalent current \underline{J}_{eq} vanishes outside the region of the dielectric coating.

Let $(\underline{E}, \underline{H})$ denote the field generated by $(\underline{J}_i, \underline{M}_i)$ in the presence of a dielectric-coated conducting scatterer. Outside the scatterer, this field may also be generated by $(\underline{J}_i, \underline{M}_i)$, $(\underline{J}_s, \underline{M}_s)$ and \underline{J}_{eq} , radiating in free space. These sources, radiating in free space, generate a null field in the interior region of the conducting body. The surface currents $(\underline{J}_s, \underline{M}_s)$ are located on the surface of the conducting body and are related to the field $(\underline{E}, \underline{H})$ by Eqs. (1) and (2).

For a coated conducting body, the reaction integral equation (Eq. (7)) is modified by replacing \underline{J}_i with $\underline{J}_i + \underline{J}_{eq}$. The current density \underline{J}_{eq} may be regarded as an additional source which plays much the same role as the impressed source \underline{J}_i . However, \underline{J}_{eq} is an unknown quantity because \underline{E} is unknown. If the dielectric coating is thin, Maxwell's equations and boundary conditions can be employed to express the polarization-current distribution \underline{J}_{eq} in terms of the surface-current density on the conducting surface. Therefore, \underline{J}_{eq} may be regarded as a dependent unknown function because it is simply related to \underline{J}_s .

The polarization-current distribution is expanded as follows:

$$(13) \quad \underline{J}_{eq} = \sum_{n=1}^N I_n \tilde{\underline{J}}_n$$

where the $\tilde{\underline{J}}_n$ are functions simply related to J_n . Thus, for a coated conducting body, each expansion mode J_n in Eq. (8) has associated with it a polarization current $\tilde{\underline{J}}_n$, and the reaction C_{mn} between the electric test source m and the expansion mode n has an additional term given by

$$(14) \quad \Delta C_{mn} = - \iint_n \tilde{\mathcal{J}}_n \cdot \underline{E}_m \, ds$$

where the integration extends through the dielectric coating in the range of the expansion mode n . The functions \underline{J}_n are defined over a surface, while the $\tilde{\mathcal{J}}_n$ are defined in a volumetric region.

It may be noted that in the reaction formulation, the effects of a dielectric coating are accounted for entirely through a modification of the square reaction matrix C_{mn} . This modification influences the current distribution, field patterns and scattering properties.

The following chapter discusses the electric sources which are employed as test sources and expansion modes for the current distribution on the conducting surface.

CHAPTER III
ELECTRIC TEST SOURCES AND EXPANSION MODES

In the preceding chapter, the reaction integral equation is reduced to a matrix equation via the moment method in two steps. First the unknown current distribution is expanded with basis functions. Test sources with the same functional form are then employed to perform the reaction tests. In the following sections three types of test sources employed in this dissertation are discussed.

A. LONGITUDINAL STRIP SOURCES

For an infinitely long cylinder with transverse magnetic incident wave, the electric current density induced on the conducting surface is in the longitudinal direction. Thus a suitable choice of the bases is the longitudinal strip source.

Consider the "strip source" illustrated in Fig. 3. This source is an electric surface-current distribution $\underline{J} = \hat{z} J(x)$ located on the xz plane. This source has width h and infinite length and radiates in free space. For the strip source shown in Fig. 3, the fields are given as follows:

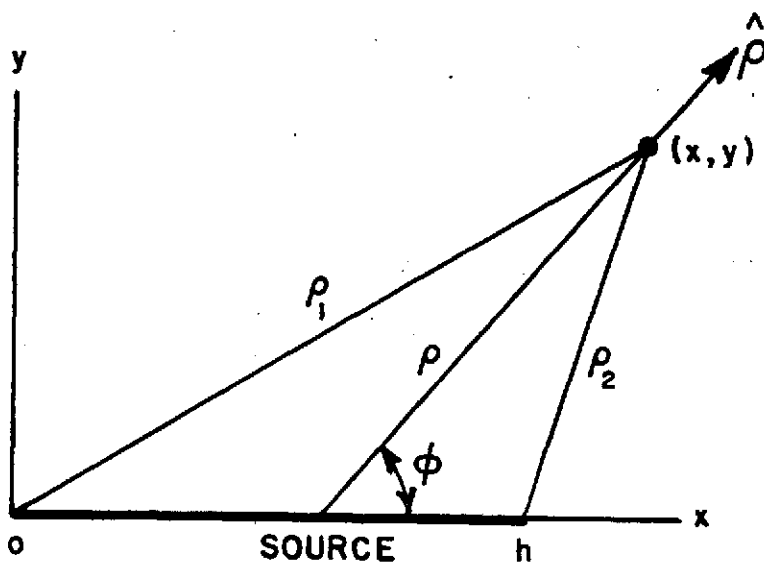


Fig. 3--An electric strip source and the coordinate system.

$$(15) \quad \underline{E} = \frac{k\eta}{4} \int_0^h \underline{J} H_0^{(2)}(k\rho) dx'$$

$$(16) \quad \underline{H} = -\frac{jk}{4} \int_0^h \underline{J} \times \hat{\rho} H_1^{(2)}(k\rho) dx'$$

where

$$(17) \quad \rho = \sqrt{(x-x')^2 + y^2}$$

$$(18) \quad k = \omega\sqrt{\mu\epsilon}$$

$$(19) \quad \eta = \sqrt{\mu/\epsilon}$$

If the electric strip source has a uniform distribution,

$$(20) \quad \underline{J}(x) = \hat{z}$$

Eqs. (15) and (16) can be written as

$$(21) \quad E_z = -\frac{k\eta}{4} \int_0^h H_0^{(2)}(k\rho) dx'$$

$$(22) \quad \underline{H} = -\frac{jk}{4} \int_0^h \hat{z} \times \hat{\rho} H_1^{(2)}(k\rho) dx' .$$

B. TRANSVERSE STRIP SOURCES [9]

In the case of a conducting cylinder illuminated by a transverse-electric incident wave, the electric current induced on the surface is in the transverse direction. Therefore, transverse electric sources are the natural choice for the induced current density.

Again consider the "strip source" illustrated in Fig. 3. But this time the source is an electric surface-current distribution $\underline{J} = \hat{x} J(x)$ located on the xz plane. For this transverse electric source the free space fields are

$$(23) \quad \underline{E} = -\frac{k\eta}{4} \int_0^h \underline{J} H_0^{(2)}(k\rho) dx' + \frac{\eta}{4} \int_0^h \hat{\rho} J' H_1^{(2)}(k\rho) dx'$$

$$(24) \quad \underline{H} = -\frac{jk}{4} \int_0^h \underline{J} \times \hat{\rho} H_1^{(2)}(k\rho) dx'$$

where

$$(25) \quad J' = dJ/dx'$$

For most current functions $J(x)$, the field integrals must be evaluated with infinite-series expansions or numerical integration procedures. For the sinusoidal current distribution, however, E_x is obtained in simple closed form [9]. Thus, if

$$(26) \quad \underline{J}(x) = \hat{x}[I_1 \sin(kh-kx) + I_2 \sin(kx)]/\sin(kh)$$

then

$$(27) \quad E_x = \frac{\eta}{4 \sin(kh)} [I_1 H_0^{(2)}(k\rho_1) \cos(kh) - I_1 H_0^{(2)}(k\rho_2)] \\ + [I_2 H_0^{(2)}(k\rho_2) \cos(kh) - I_2 H_0^{(2)}(k\rho_1)]$$

where I_1 and I_2 represent $J(0)$ and $J(h)$, respectively, and ρ_1, ρ_2 are illustrated in Fig. 3.

For the purpose of representing a continuous surface-current distribution on a conducting cylinder, it is useful to define a strip dipole which is comprised of two strip monopoles. Fig. 4a illustrates a planar strip dipole. This dipole lies on the xz plane and has infinite length in the z direction. The surface-current density is

$$(28) \quad \underline{J} = \hat{x} \frac{\sin k(x-x_1)}{\sin k(x_2-x_1)} \quad \text{for} \quad x_1 \leq x \leq x_2$$

$$(29) \quad \underline{J} = \hat{x} \frac{\sin k(x_3-x)}{\sin k(x_3-x_2)} \quad \text{for} \quad x_2 \leq x \leq x_3$$

As indicated in Fig. 4b, the current density vanishes at the edges x_1 and x_3 , is continuous across the terminals at x_2 and has a slope discontinuity at x_2 .

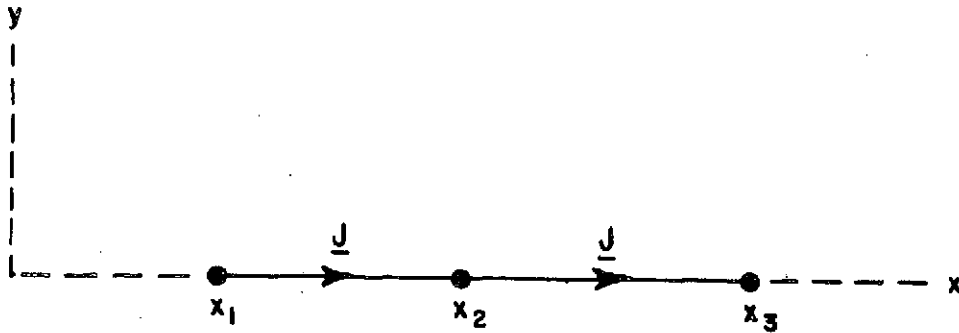


Fig. 4a--A planar strip dipole with edges at x_1 and x_3 and terminals at x_2 .

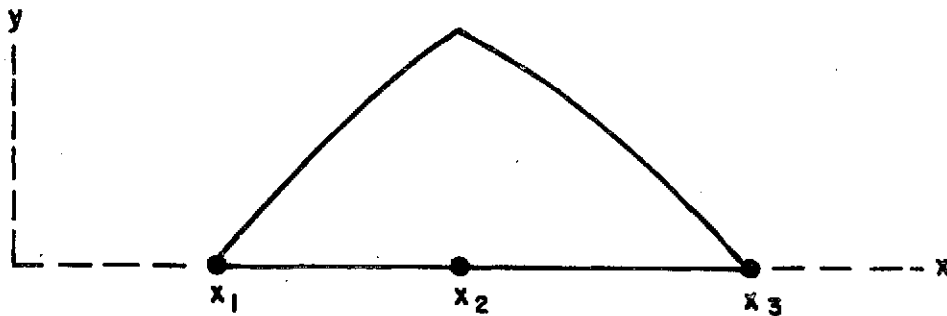


Fig. 4b--The current-density distribution \underline{J} on the sinusoidal strip dipole.

Fig. 5 illustrates a strip V-dipole. Distance along the dipole arms is measured by the coordinates s and t with origin at the terminals 0. The surface-current density is

$$(30) \quad \underline{J} = -\hat{s} \frac{\sin k(s_1 - s)}{\sin ks_1} \quad \text{on arm } s$$

$$(31) \quad \underline{J} = \hat{t} \frac{\sin k(t_1 - t)}{\sin kt_1} \quad \text{on arm } t,$$

where the unit vectors \hat{s} and \hat{t} are perpendicular to the z -axis. Thus, the current density vanishes at edges s_1 and t_1 and has unit value at the terminals 0. The edges are parallel with the z -axis. If the wedge angle ψ is adjusted to 180 degrees, the V-dipole in Fig. 5 reduces to the planar dipole in Fig. 4.

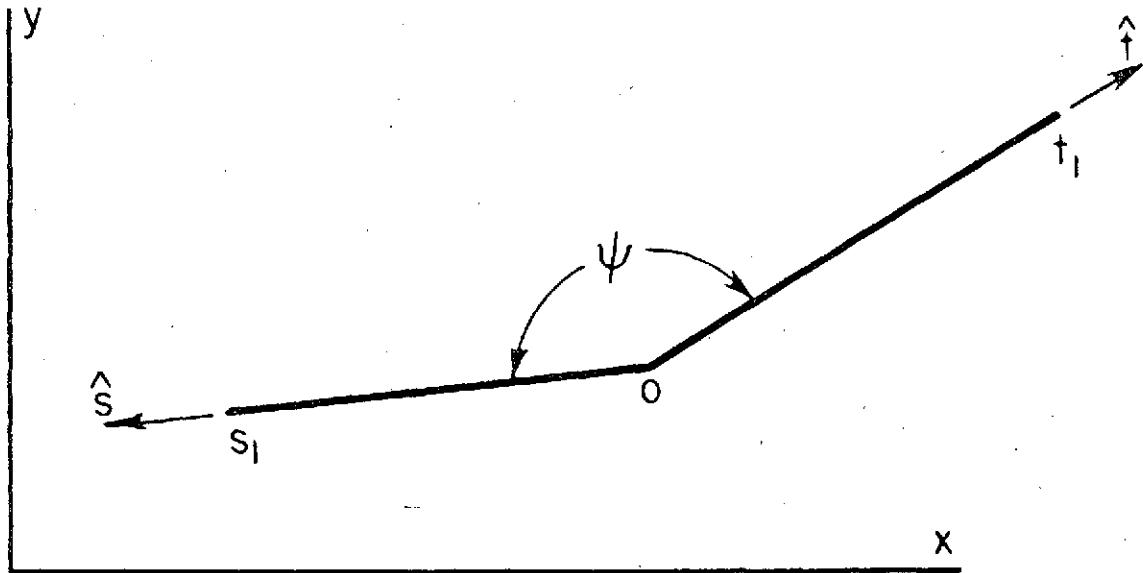


Fig. 5--Nonplanar strip dipole with edges at s_1 and t_1 and terminals at 0.

C. RECTANGULAR SURFACE SOURCES

Consider a "surface monopole" radiating in free space as shown in Fig. 6. This source is an electric surface-current density $\underline{J} = \hat{z} J(z)$ located on the yz plane. This source has height $a/2$ and width b . The surface-current density is related to the current by $I = b J$. For the electric surface monopole illustrated in Fig. 6, the fields are

$$(32) \quad \underline{E} = \frac{-j}{\omega\epsilon} \left[k^2 \int_0^{a/2} \int_0^b \underline{J} G_0(kR) dy' dz' + \nabla \int_0^{a/2} \int_0^b J' G_0(kR) dy' dz' \right]$$

$$(33) \quad \underline{H} = \nabla \times \int_0^{a/2} \int_0^b \underline{J} G_0(kR) dy' dz'$$

where

$$(34) \quad R = \sqrt{(x-x')^2 + (y-y')^2 + (z-z')^2}$$

$$(35) \quad J' = dJ/dz'$$

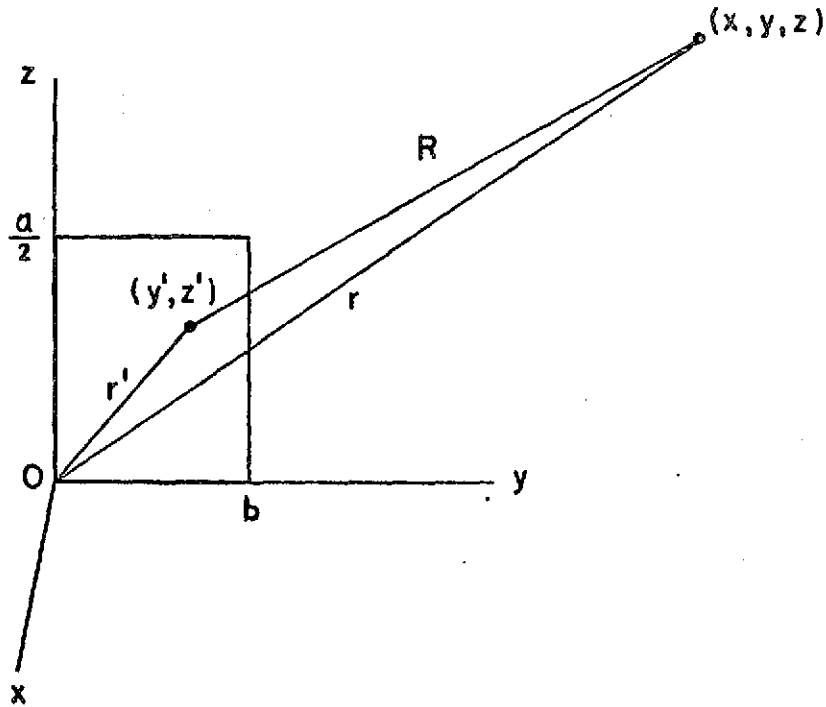


Fig. 6--An electric surface monopole and the coordinate system.

$$(36) \quad G_0(kR) = e^{-jkR}/4\pi R$$

Numerical integration techniques must be employed to perform the field integrals.

A planar sinusoidal dipole source located on the yz plane as shown in Fig. 7a will be considered. This source is an electric surface-current density with height a and width b. The surface-current density is given by

$$(37) \quad \underline{J} = \hat{z} \cos\left(\frac{(z-z_2)\pi}{2(z_2-z_1)}\right) \quad \text{for} \quad z_1 \leq z \leq z_2$$

$$(38) \quad \underline{J} = \hat{z} \cos\left(\frac{(z-z_2)\pi}{2(z_3-z_2)}\right) \quad \text{for} \quad z_2 \leq z \leq z_3$$

As illustrated in Fig. 7b and 7c, the current density vanishes at the edges $z = z_1$ and $z = z_3$, and is uniformly distributed in the

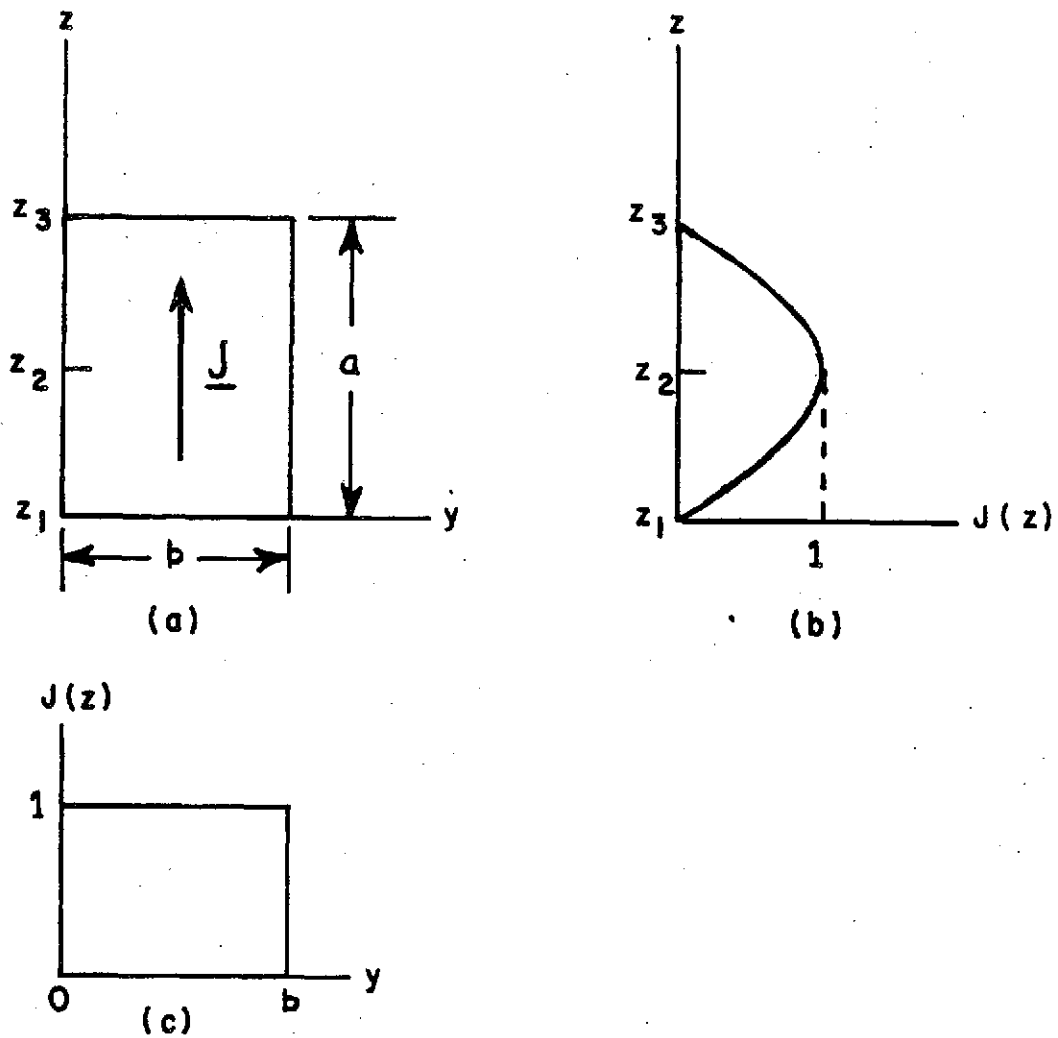


Fig. 7--An electric surface dipole and its current-density distribution.

transverse direction. The surface-current density and its slope are continuous across the terminals at $z = z_2$ for $z_2 - z_1 = z_3 - z_2 = a/2$.

Fig. 8 illustrates a surface V-dipole. Distance along the dipole arms is measured by the coordinates s and t with origin at the terminal 0. The surface-current density for this electric source is

$$(39) \quad \underline{J} = -\hat{s} \cos\left(\frac{\pi s}{2s_1}\right) \quad \text{on arm } s$$

$$(40) \quad \underline{J} = \hat{t} \cos\left(\frac{\pi t}{2t_1}\right) \quad \text{on arm } t.$$

When the wedge angle ψ is adjusted to 180 degrees, the V-dipole in Fig.8 reduces to the planar surface dipole in Fig. 7a.

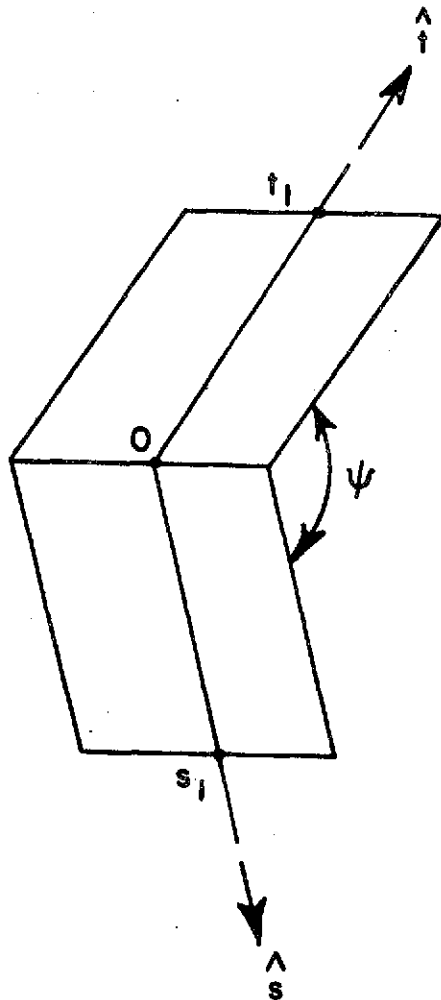


Fig. 8--A nonplanar surface dipole with edges at s_1 and t_1 and terminal at O .

The electric sources defined in the previous sections are all hypothetical sources. The current density on a conducting strip is neither uniform nor sinusoidal and the current density induced on a rectangular plate is not sinusoidal. The relevance of these sources will now be explained. The electric current distributions (Eqs. (20),

(30), (31), (39), and (40)) will be used as the basis functions (Eq. (8)) for expanding the unknown current distribution induced on conducting surfaces for various problems. Furthermore, test sources with the same size, shape, and functional form as the expansion functions will be employed with the reaction concept to solve the integral equation.

By superposition, the field scattered by a conducting body may be regarded as the sum of the fields radiated by the mode currents:

$$(41) \quad \underline{E}^S = \sum_{n=1}^N I_n \underline{e}_n$$

$$(42) \quad \underline{H}^S = \sum_{n=1}^N I_n \underline{h}_n$$

where $(\underline{e}_n, \underline{h}_n)$ is the free space field generated by the mode current n .

CHAPTER IV
THE IMPEDANCE MATRIX

From the viewpoint of reaction, the complex number C_{mn} in Eq. (10) represents the reaction between the sources m and n . The reaction between two electric sources m and n is:

$$(43) \quad C_{mn} = -\iiint_m \underline{E}_n \cdot \underline{J}_m \, dv$$

Although the electric sources defined in Chapter III are hypothetical, it is useful to define self impedance with the induced-emf formulation [13]:

$$(44) \quad Z_{mm} = \frac{V_{mm}}{I_{mm}} = \frac{C_{mm}}{I_{mm}^2}$$

From Eqs. (43) and (44):

$$(45) \quad Z_{mm} = \frac{-1}{I_{mm}^2} \iiint_m \underline{E}_m \cdot \underline{J}_m \, dv$$

where \underline{J}_m is the current density of source m and \underline{E}_m is the free-space electric field. The self impedance of the longitudinal strip source (Eq. (20)), the transverse strip dipole [9] (Eq. (30) and Eq. (31)), and the rectangular surface dipole (Eqs. (39) and (40)), as a function of size, are listed in Table I, II, and III, respectively.

The mutual impedance between two sources is defined by

$$(46) \quad Z_{mn} = \frac{-1}{I_{mm} I_{nn}} \iiint_m \underline{E}_n \cdot \underline{J}_m \, dv.$$

Tables IV, V and VI list the mutual impedance between two longitudinal strip sources, transverse strip sources [9], and rectangular surface dipoles, respectively.

TABLE I

Self Impedance of Longitudinal Strip Source
shown in Fig. 9.

h/λ	R_{11}	X_{11}
0.1	582.38	771.74
0.2	554.63	488.50
0.3	511.90	317.22
0.4	458.70	199.36
0.5	400.65	118.30

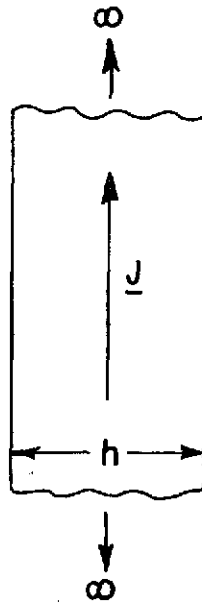


Fig. 9--Strip Source with $\underline{j} = \hat{z}$.

TABLE II

Self Impedance of Center-Fed Strip-Dipole
shown in Fig. 10

$$s_1 = t_1 = h$$

ψ	$h/\lambda = 0.05$	$h/\lambda = 0.10$	$h/\lambda = 0.15$	$h/\lambda = 0.20$
45°	0.11 -j 14.1	0.47 -j 13.4	1.20 -j 12.1	2.53 -j 10.4
90°	0.38 -j 20.9	1.59 -j 19.3	3.94 -j 17.1	8.10 -j 14.0
135°	0.64 -j 24.3	2.68 -j 22.2	6.49 -j 19.5	12.95 -j 16.4
180°	0.75 -j 25.3	3.11 -j 23.0	7.50 -j 20.3	14.77 -j 17.4

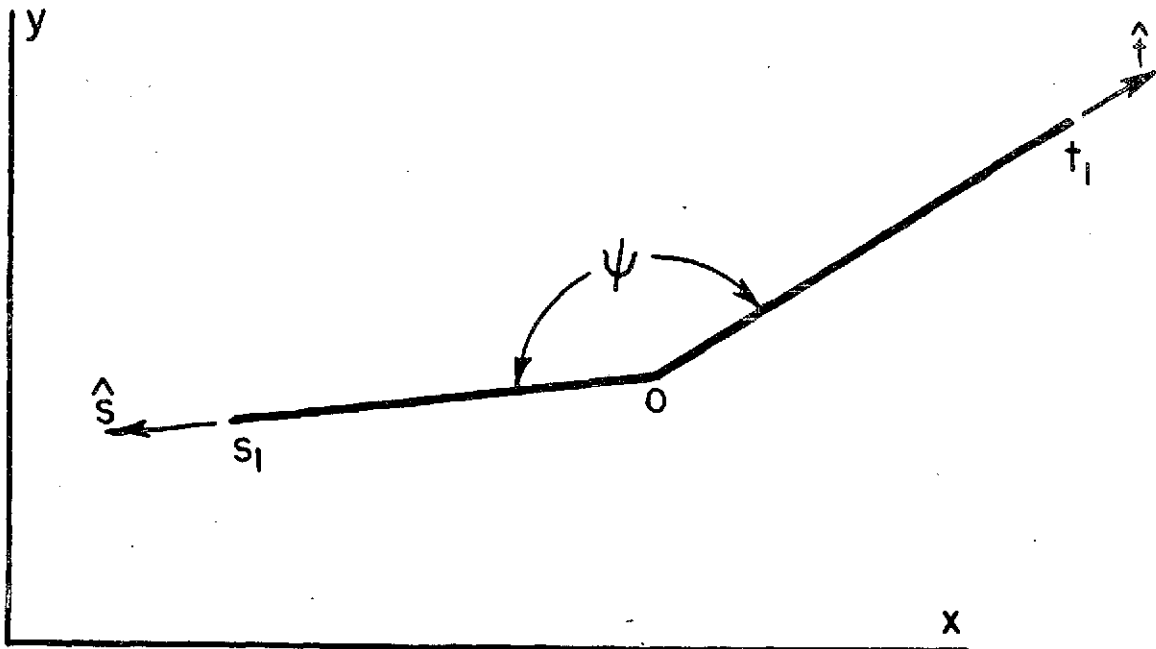


Fig. 10--Nonplanar strip dipole with edges at s_1 and t_1
and terminals at 0.

TABLE III

Self Impedance of Center-Fed Planar Surface-Dipole
shown in Fig. 11

a/λ	R_{11}	X_{11}
0.2	11.48	-69.76
0.3	23.98	-35.26
0.4	38.80	-15.36
0.5	52.98	- 4.52

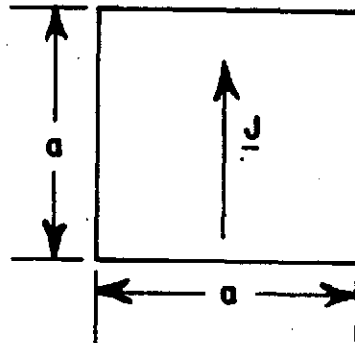


Fig. 11--Surface Dipole with $\underline{J} = \hat{z} \cos(\pi z/a)$

TABLE IV

Mutual Impedance of Coplanar Strip Sources
shown in Fig. 12

$$h_1 = h_2 = 0.1/\lambda$$

d/λ	R_{12}	X_{12}
0.0	582.38	771.74
0.1	526.74	205.89
0.2	376.25	-140.97
0.3	171.77	-283.09
0.4	-27.43	-283.44
0.5	-172.11	-190.34

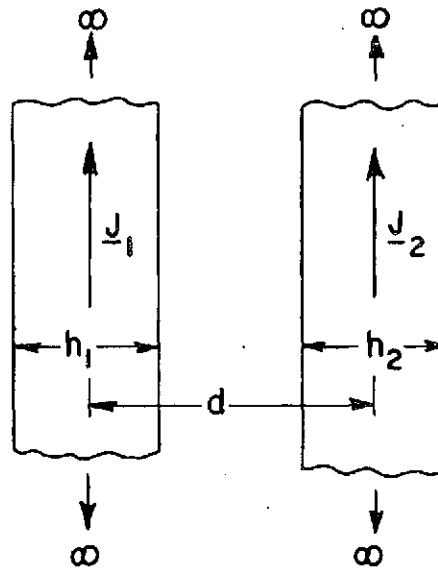


Fig. 12--Coupled Coplanar Strip Sources with $\underline{J}_1 = \underline{J}_2 = \hat{z}$

TABLE V

Mutual Impedance of Center-Fed Planar Strip-Dipoles
shown in Fig. 13

Segment length: $h/\lambda = 0.1$
Distance between midpoints: $\rho/\lambda = 0.3$

ϕ	$\beta = 0^\circ$	$\beta = 45^\circ$	$\beta = 90^\circ$	$\beta = 135^\circ$
0°	$1.94 + j 0.81$	$1.36 + j 0.39$	$0.00 + j 0.00$	$-1.36 - j 0.39$
30°	$1.42 - j 0.58$	$1.62 + j 1.07$	$0.87 + j 1.80$	$-0.38 + j 1.73$
60°	$0.39 - j 2.68$	$0.90 - j 0.66$	$0.87 + j 1.80$	$0.34 + j 3.03$
90°	$-.13 - j 3.53$	$-.08 - j 2.57$	$0.00 + j 0.00$	$0.08 + j 2.57$

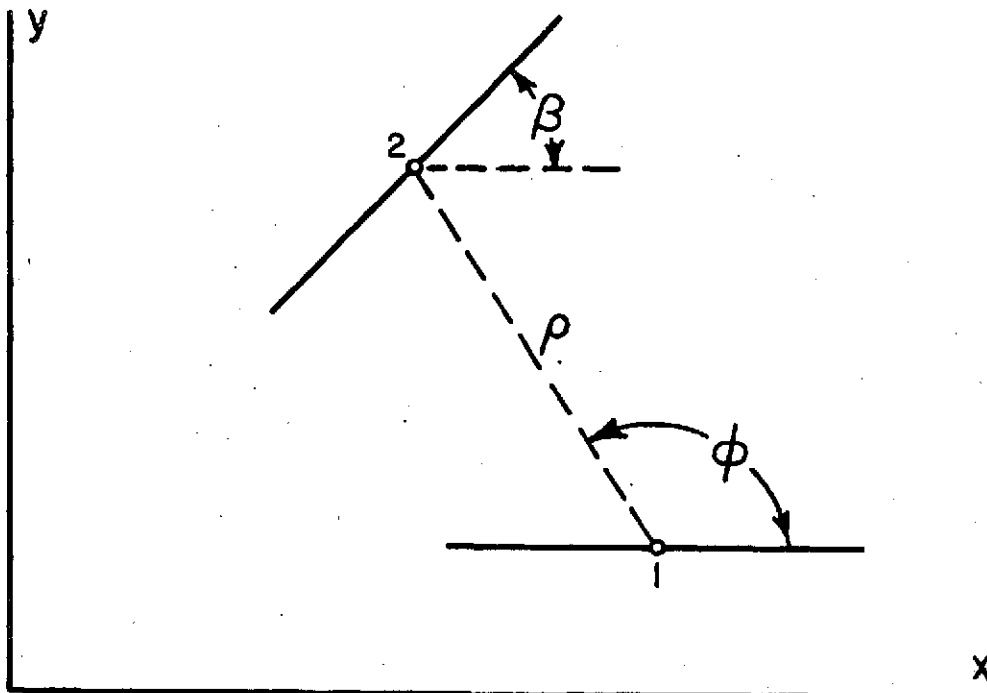


Fig. 13--Coupled strip dipoles

TABLE VI

Mutual Impedance of Center-Fed Coplanar Surface-Dipoles
shown in Fig. 14

	$a/\lambda = 0.5$		$b/\lambda = 0.25$		
0.75	1.076 -j 7.913	-2.925 -j 5.950	-5.968 +j 1.761	0.8871 +j 7.019	
0.50	24.43 +j 5.997	10.04 -j 9.321	-9.568 -j 6.65	-7.194 +j 8.971	
0.25	53.10 +j 55.87	29.54 -j 9.070	-9.468 -j 19.33	-15.74 +j 6.426	
0.0	67.09 +j 13.23	39.07 -j 22.49	-8.659 -j 26.75	-19.32 +j 4.263	
s_z/λ / s_y/λ	0.0	0.25	0.50	0.75	

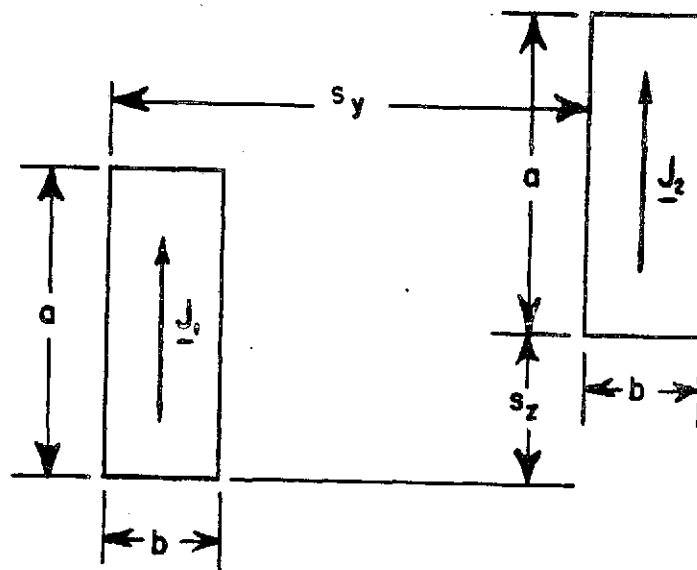


Fig. 14--Coupled surface dipoles

CHAPTER V
THE EXCITATION COLUMN

The complex quantities A_m in Eq. (9) form the excitation column in the matrix equation $C_{mn} I_n = A_m$. Physically, A_m is the reaction between the impressed source and the test source m . These reactions are independent of the surface impedance or the dielectric coating. For arbitrary impressed sources which generate \underline{E}_j in free space, Eq. (11) gives

$$(47) \quad A_m = \iiint_m \underline{J}_m \cdot \underline{E}_j \, dv .$$

The above expressions require numerical integration over test source m .

A. PLANE WAVE ILLUMINATION (TWO-DIMENSIONAL TM CASE)

If an infinitely long, electric line source, parallel with the z axis, is located at a great distance from the conducting cylinder, the incident field $(\underline{E}_j, \underline{H}_j)$ may be regarded as a plane wave with

$$(48) \quad \underline{E}_j = \hat{z} E_0 e^{jk(x \cos \phi_j + y \sin \phi_j)}$$

where ϕ_j is the angular coordinate of the source, and E_0 is the incident electric field intensity at the origin. Fig. 15 illustrates an incident plane wave illuminating a longitudinal strip source with unit current density in the z direction. The integration in Eq. (47) is readily performed to yield

$$(49) \quad A_m = E_0 \frac{e^{j\psi_2} - e^{j\psi_1}}{jk \cos(\alpha - \phi_j)}$$

where $\psi_j = k(x_j \cos \phi_j + y_j \sin \phi_j)$ and α is the angle between the positive x axis and the \underline{j} vector directed from point 1 to point 2.

B. PLANE WAVE ILLUMINATION (TWO-DIMENSIONAL TE CASE)

Consider a magnetic line source, parallel with the z axis and located at a great distance away, illuminating a strip dipole with sinusoidal electric current density (Eqs. (30) and (31)) flow in the direction from 1 to 2 and from 2 to 3 as shown in Fig. 16. The incident electric field may be regarded as a plane wave with

$$(50) \quad \underline{E}_j = -\hat{\phi}_j H_0 e^{jk(x \cos \phi_j + y \sin \phi_j)}$$

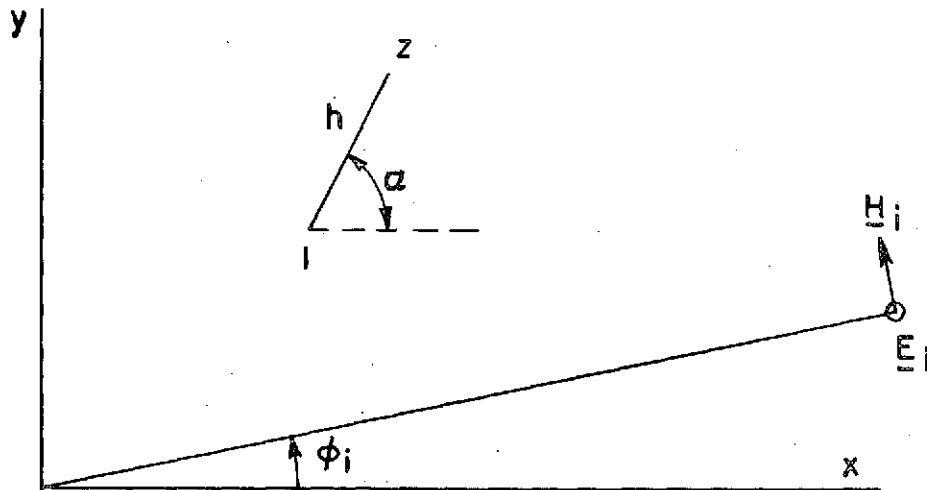


Fig. 15--A plane wave illuminates a strip source

In this case, Eq. (47) is readily evaluated to yield

$$(51) \quad A_m = -\eta H_0 \frac{[e^{j\psi_1} - (\cos kh_1 - j \cos(\alpha_1 - \phi_i) \sin kh_1) e^{j\psi_2}]}{k \sin kh_1 \sin(\alpha_1 - \phi_i)} + \eta H_0 \frac{[e^{j\psi_3} - (\cos kh_2 - j \cos(\alpha_2 - \phi_i) \sin kh_2) e^{j\psi_2}]}{k \sin kh_2 \sin(\alpha_2 - \phi_i)}$$

where h_1 and h_2 are the dipole segment lengths. The angle between the positive x axis and the vector directed to the terminals from point 1 is denoted α_1 . Similarly α_2 is the angle of the vector directed to the terminals from point 3.

C. PLANE WAVE ILLUMINATION (THREE-DIMENSIONAL CASE)

If an impressed source is located at a great distance away from a surface dipole with current distribution $\underline{J} = \hat{z}' \cos(\pi z'/a)$ as shown in Fig. 17, the incident field may be regarded as a plane wave with

$$(52) \quad \underline{E}_i = \underline{E}_0 e^{jk(x' \sin \theta'_i \cos \phi'_i + y' \sin \theta'_i \sin \phi'_i + z' \cos \theta'_i)}$$

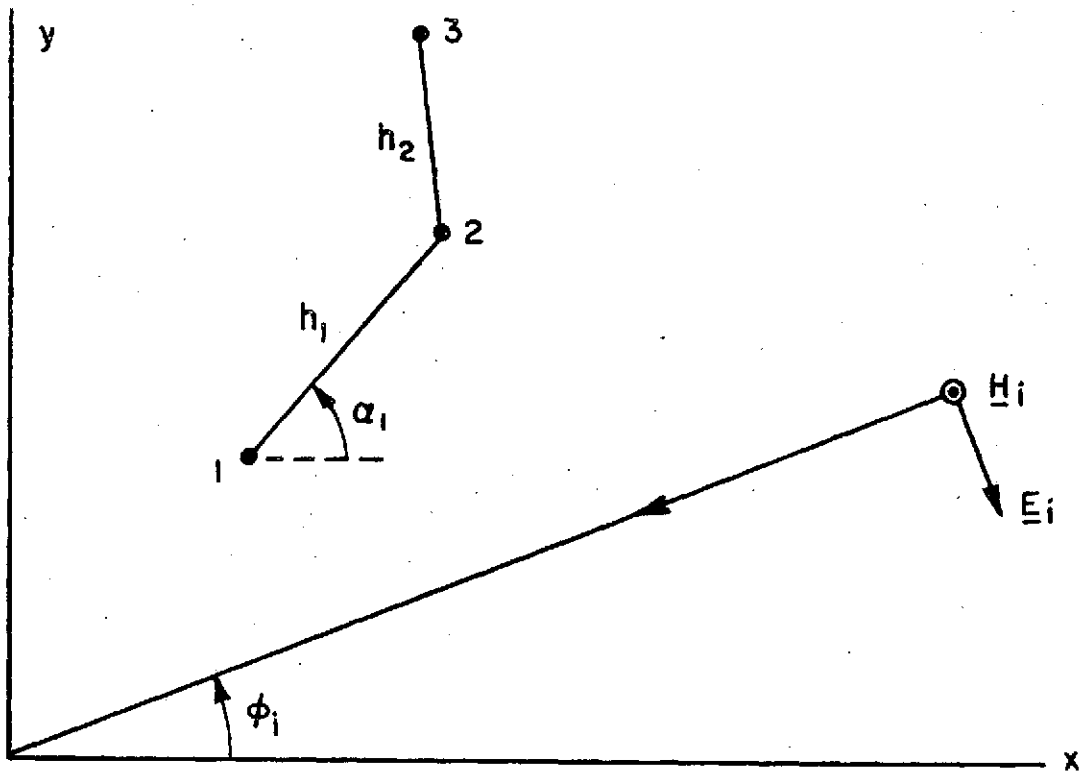


Fig. 16--A plane wave illuminates an electric strip dipole.

From Eqs. (52) and (47),

$$(53) \quad A_m = (\underline{E}_0 \cdot \hat{z}') 2\pi ab \frac{\sin(X_i) \cos(Y_i/2)}{X_i(Y_i^2 - \pi^2)}$$

where $X_i = 0.5 kb \sin \epsilon_i' \sin \phi_i'$

$Y_i = ka \cos \epsilon_i'$.

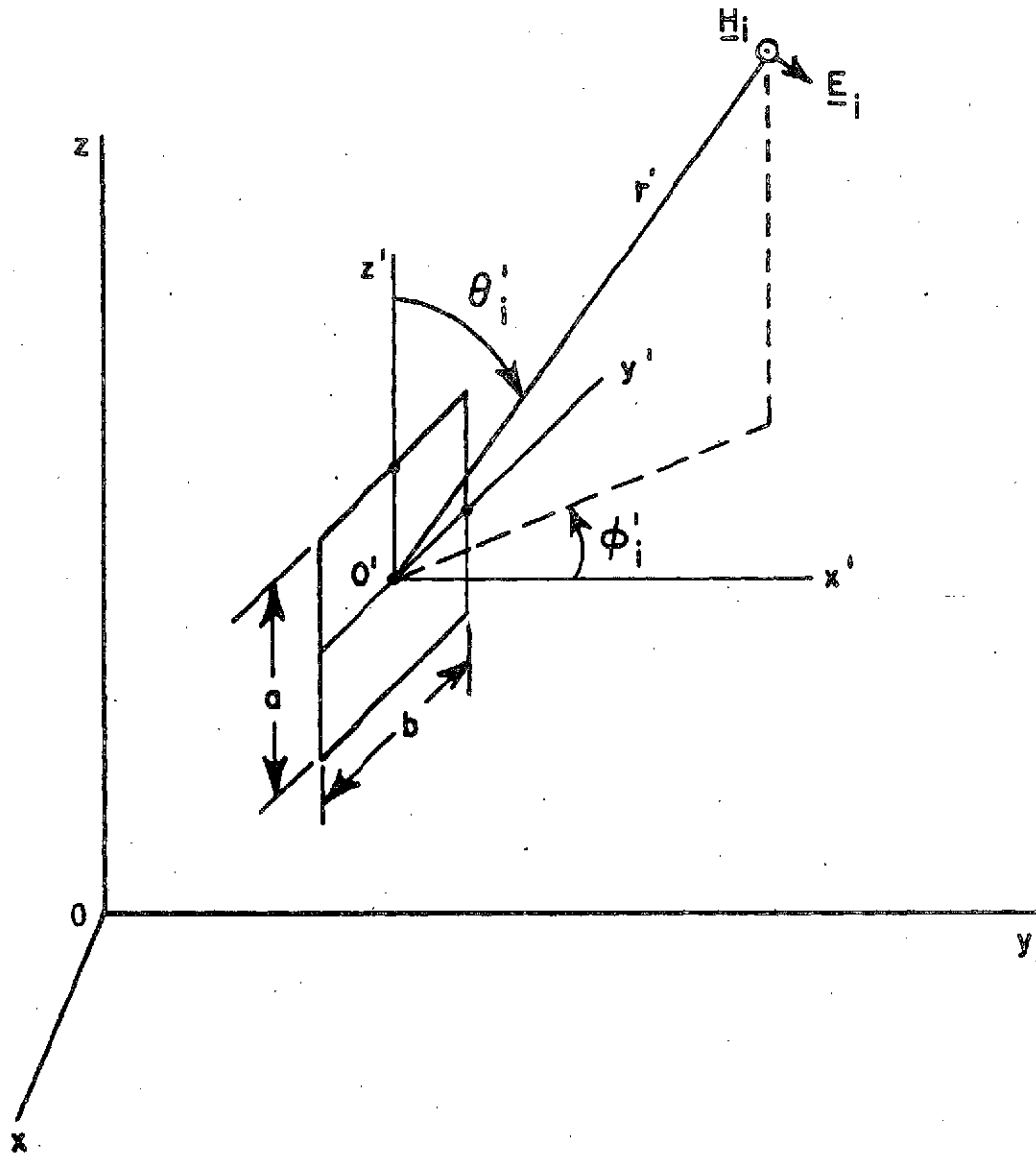


Fig. 17--A plane wave (\vec{E}_i, \vec{H}_i) illuminates an electric surface dipole.

CHAPTER VI APPLICATIONS

In the preceding chapters, attention has been directed to the general theory of the reaction integral formulation for scattering problems. Suitable bases and test sources have been defined and the mutual impedance between them has been evaluated. In the following, scattering from dielectric-coated cylinders with transverse magnetic incident wave will first be investigated.

A. CYLINDERS WITH THIN DIELECTRIC COATING (TM CASE)

Consider a dielectric-coated conducting cylinder illuminated by an electric line source. Let $(\underline{J}_S, \underline{M}_S)$ denote the surface-current density induced on the conducting surface, and \underline{J}_{eq} denotes the polarization-current density induced in the dielectric layer. The first step in the reaction-Galerkin approach is to approximate the cylinder by a polygon cylinder with N segments. This is accomplished by fitting the cylinder with segments such that the perimeter of the polygon cylinder is equal to that of the original cylinder.

Fig. 18a illustrates a dielectric-coated, conducting polygon cylinder illuminated by a parallel electric line source $\underline{J}_i \hat{z}$. Let I_n denote the current density \underline{J}_S on segment n of the polygon cylinder. Each modal current \underline{J}_n has a uniform current distribution as in Eq. (20). Now one represents \underline{J}_S as the superposition of the N modal currents with weighting I_n . This gives a piecewise uniform expansion for \underline{J}_S with N unknown constants. The expansion for \underline{J}_{eq} will be considered next.

For a transverse magnetic source such as the electric line source $\underline{J}_i \hat{z}$ shown in Fig. 18a, the electric field has only a \hat{z} -component. For a conducting cylinder with thin dielectric coating, Maxwell's equations and the boundary conditions can be employed to obtain a suitable approximation for the electric field in the dielectric layer (Appendix):

$$(54) \quad \underline{E} = \frac{-k_1 \sin(k_1 \zeta) \underline{J}_S}{j\omega \epsilon} \quad (\text{TM case})$$

where \underline{J}_S is the \hat{z} -directed surface-current distribution on the conducting surface and ϵ is the permittivity of the layer. Distance measured normally outward from the conducting surface is denoted by the coordinate ζ , and k_1 is the propagation constant in the dielectric.

⊙ \underline{J}_i

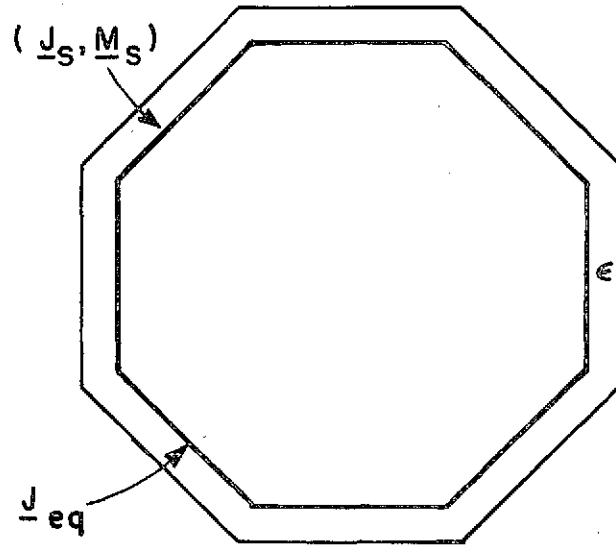


Fig. 18a--Dielectric-coated, conducting polygon cylinder illuminated by a parallel electric line source.

From Eq. (12) and (54), the polarization-current density can be expressed in terms of the surface-current density as follows.

$$(55) \quad \underline{J}_{eq} = -\left(\frac{\epsilon - \epsilon_0}{\epsilon}\right) k_1 \sin(k_1 \zeta) \underline{J}_s \quad (\text{TM case})$$

Since the surface-current distribution \underline{J}_s has been expanded with rectangular-pulse bases \underline{J}_n , one obtains a dependent expansion for the polarization-current density

$$(56) \quad \underline{J}_{eq} = \sum_{n=1}^N I_n \tilde{\underline{J}}_n$$

where

$$(57) \quad \tilde{J}_n = -\left(\frac{\epsilon - \epsilon_0}{\epsilon}\right) k_1 \sin(k_1 z) \underline{J}_n \quad (\text{TM case})$$

The magnetic current \underline{M}_s vanishes if the cylinder is a perfect conductor. If the cylinder has finite conductivity and the impedance boundary condition (Eq. (6)) is employed, then the magnetic surface-current density can be expanded as

$$(58) \quad \underline{M}_s = \sum_{n=1}^N I_n \underline{M}_n$$

where

$$(59) \quad \underline{M}_n = z_s \underline{J}_n \times \hat{n} \quad (\text{TM case})$$

and \hat{n} is the unit normal vector directed into the source region.

From the above discussions, the original problem illustrated in Fig. 18a can be replaced by its equivalent electromagnetic model, in that the dielectric-coated polygon cylinder is represented by an array of N hypothetical sources radiating in free space as shown in Fig. 18b. Each source is a modal current distribution \underline{S}_n , which is a collection of mode currents \underline{J}_n , \tilde{J}_n and \underline{M}_n , with weighting I_n .

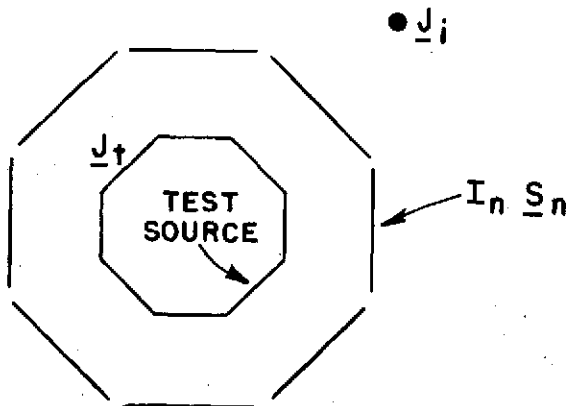


Fig. 18b--Electromagnetic model of the problem shown in Fig. 18a.

Based on the zero-reaction concept discussed in Chapter II, if one places an electric test source in the interior region, as illustrated in Fig. 18b, this interior test source has zero reaction with the other sources. To determine N current samples, one makes N independent reaction tests. This procedure generates a system of N simultaneous linear equations. Numerical solution of this system yields a stationary result [17] for the samples of the current distribution.

Let C_{mn} denote the reaction between test-source m and mode current \underline{S}_n in Fig. 18b. The reaction between the test-source m and the impressed source \underline{J}_i plus the reaction between the test-source m and all the mode currents,

$$\sum_{n=1}^N \underline{S}_n$$

must vanish, leading again to Eq. (9) in which the reaction C_{mn} is given by Eq. (10) plus an additional term ΔC_{mn} given by Eq. (14).

B. CYLINDERS WITH THIN DIELECTRIC COATING (TE CASE)

Consider a dielectric-coated, conducting polygon cylinder illuminated by a parallel magnetic line source $M_i \hat{z}$, as shown in Fig. 19a. The induced surface-current density \underline{J}_s flows in the direction transverse to z axis. Let I_n denote the current density at the corners of the polygon, and let one define N strip dipole-mode currents on the conducting surface. Mode 1 extends from point N to point 2, Mode 2 extends from point 1 to point 3, and so on. Each mode \underline{J}_n has a sinusoidal current distribution and unit terminal current density defined by Eqs. (30) and (31). Now one represents \underline{J}_s as the superposition of the N overlapping dipole-mode currents with weighting I_n . This gives a piecewise-sinusoidal expansion for \underline{J}_s with N unknown constants.

For the TE case, the electric field in the thin dielectric coating is essentially normal to the conducting surface, and can be determined from the charge density distributed on the conducting surface. Via Maxwell's equations and the boundary conditions, a suitable approximation for the electric field in the dielectric region (Appendix) is

$$(60) \quad \underline{E} = \frac{1}{j\omega\epsilon} \cos(k_\zeta \zeta) (\hat{z} \times \underline{J}'_s) \quad (\text{TE CASE})$$

where $k_\zeta = k\sqrt{\epsilon_r - 1}$ and ϵ_r is the relative permittivity. Coordinate ζ denotes the distance measured normally outward from the conducting surface. \underline{J}'_s is the derivative of the surface-current density. From Eqs. (12) and (60), one obtains a suitable expansion for the polarization-current density inside the thin dielectric layer coated on a conducting cylinder as follows:

• \underline{M}_i

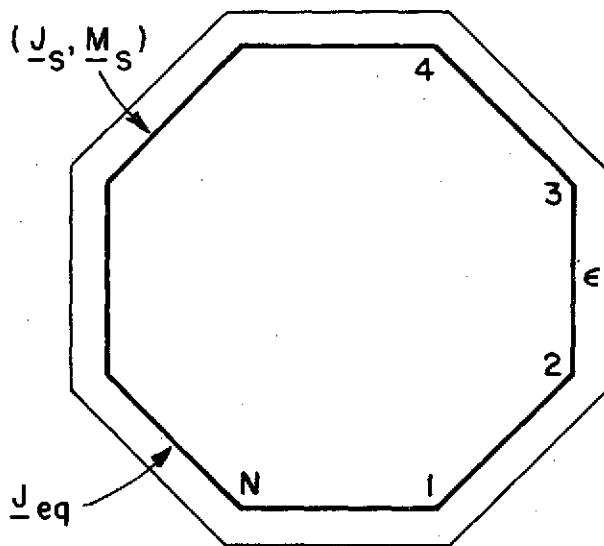


Fig. 19a--Dielectric-coated, conducting polygon cylinder illuminated by a parallel magnetic line source.

$$(61) \quad \underline{J}_{eq} = \sum_{n=1}^N I_n \underline{\mathcal{J}}_n$$

where

$$(62) \quad \underline{\mathcal{J}}_n = \frac{\epsilon_r - 1}{\epsilon_r} \cos(k_z z) (\hat{z} \times \underline{J}'_n) \quad (\text{TE case})$$

and \underline{J}'_n is the derivative of the expansion functions \underline{J}_n (Eqs. (30) and (31)) employed for the surface-current density \underline{J}_s .

If one takes the finite conductivity into account and uses the impedance boundary condition, the magnetic surface-current density can be expanded as

$$(63) \quad \underline{M}_s = \sum_{n=1}^N I_n \underline{M}_n$$

with

$$(64) \quad \underline{M}_n = z_s (\underline{J}_n \times \hat{n}) \quad (\text{TE case})$$

Thus, the electromagnetic model, in the TE case, for the problem shown in Fig. 19a is an array of N overlapping, sinusoidal-dipole sources radiating in free space as illustrated in Fig. 19b. Each source is a modal current distribution \underline{S}_n , which is comprised of the mode currents \underline{J}_n , $\underline{\tilde{J}}_n$ and \underline{M}_n , with weighting I_n .

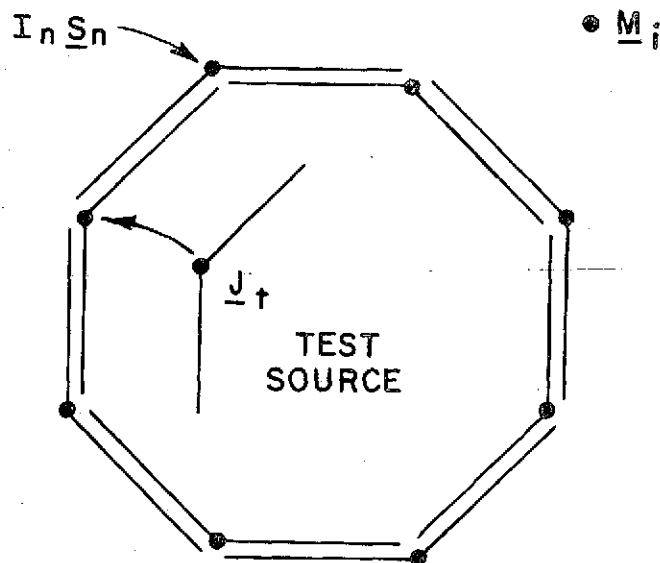


Fig. 19b--Electromagnetic model for the problem of Fig. 19a.

Following the same argument used in the previous section, one performs N independent reaction tests by moving an electric test source to the conducting surface all illustrated in Fig. 19b. Again, the zero-reaction concept leads to the matrix equation, Eq. (9), which can be solved numerically for the stationary current samples.

In the reaction formulation, a polygon cylinder with N segments is employed to represent a cylinder with arbitrary contour. It is found that in order to obtain accurate results one must use at least five segments per wavelength.

C. PLATES AND CORNER REFLECTORS WITH PERFECT CONDUCTIVITY

Electromagnetic modeling of dielectric-coated, conducting bodies with finite extent can be accomplished through the procedure described in the previous sections. In this section, however, two specific cases, namely, scattering from perfectly-conducting plates and corner reflectors are discussed. The plates and corner reflectors are assumed to have an infinitesimal thickness. Therefore, the total surface-current density \underline{J}_s (the vector sum of the current density on the front and back of the plates) is employed in the analysis.

Consider the problems of plane wave scattering by rectangular plates and corner reflectors. The planar surfaces are divided into rectangular cells as illustrated in Fig. 20. The surface-current density is then expanded into two orthogonal sets of overlapping dipole-mode currents. Each dipole-mode current covers two cells and has a sinusoidal current distribution as defined by Eqs. (39) and (40). In Fig. 20 the arrows represent the mode current densities \underline{J}_m . Thus, in the reaction calculation, the plates or the corner reflectors are represented by an array of overlapping mode currents radiating in free space and the reaction tests are enforced with a set of electric test sources.

The zero-reaction concept leads again to the matrix equation, Eq. (9), which is then solved for the samples of the surface-current density.

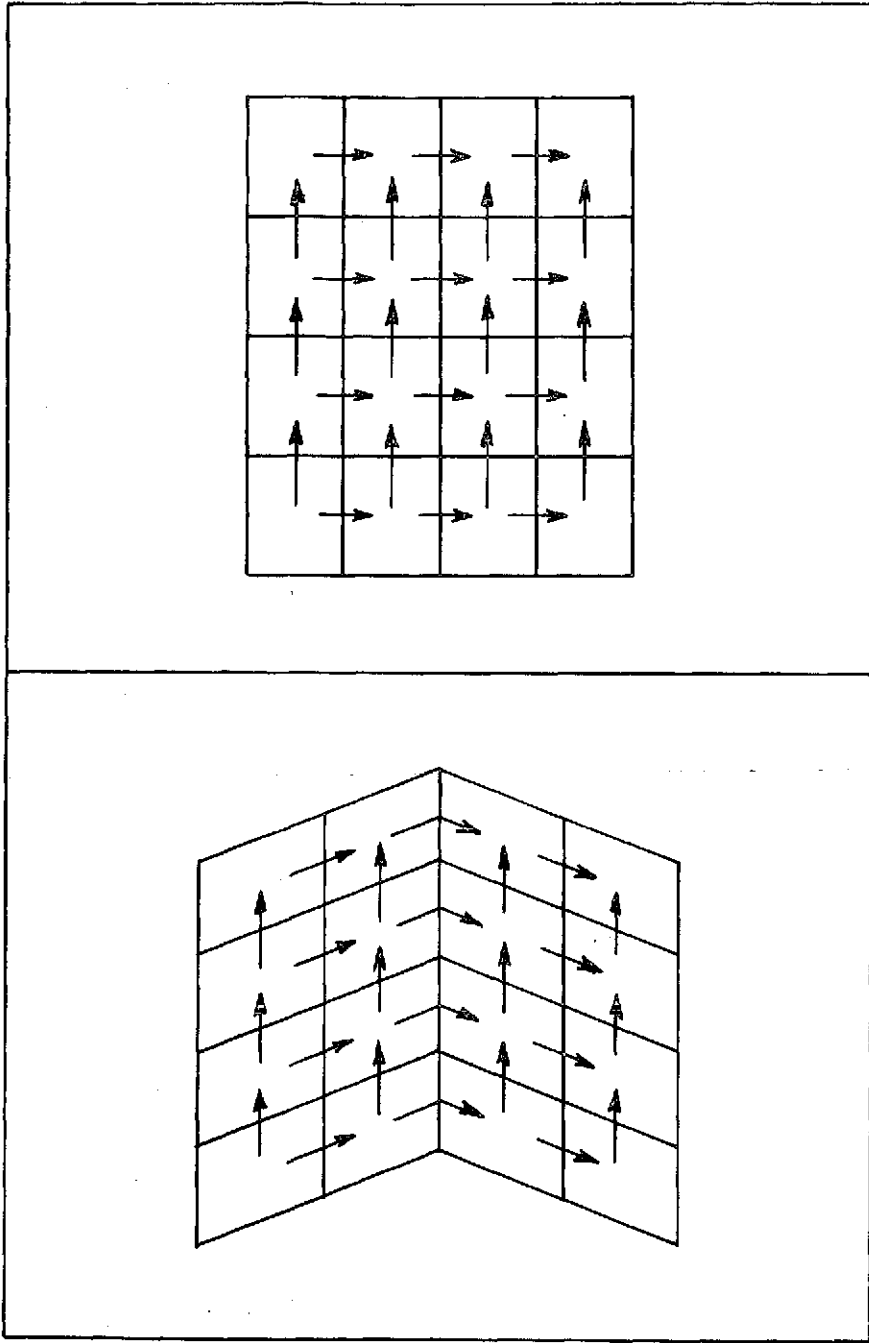


Fig. 20--Electromagnetic model of plate and corner reflector.

CHAPTER VII
FAR-FIELD RADIATION AND SCATTERING

The field scattered by a conducting body is the sum of the free space fields generated by the electric surface-current distribution \underline{J}_s and the magnetic surface-currents \underline{M}_s induced on the conducting surface. If the body has a dielectric coating, the contribution from the polarization-current density \underline{J}_{eg} should be included. To obtain the total field one adds the free space field of the impressed current source ($\underline{J}_i, \underline{M}_i$).

In the reaction calculation the continuous conducting surface is segmented and the current distribution is represented by a set of modal currents. Thus, the field scattered by a conducting body is the sum of the free space fields generated by these modal currents. The far-field contribution due to three types of modal currents employed in this dissertation will be examined in the following sections.

A. LONGITUDINAL, DIELECTRIC-COATED STRIP SOURCE

For an electric line source J_z of infinite length located on the z axis, the free space field is

$$(65) \quad \underline{E} = -\hat{z} k_\eta J_z H_0^{(2)}(k\rho)/4$$

$$(66) \quad \underline{H} = -\hat{\phi} J_z H_1^{(2)}(k\rho)/4k.$$

If the electric line source is parallel with the z axis and passes through the point (x,y), its free space field at a distant point (ρ, ϕ) is

$$(67) \quad \underline{E} = -\hat{z} \frac{k_\eta J_z \sqrt{2j} e^{-jk\rho}}{4\sqrt{\pi k\rho}} e^{jk(x \cos \phi - y \sin \phi)}$$

Fig. 21 illustrates an electric surface-current distribution $J(t) = \hat{z} J(t)$ on a dielectric-coated, conducting strip extending from (x_1, y_1) to (x_2, y_2) . Distance along the strip is measured by the coordinate t, and distance perpendicular to the strip is measured by the coordinate ζ . For an arbitrary point on the strip,

$$(68) \quad x = x_1 + t \cos \alpha$$

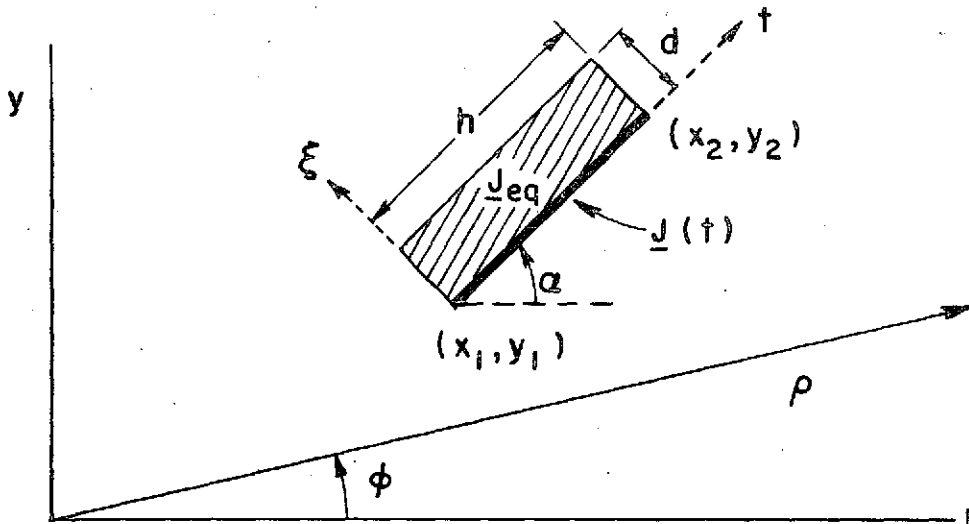


Fig. 21--A dielectric-coated strip source.

$$(69) \quad y = y_1 + t \sin \alpha .$$

From Eq. (67), the free space field of this source $\underline{J}(t) = \hat{z} J_z(t)$ at a distant point (ρ, ϕ) is

$$(70) \quad \underline{E}^J = -\hat{z} \frac{k\eta\sqrt{2j}}{4\sqrt{\pi}k\rho} e^{-jk\rho} e^{j\psi_1} \int_0^h J_z(t) e^{jkct} dt$$

where

$$(71) \quad \psi_1 = k(x_1 \cos \phi + y_1 \sin \phi)$$

$$(72) \quad c = \cos(\alpha - \phi)$$

Using the approximation (Eq. (55)), the far-field contribution from the volume current density \underline{J}_{eq} is

$$(73) \quad \underline{E}^{J_{eq}} = \hat{z} \frac{kn\sqrt{2j} e^{-jk\rho}}{4\sqrt{\pi k\rho}} e^{j\psi_1} \left(\frac{\epsilon_r - 1}{\epsilon_r} \right) \int_0^h \int_0^d k_1 \sin(k_1 \zeta) J_z(t) e^{jkct} e^{-jk\zeta \sin(\alpha - \phi)} d\zeta dt.$$

The integration along ζ can be readily performed to yield

$$(74) \quad \underline{E}^{J_{eq}} = g_{TM} \underline{E}^J$$

where

$$(75) \quad g_{TM} = \left(\frac{\epsilon_r - 1}{2\epsilon_r} \right) k_1 \left[\frac{e^{j[k_1 - k \sin(\alpha - \phi)]d} - 1}{k_1 - k \sin(\alpha - \phi)} + \frac{e^{-j[k_1 + k \sin(\alpha - \phi)]d} - 1}{k_1 + k \sin(\alpha - \phi)} \right]$$

If one introduces finite conductivity to the conducting strip and uses the impedance boundary condition (Eq. (6)), the free space field due to this magnetic current distribution is

$$(76) \quad \underline{E}^M = \frac{z_s \sin(\alpha - \phi)}{\eta} \underline{E}^J.$$

From Eqs. (70), (74), and (76), the distant scattered field generated by the dielectric-coated conducting strip (shown in Fig. 21) with $J_z(t) = I$ is

$$(77) \quad E_z^S = \frac{-n e^{-j\pi/4}}{\sqrt{8\pi k\rho}} e^{-jk\rho} \left(1 + g_{TM} + \frac{z_s \sin(\alpha - \phi)}{\eta} \right) F_{TM}$$

where

$$(78) \quad F_{TM} = \frac{e^{j\psi_2} - e^{j\psi_1}}{c}$$

$$(79) \quad \psi_2 = k(x_2 \cos \phi + y_2 \sin \phi).$$

For broadside direction, i.e., $\alpha - \phi = \pi/2$ or $3\pi/2$,

$$(80) \quad F_{TM} = jkh e^{j\psi_1} .$$

B. TRANSVERSE, DIELECTRIC-COATED STRIP MONOPOLE

Consider again the dielectric-coated strip monopole shown in Fig. 21. This time the source is a transverse electric surface-current distribution $\underline{J}(t) = \hat{t} J_t(t)$. From Eq. (24), the magnetic field at a distant point (ρ, ϕ) is

$$(81) \quad \underline{H}^J = -\hat{z} \frac{k\sqrt{2j} \sin(\alpha-\phi)}{4\sqrt{\pi k\rho}} e^{-jk\rho} e^{j\psi_1} \int_0^h J_t(t) e^{jkct} dt$$

From Eq. (62), the far-field contribution from the volume current density is

$$(82) \quad \underline{H}^{J_{eq}} = \hat{z} \frac{k\sqrt{2j} \cos(\alpha-\phi)}{4\sqrt{\pi k\rho}} e^{-jk\rho} e^{j\psi_1} \left(\frac{\epsilon_r - 1}{\epsilon_r} \right) \int_0^h \int_0^d \cos(k_\zeta \zeta) J'_t(t) e^{jkct} e^{-jk \sin(\alpha-\phi)\zeta} d\zeta dt .$$

The integration along ζ is performed to yield

$$(83) \quad \underline{H}^{J_{eq}} = \frac{\hat{z} k\sqrt{2j}}{4\sqrt{\pi k\rho}} \cos(\alpha-\phi) e^{-jk\rho} e^{j\psi_1} g_{TE} \int_0^h J'_t(t) e^{jkct} dt$$

where

$$(84) \quad g_{TE} = \left(\frac{\epsilon_r - 1}{2j\epsilon_r} \right) \left[\frac{e^{j[k_\zeta - k \sin(\alpha-\phi)]d} - 1}{k_\zeta - k \sin(\alpha-\phi)} - \frac{e^{-j[k_\zeta + k \sin(\alpha-\phi)]d} - 1}{k_\zeta + k \sin(\alpha-\phi)} \right]$$

Consider a magnetic surface-current distribution $M_z(t)$ on the planar strip extending from (x_1, y_1) to (x_2, y_2) as in Fig. 21. From duality relations in electric and magnetic systems and Eq. (70), the free space field of this source at a distant point (ρ, ϕ) is

$$(85) \quad \underline{H}^M = \frac{-\hat{z} k\sqrt{2j}}{4\sqrt{\pi k\rho}} e^{-jk\rho} e^{j\psi_1} \int_0^h M_z(t) e^{jkct} dt .$$

If the magnetic surface-current density $M_z(t)$ in Eq. (85) arises through the finite conductivity of the cylinder, the impedance boundary condition in Eq. (6) yields

$$(86) \quad M_z(t) = s Z_s J_t(t)$$

where

$$(87) \quad s = (\hat{t} \times \hat{n}) \cdot \hat{z} = \pm 1$$

and the unit normal \hat{n} is directed into the source region.

From Eqs. (81), (83), (85), and (86), the distant scattered field from one segment of the dielectric-coated conducting cylinder (the segment in Fig. 21) is

$$(88) \quad H_z^S = - \frac{\sqrt{2j} [(\eta \sin(\alpha - \phi) + s Z_s) F_1 - \eta \cos(\alpha - \phi) g_{TE} F_2] e^{-jk\rho}}{4\eta \sin kh \sqrt{\pi k\rho}}$$

where

$$(89) \quad F_1 = k \sin(kh) e^{j\psi_1} \int_0^h J_t(t) e^{jkct} dt$$

and

$$(90) \quad F_2 = k \sin(kh) e^{j\psi_1} \int_0^h J'_t(t) e^{jkct} dt .$$

If the transverse electric current on this segment has a sinusoidal distribution as follows

$$(91) \quad J_t(t) = \frac{I_1 \sin(kh - kt) + I_2 \sin(kt)}{\sin(kh)} ,$$

Eqs. (89) and (90) yield

$$(92) \quad F_1 = \frac{I_1}{\sin^2(\alpha - \phi)} \left[e^{j\psi_2} - (\cos kh + j c \sin kh) e^{j\psi_1} \right] \\ + \frac{I_2}{\sin^2(\alpha - \phi)} \left[e^{j\psi_1} - (\cos kh - j c \sin kh) e^{j\psi_2} \right]$$

and

$$(93) \quad F_2 = \frac{I_1}{\sin^2(\alpha - \phi)} \left[j c e^{j\psi_2} + (\sin kh - j c \cos kh) e^{j\psi_1} \right] \\ + \frac{I_2}{\sin^2(\alpha - \phi)} \left[j c e^{j\psi_1} - (\sin kh + j c \cos kh) e^{j\psi_2} \right].$$

In the end-fire direction where $(\alpha - \phi)$ is zero or π ,

$$(94) \quad F_1 = \left[e^{j\psi_1} \sin kh - kh e^{j\psi_2} \right] j c I_1/2 \\ - \left[e^{j\psi_2} \sin kh - kh e^{j\psi_1} \right] j c I_2/2$$

and

$$(95) \quad F_2 = \left[kh e^{j\psi_2} + \sin kh e^{j\psi_1} \right] I_1/2 \\ - \left[kh e^{j\psi_1} + \sin kh e^{j\psi_2} \right] I_2/2$$

C. RECTANGULAR SURFACE DIPOLE

Consider an electric surface dipole with current density $\underline{J} = \hat{z}' \cos(\pi z'/a)$ located on the $y'z'$ plane as shown in Fig. 22. From reciprocity, the free space electric field generated by this source at a distant point (r, θ'_S, ϕ'_S) (from Eq. (53)) is

$$(96) \quad \underline{E}^S = \hat{\theta}'_S \frac{j\omega\mu}{2} a b \sin \theta'_S \frac{\sin(X_S)}{X_S} \frac{\cos(Y_S/2)}{(Y_S^2 - \pi^2)} \frac{e^{-jkr}}{r}$$

where

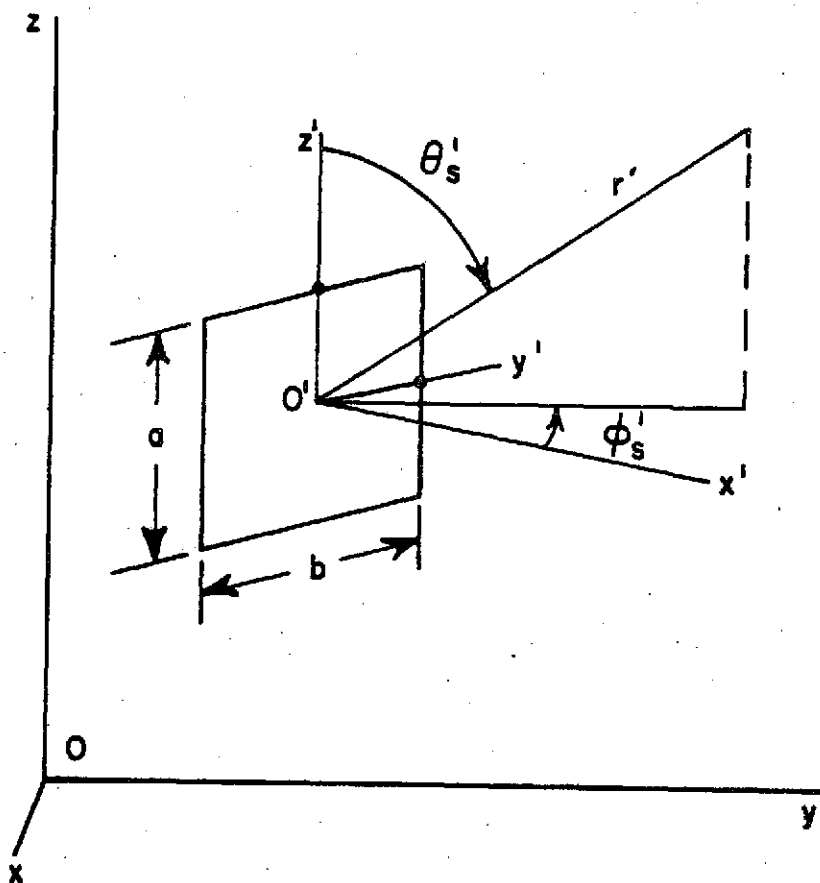


Fig. 22--A surface dipole radiates in free space.

$$(97) \quad X_s = 0.5 kb \sin \theta'_s \sin \phi'_s$$

$$(98) \quad Y_s = ka \cos \theta'_s .$$

The $\hat{\theta}$ - and $\hat{\phi}$ -components of the scattered field with respect to the reference coordinate system 0 can be obtained easily via appropriate coordinate transformation.

In plane-wave scattering problems, one is usually interested in the echo information defined as follows:

$$(99) \quad \text{echo width} = \lim_{\rho \rightarrow \infty} 2\pi\rho \frac{|E^S|^2}{|E^i|^2} \quad (\text{TM case}),$$

$$(100) \quad \text{echo width} = \lim_{\rho \rightarrow \infty} 2\pi\rho \frac{|H^S|^2}{|H^i|^2} \quad (\text{TE case}),$$

and

$$(101) \quad \text{echo area} = \lim_{r \rightarrow \infty} 4\pi r^2 \frac{|E^S|^2}{|E^i|^2} \quad (\text{three-dimensional case}).$$

In three-dimensional antenna problems, one is interested in the power gain:

$$(102) \quad \text{gain} = \frac{4\pi r^2 |E|^2}{\eta |V|^2 G}$$

where V is the terminal voltage and G is the conductance of the antenna.

CHAPTER VIII NUMERICAL RESULTS

A. TM DIELECTRIC-COATED CYLINDERS

In this section numerical results are presented for the backscattering echo width of cylinders with thin dielectric coating. The incident wave is a transverse-magnetic plane wave. Fig. 23 presents the backscattering echo width of a circular cylinder with a thin dielectric coating. In the reaction calculation the cylinder is divided into N segments with $N = 12 + 20 d/\lambda$ and d is the diameter. Similar results for a square cylinder with 16 segments are shown in Fig. 24. For comparison, similar results are presented in Figs. 25 and 26 for uncoated cylinders with finite conductivity. Bistatic echo width as a function of aspect angle is presented in Fig. 27 through 29 for circular and square cylinders with a thin dielectric coating. In all cases, the dielectric layer has a relative dielectric constant of 10.

B. TE DIELECTRIC-COATED CYLINDERS

Numerical results are presented for cylinders with a thin dielectric coating illuminated by a transverse-electric incident plane wave. Fig. 30 presents the backscattering echo width of a circular cylinder with a thin dielectric coating. As before, the cylinder is divided into N segments with $N = 12 + 20 d/\lambda$ and d is the diameter. Similar results for a square cylinder with 16 segments are presented in Fig. 31. In Figs. 30 and 31, backscattering echo width for uncoated cylinders are also included for comparison. Bistatic echo width as a function of observation angle for coated cylinders are shown in Figs. 32, 33 and 34. The relative dielectric constant is 1.5 in each case.

Examining the results, one can note that the reaction calculation gives accurate data for uncoated conducting cylinders. Satisfactory results are also obtained for cylinders with a thin dielectric coating.

C. PERFECTLY-CONDUCTING PLATES AND CORNER REFLECTORS

Fig. 35 presents the backscattering echo area of a square plate with perfect conductivity for the broadside aspect. In the reaction calculation, the plate is divided into cells, and overlapping current modes were employed as illustrated in Fig. 36. In this case the transverse current was neglected and 45 modes were used for the current distribution. Useful results can be obtained with as few as one mode per square wavelength of surface area. For comparison, Fig. 35 also shows the experimental measurements of Kouyoumjian [18].

The magnitude and phase of the induced current density on a perfectly-conducting rectangular plate are illustrated in Figs. 37 and

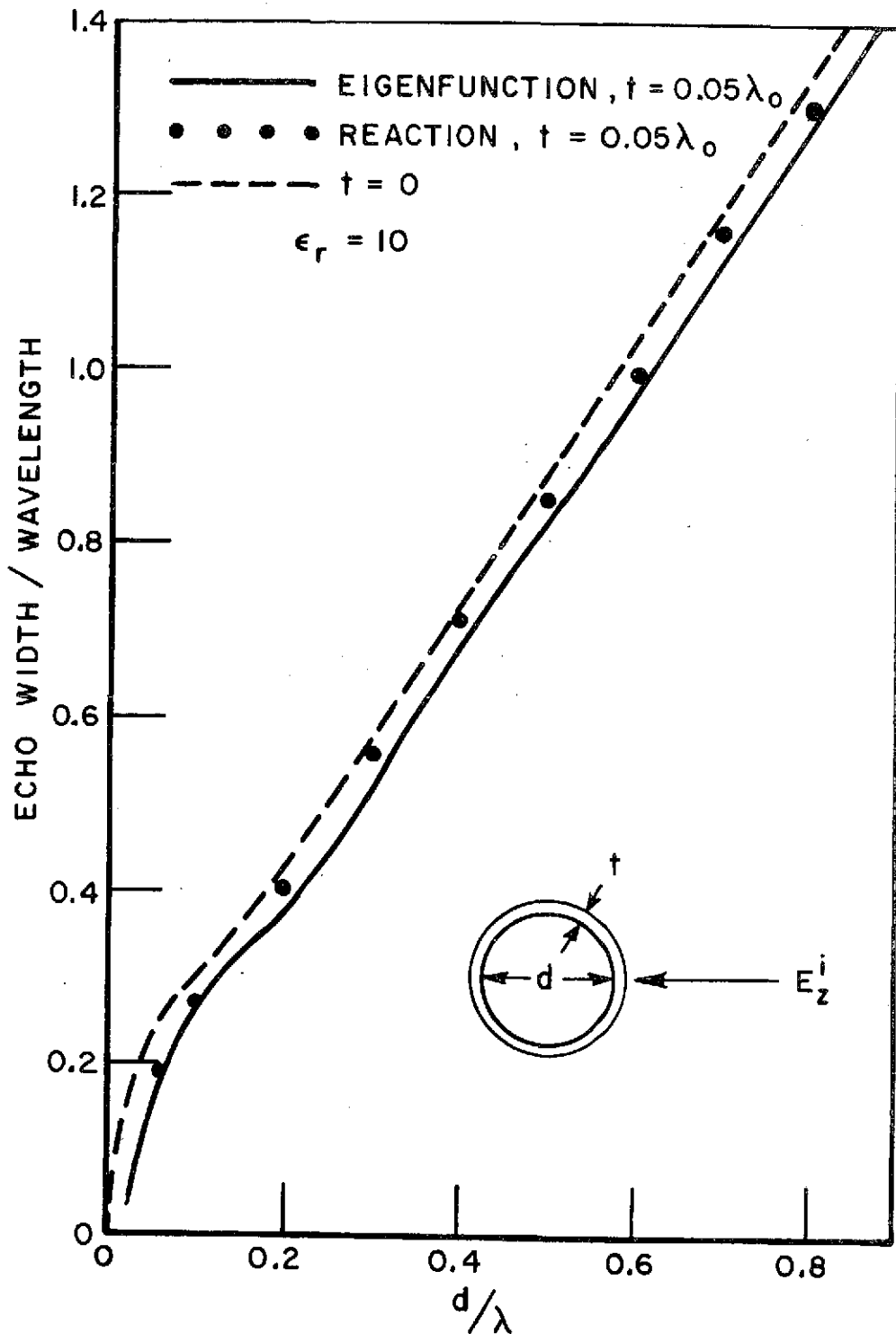


Fig. 23--Backscattering echo width of dielectric-coated circular cylinder.

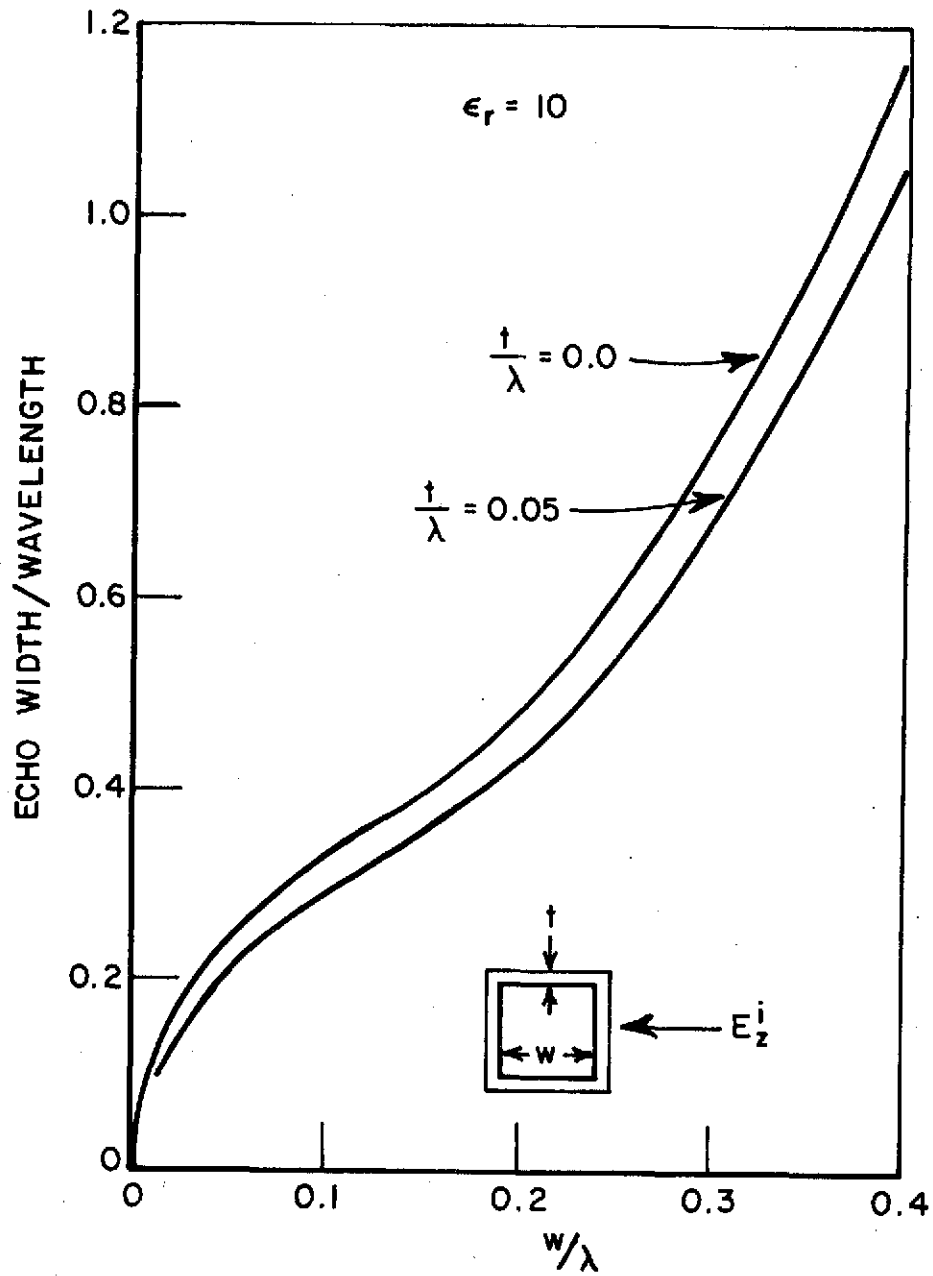


Fig. 24--Broadside backscattering echo width of dielectric-coated square cylinder.

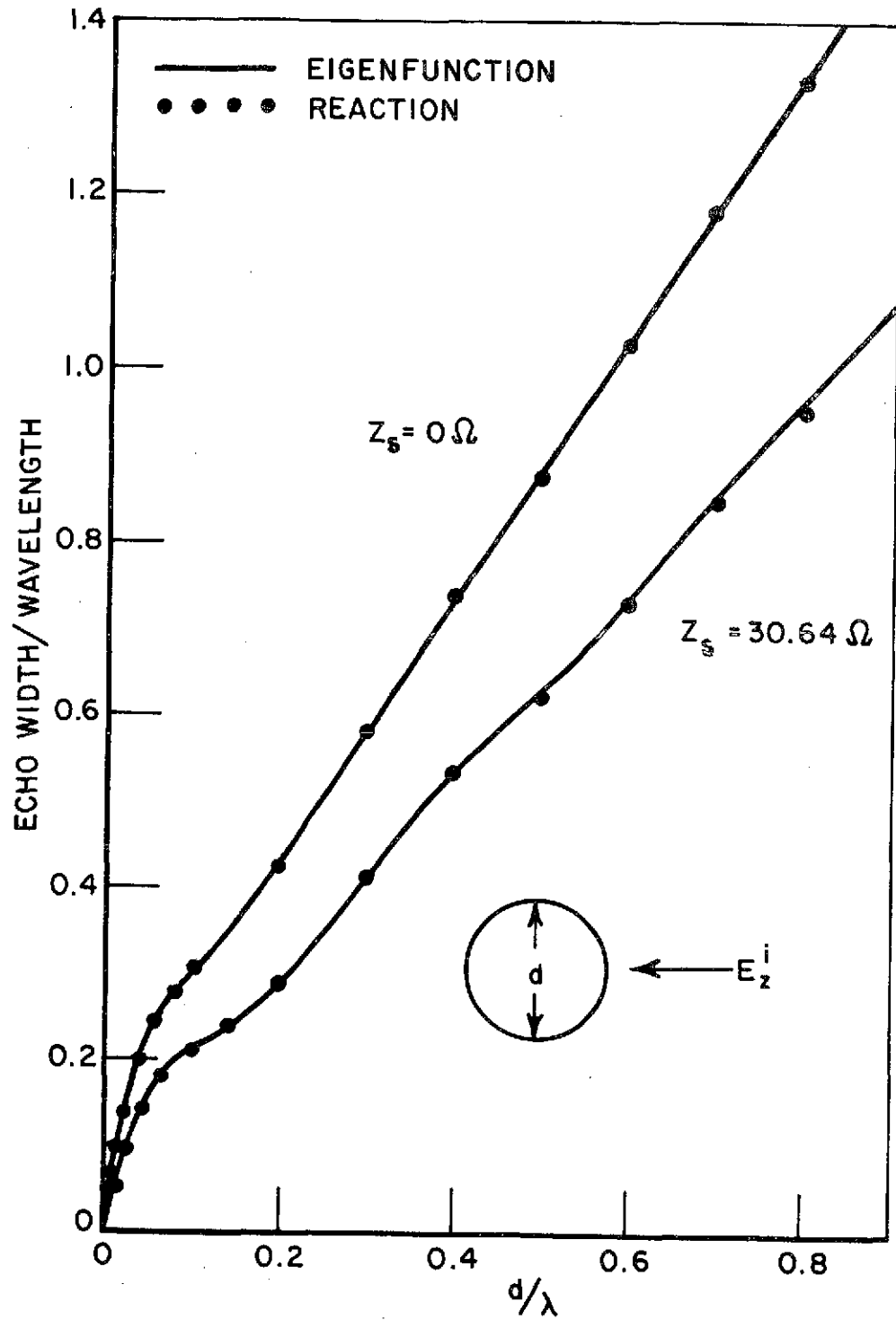


Fig. 25--Backscattering echo width of circular cylinder.

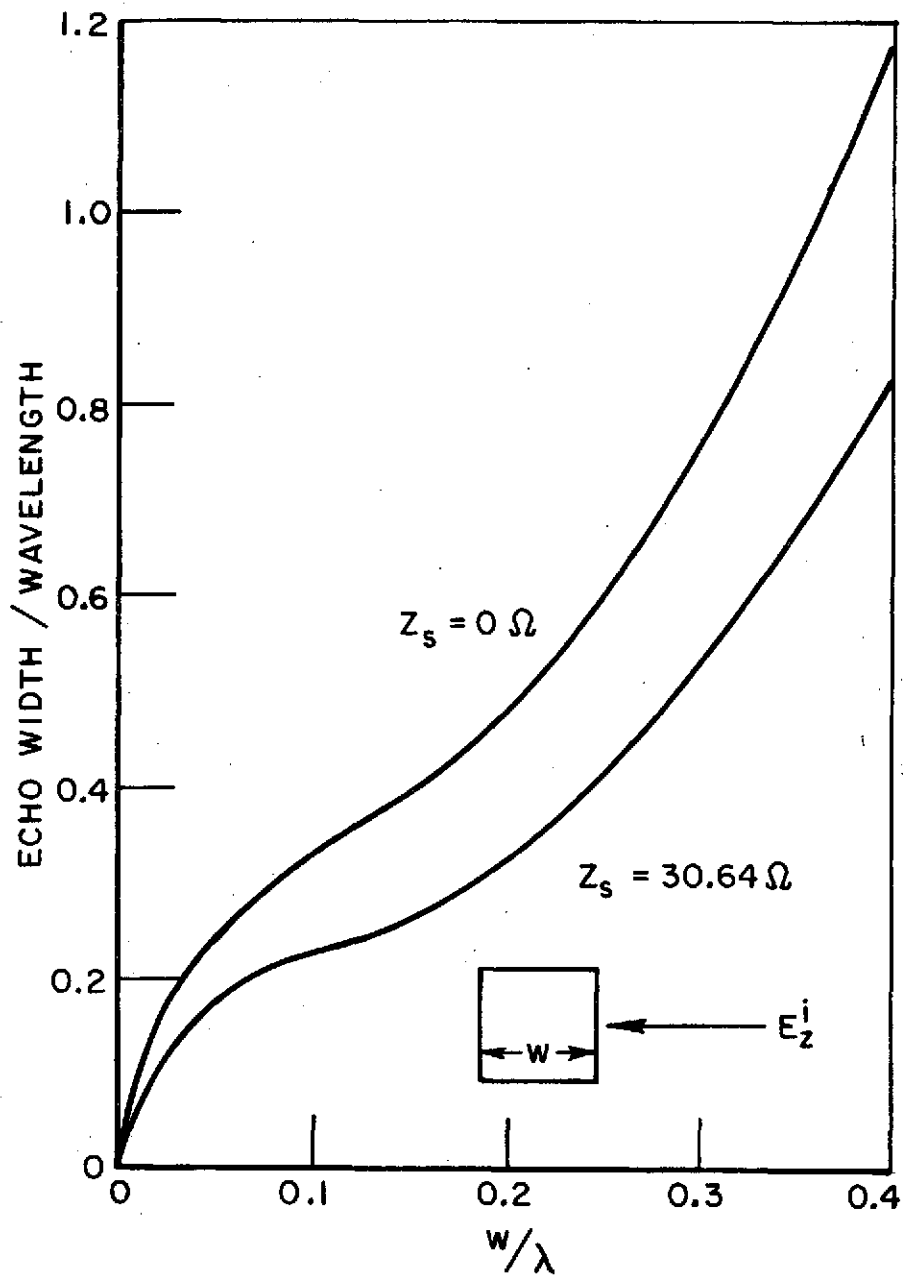


Fig. 26--Broadside backscattering echo width of square cylinder.

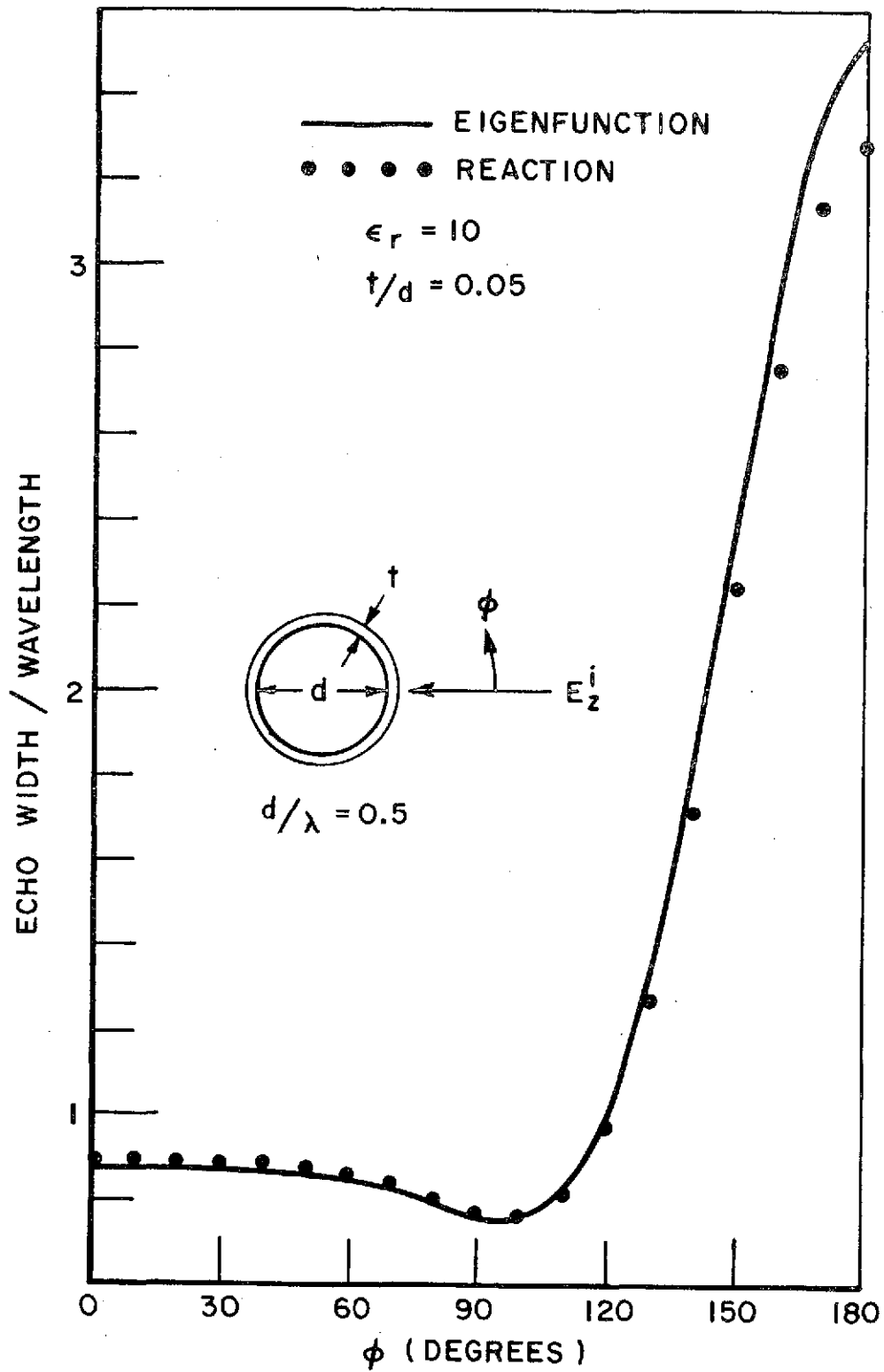


Fig. 27--Bistatic echo width of dielectric-coated circular cylinder.

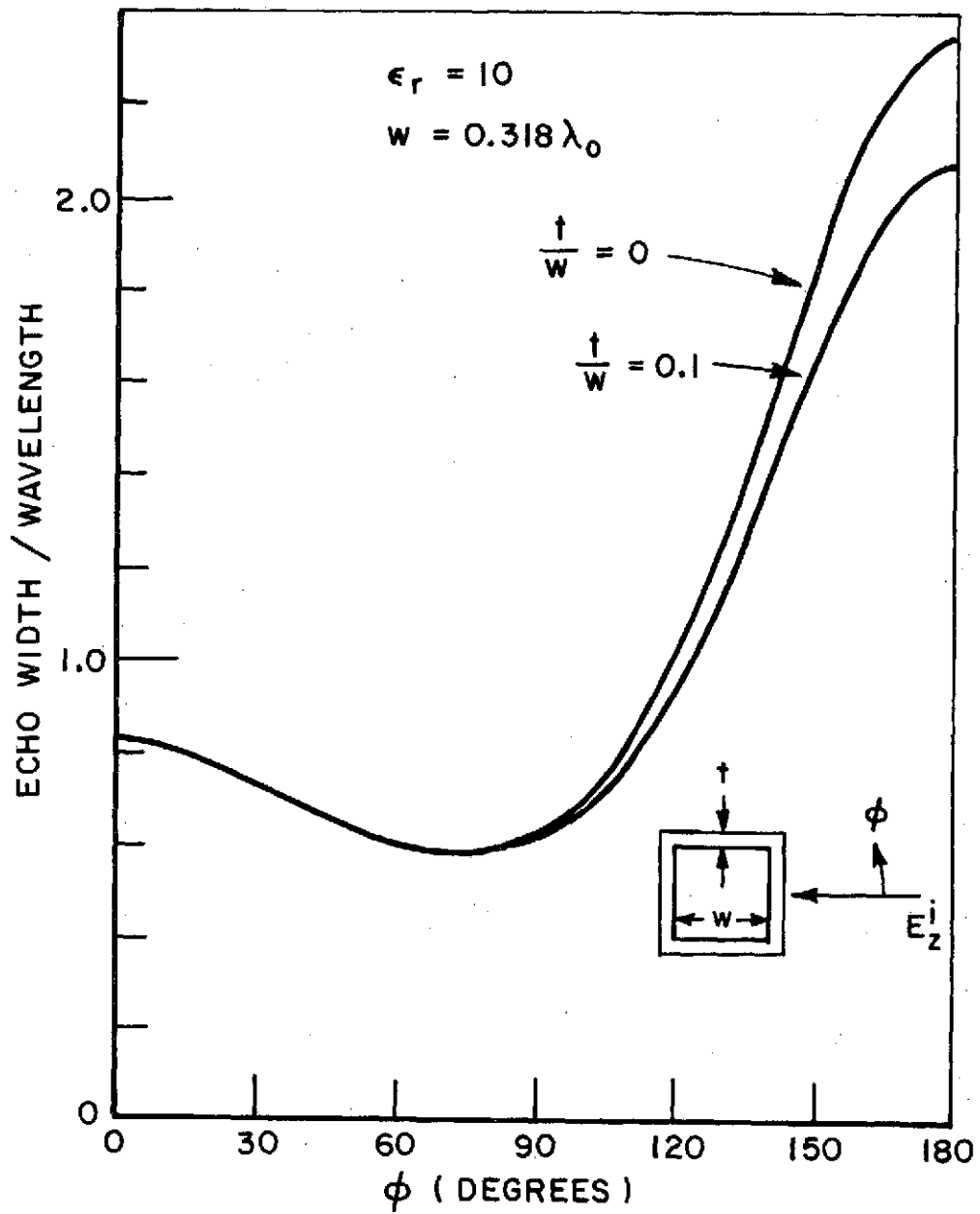


Fig. 28--Bistatic echo width of dielectric-coated square cylinder for broadside incidence.

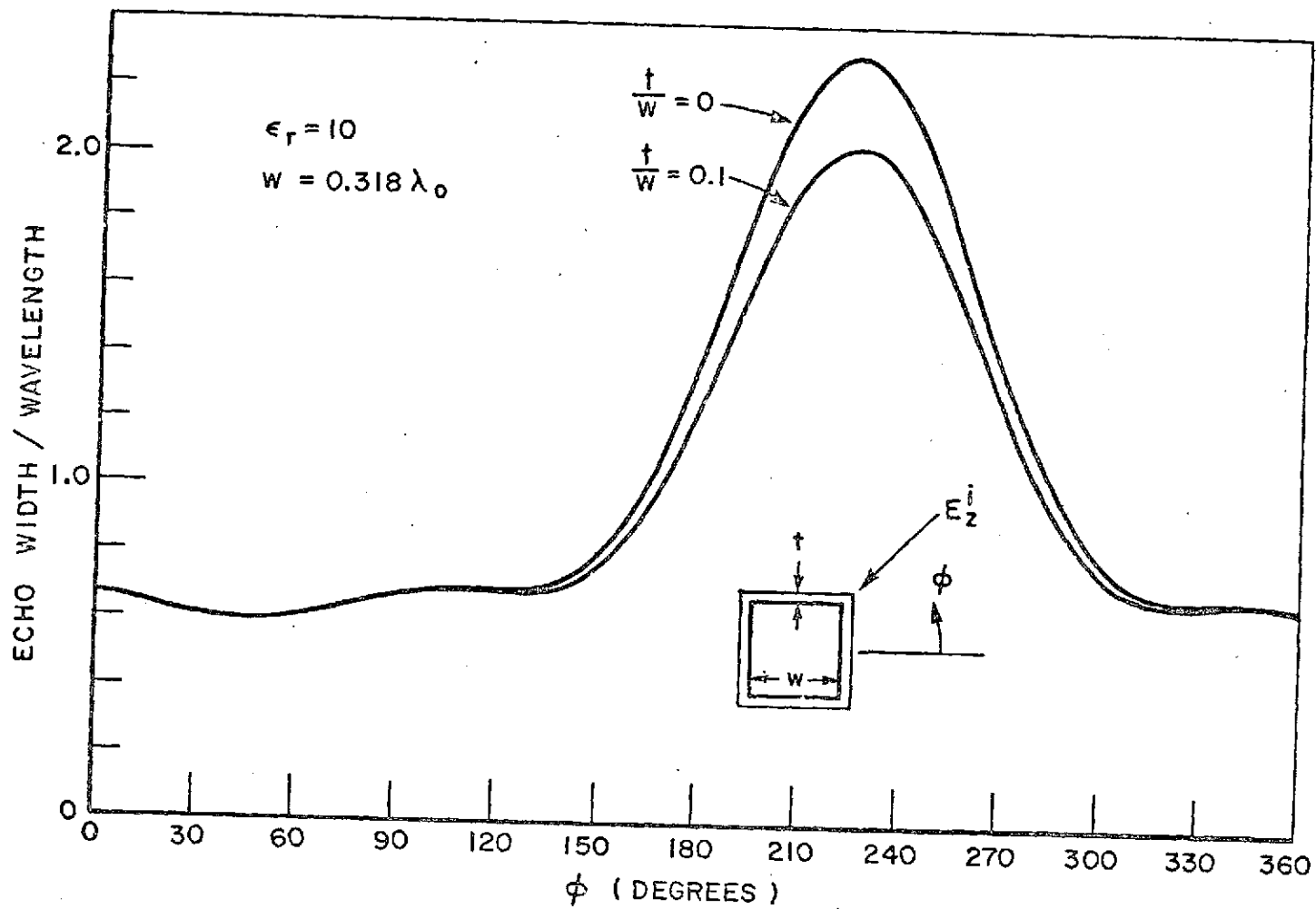


Fig. 29--Bistatic echo width of dielectric-coated square cylinder for oblique incidence.

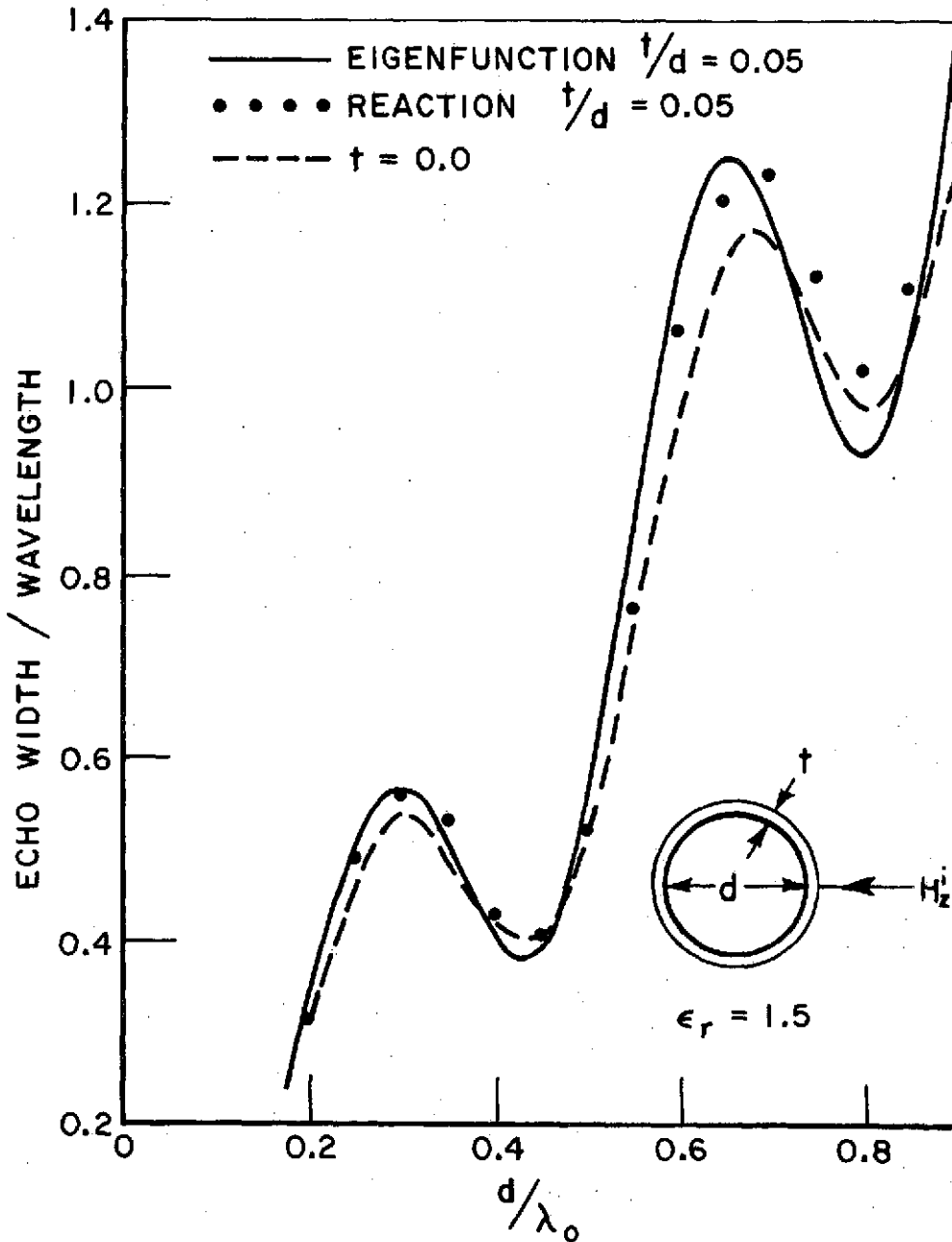


Fig. 30--Backscattering echo width of dielectric-coated circular cylinder.

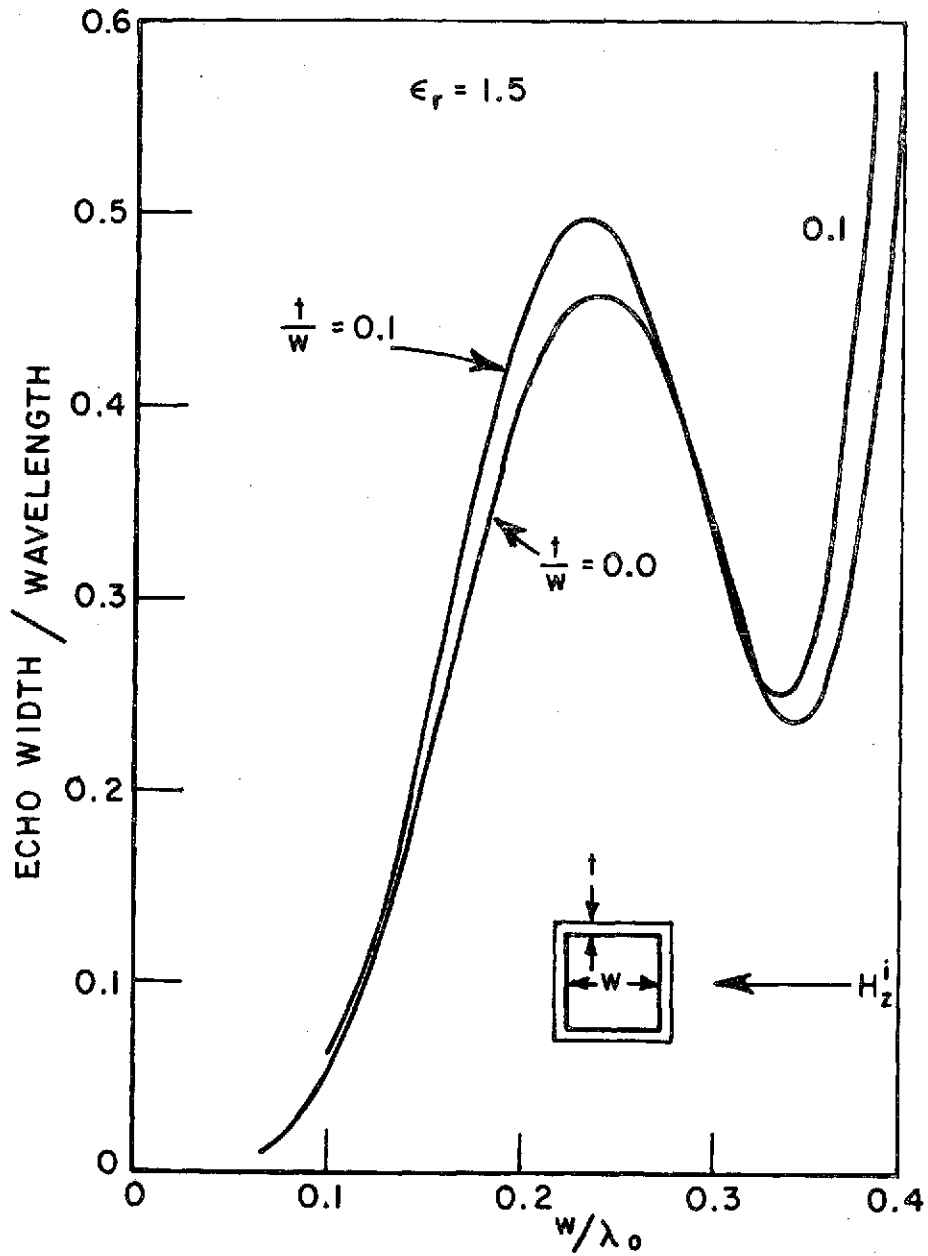


Fig. 31--Broadside backscattering echo width of dielectric-coated square cylinder.

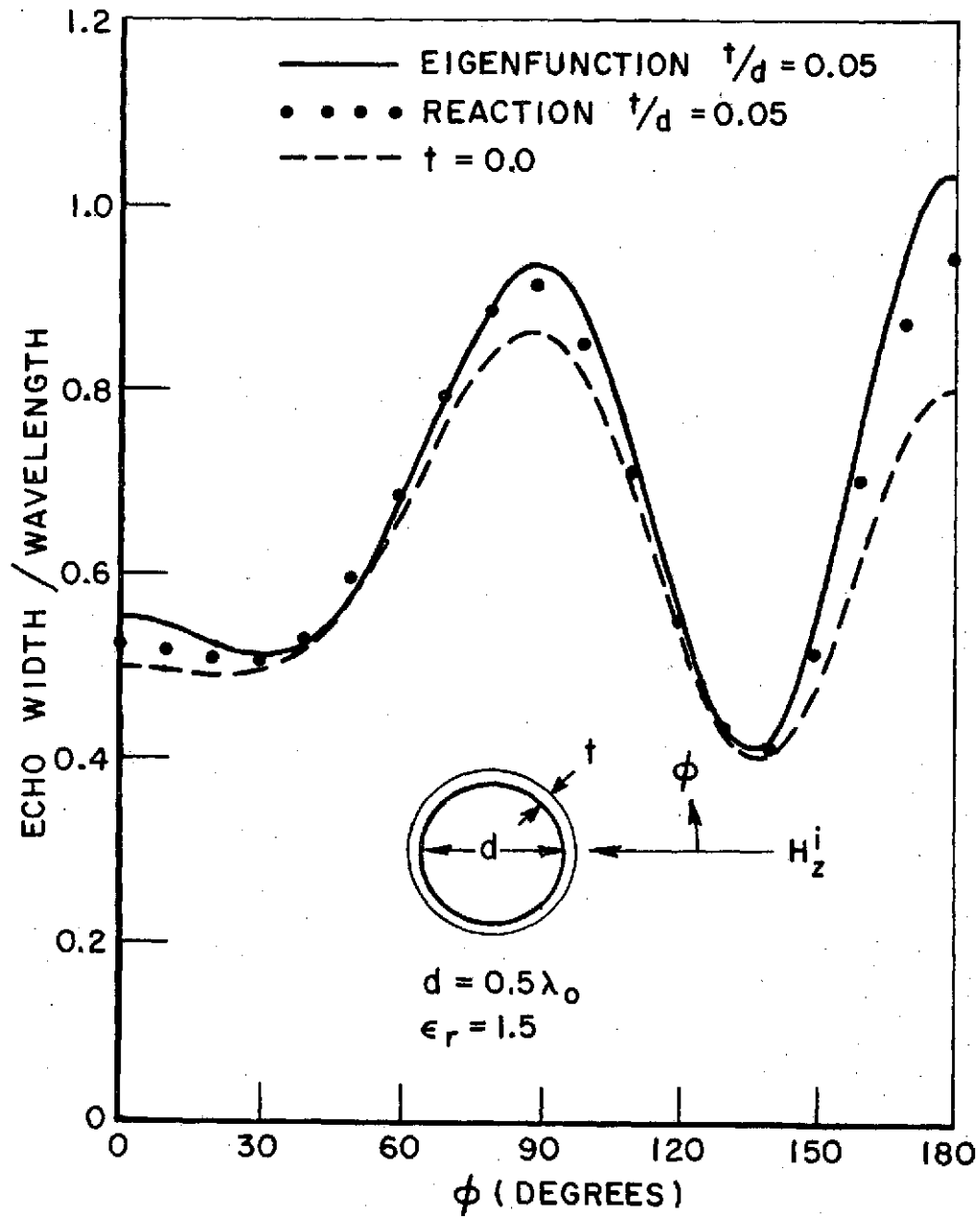


Fig. 32--Bistatic echo width of dielectric-coated circular cylinder.

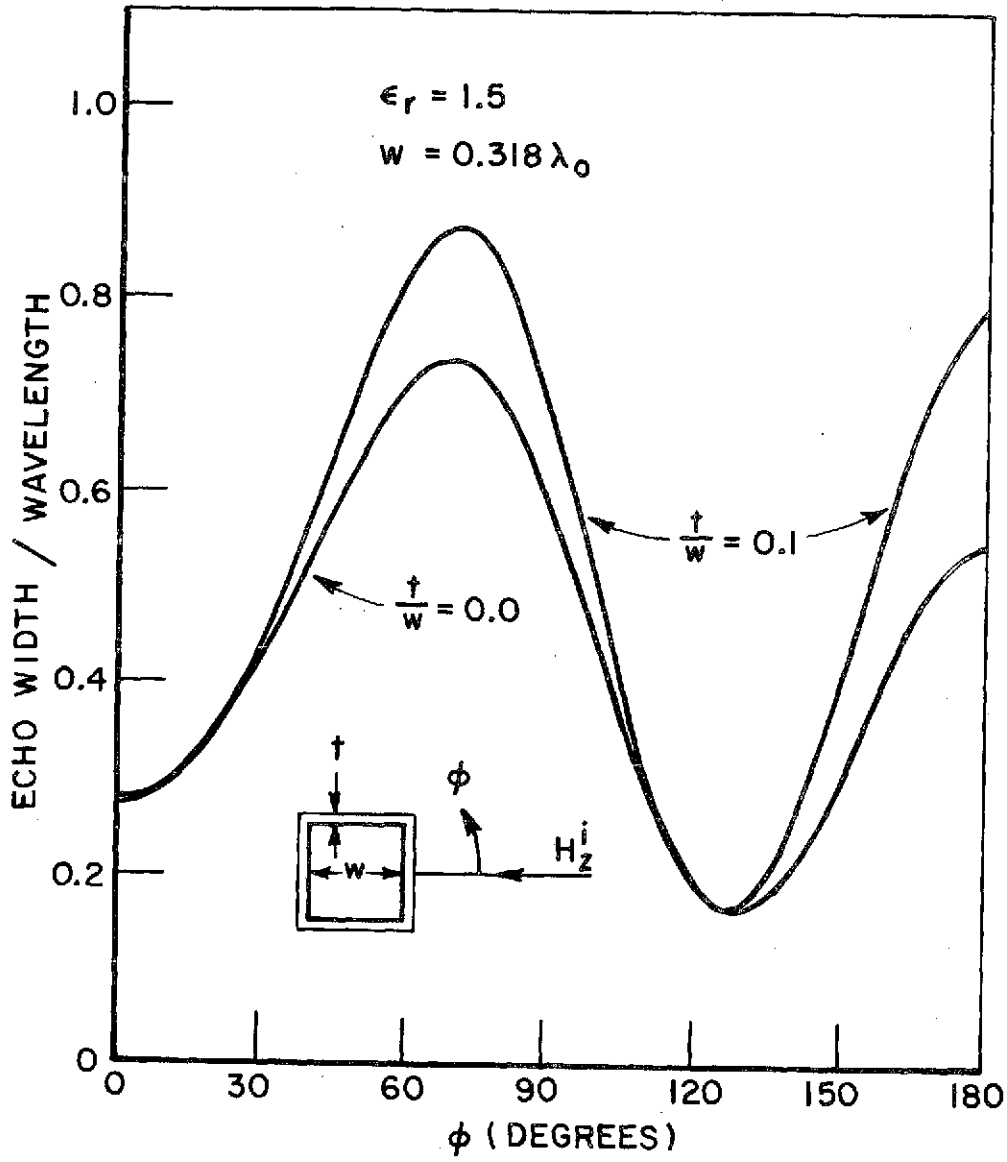


Fig. 33--Bistatic echo width of dielectric-coated square cylinder for broadside incidence.

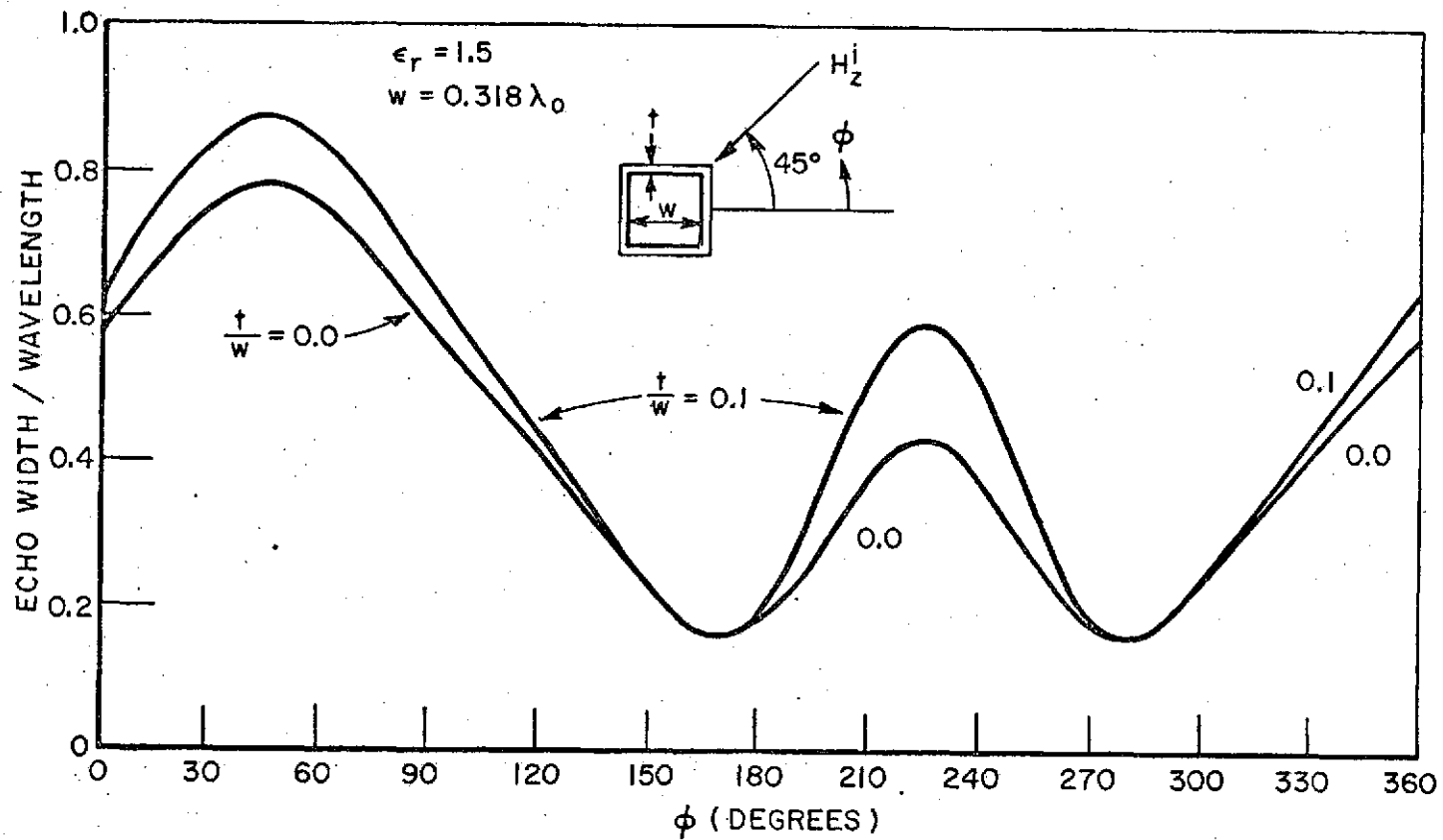


Fig. 34--Bistatic echo width of dielectric-coated square cylinder for oblique incidence.

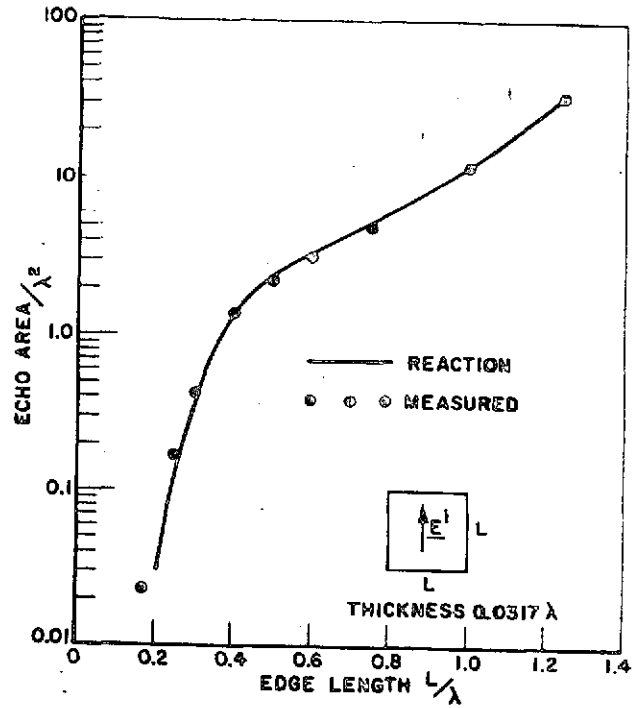


Fig. 35--Backscatter cross-section of perfectly conducting square plate for the broadside aspect.

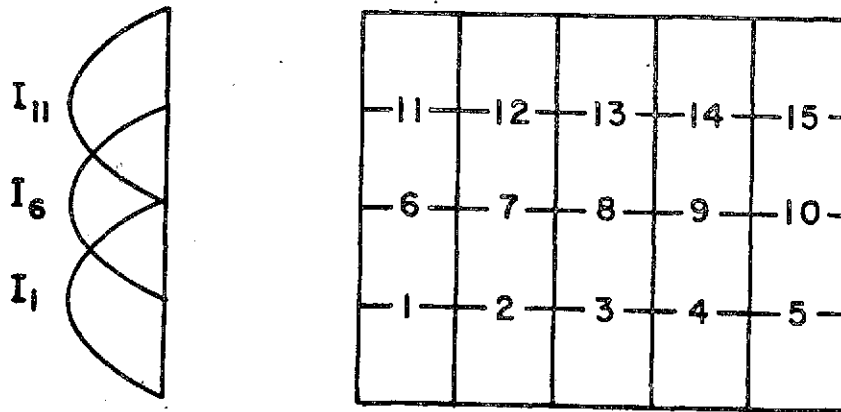


Fig. 36--Electromagnetic modeling of plate.

38. Figs. 39 through 42 show the normalized backscatter cross section of a rectangular plate. Figs. 43 and 44 show the normalized backscatter cross section of a corner reflector. The title of each figure gives the echo area at the broadside aspect in terms of $\text{dB} = 10 \log(\sigma/\lambda^2)$.

Figs. 46 through 49 show the E-plane gain of the corner-reflector antenna illustrated in Fig. 45. Figs. 50 through 53 show the H-plane gain of the same antenna. For comparison, Figs. 46 through 53 include experimental measurements obtained by Melvin Gilreath at NASA Langley Research Center. In the experimental measurements the receiving antenna was linearly polarized in the theta direction. Similarly, the calculated gain is based on E_θ . The dipole length is $\lambda/2$ and the radius is 0.005λ .

In the reaction calculation, only vertical modes were employed to approximate the current distribution. The number of modes used to obtain the results given in Figs. 37 through 53 are listed below. In each case, the matrix size is equal to the number of modes.

<u>Figs.</u>	<u>Number of Modes</u>
37,38	45
39,40	55
41,42	75
43,44	30
46-53	61

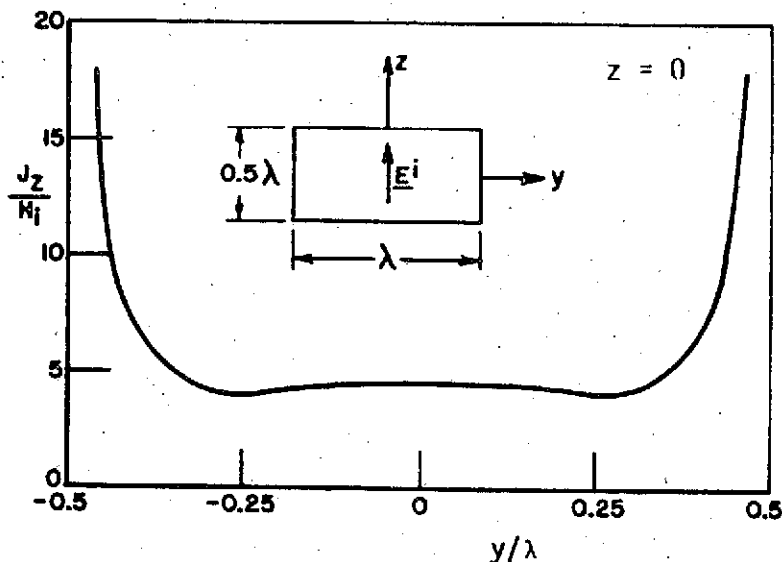


Fig. 37--Magnitude of surface-current density induced on a perfectly-conducting rectangular plate for a plane wave incident at broadside.

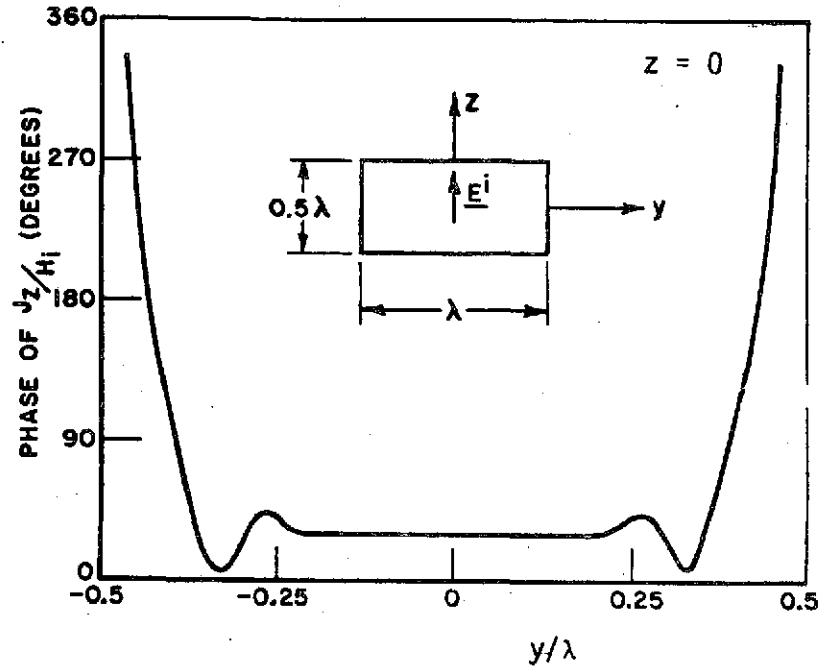


Fig. 38--Phase of surface-current density induced on a rectangular plate for a plane wave incident at broadside.

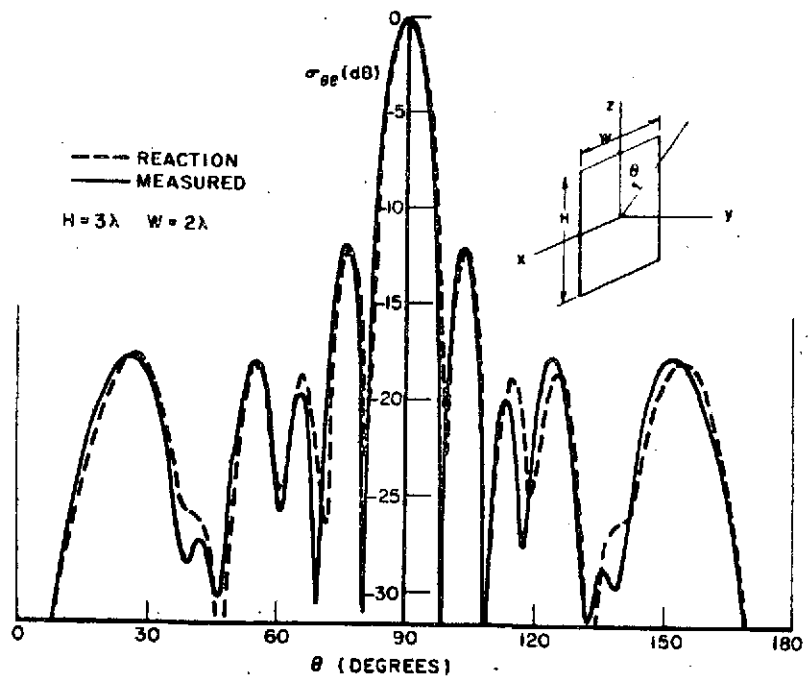


Fig. 39--Normalized backscatter cross-section in the yz plane of a rectangular plate. $\sigma_{\theta\theta}(\theta, \phi) = 15.25$ dB at $(90^\circ, 90^\circ)$.

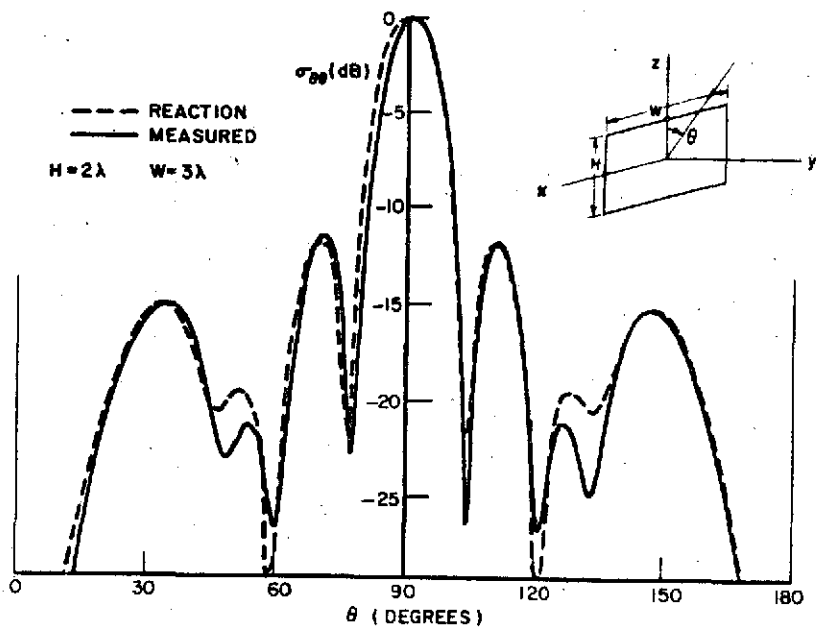


Fig. 40--Normalized backscatter cross-section in the yz plane of a rectangular plate. $\sigma_{\theta\theta}(\theta, \phi) = 15.23$ dB at $(90^\circ, 90^\circ)$.

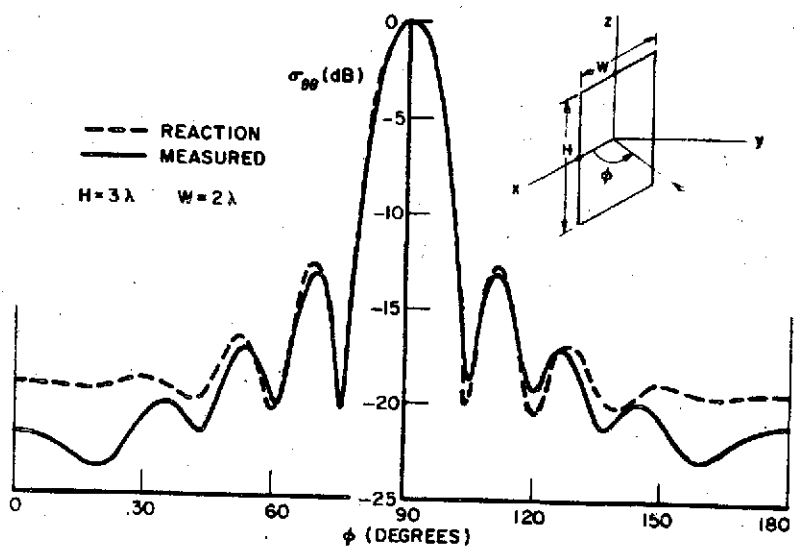


Fig. 41--Normalized backscatter cross-section in the xy plane of a rectangular plate. $\sigma_{\theta\theta}(\theta, \phi) = 15.25$ dB at $(90^\circ, 90^\circ)$.

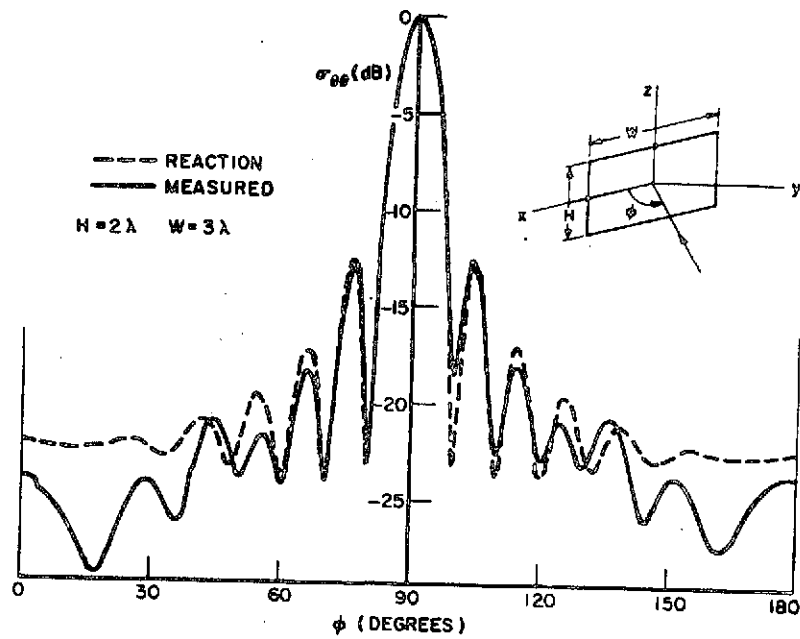


Fig. 42--Normalized backscatter cross-section in the xy plane of a rectangular plate. $\sigma_{\theta\theta}(\theta, \phi) = 15.23$ dB at $(90^\circ, 90^\circ)$.

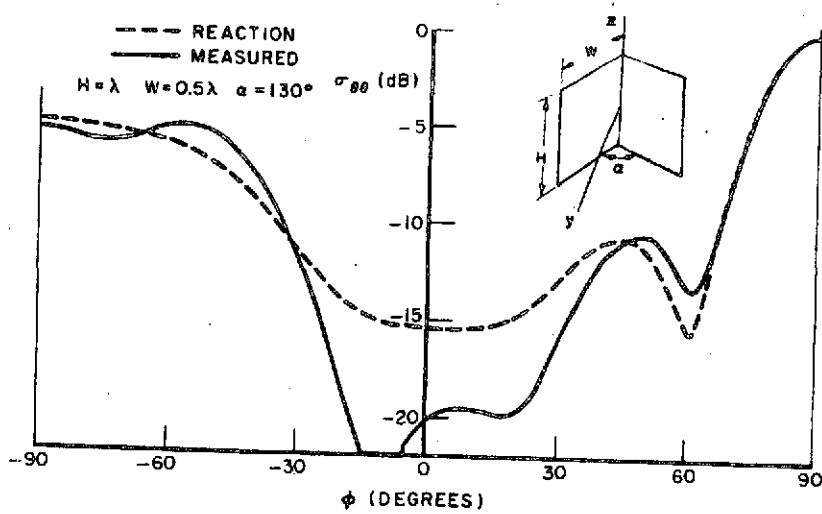


Fig. 43--Normalized backscatter cross-section in the xy plane of a corner reflector. $\sigma_{\theta\theta}(\theta, \phi) = -0.38$ dB at $(90^\circ, 90^\circ)$.

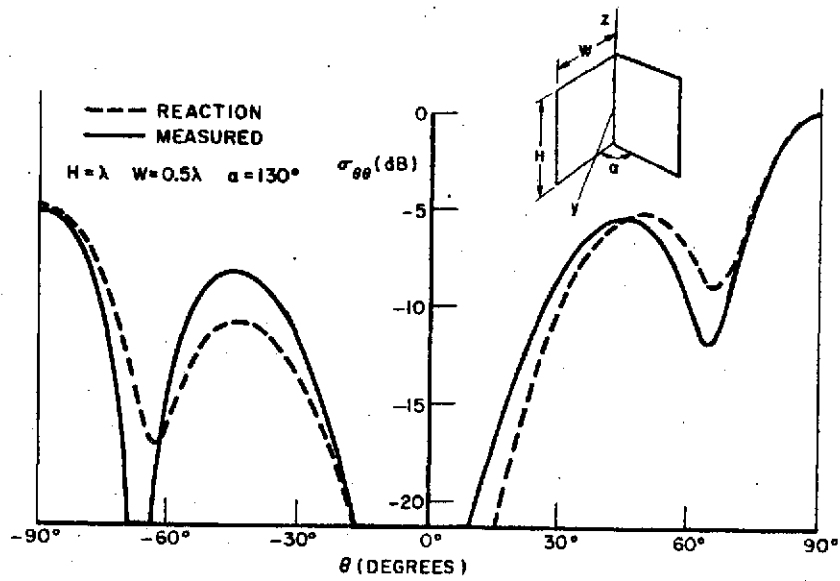


Fig. 44--Normalized backscatter cross-section in the yz plane of a corner reflector. $\sigma_{\theta\theta}(\theta, \phi) = -0.38$ dB at $(90^\circ, 90^\circ)$.

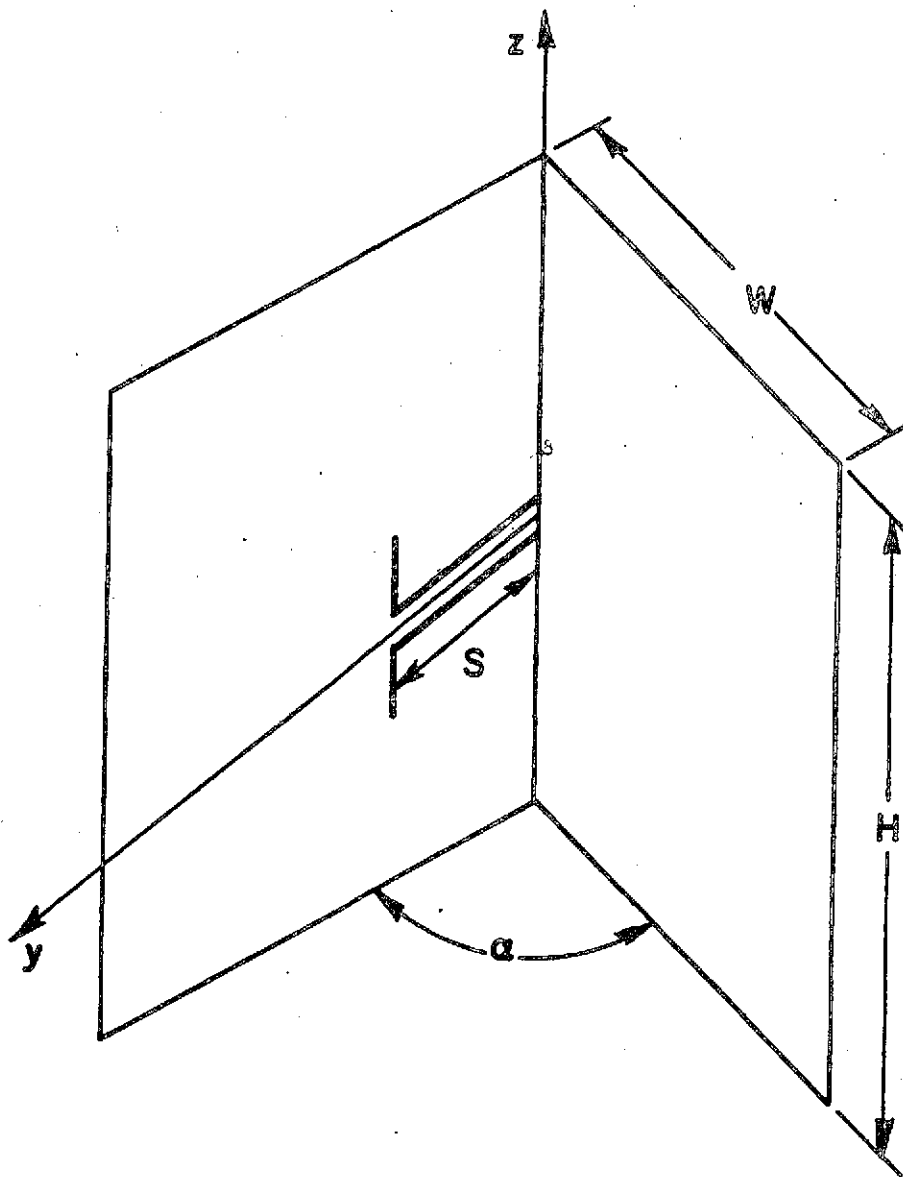


Fig. 45--Corner-reflector antenna.

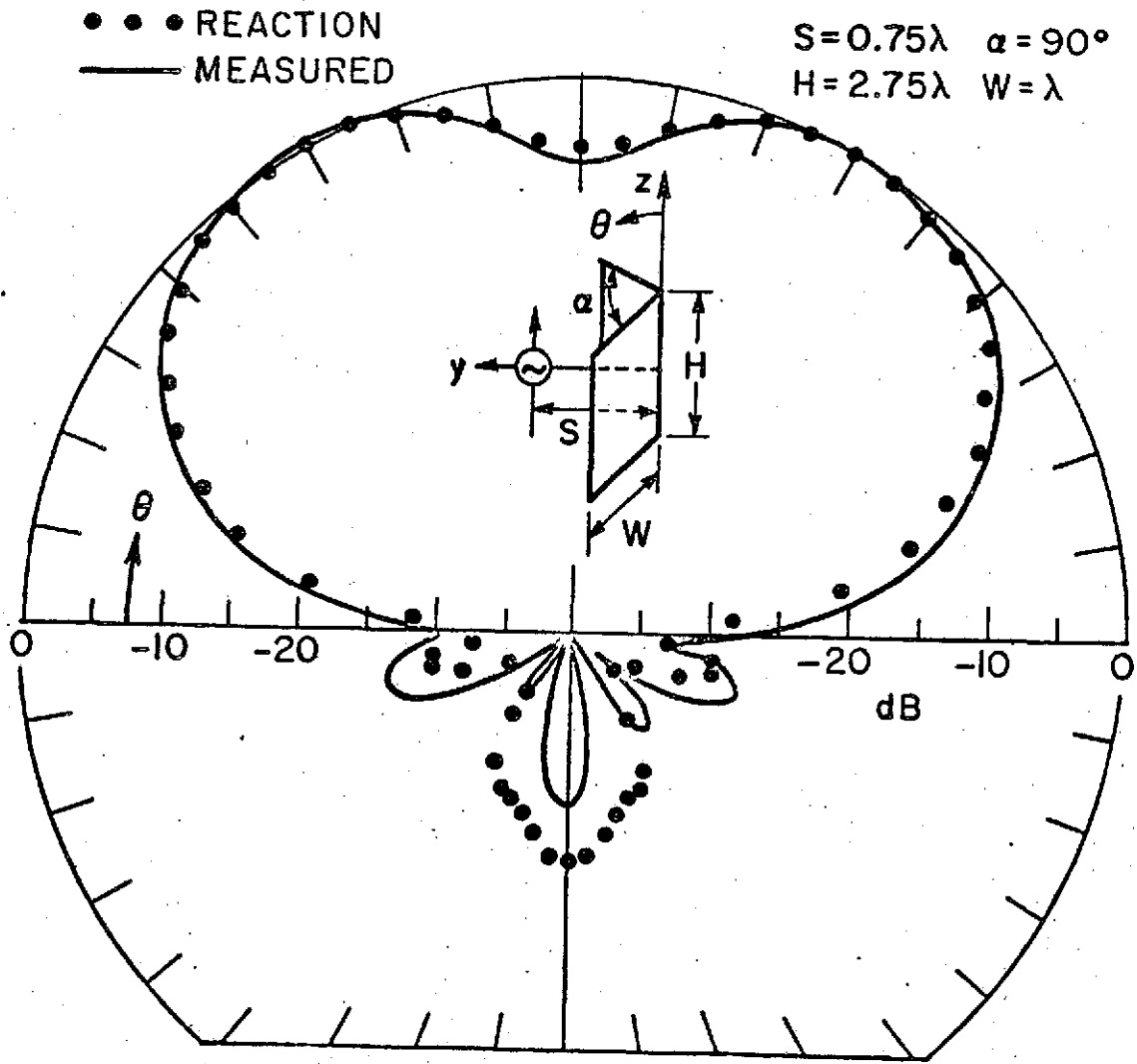


Fig. 46--Relative gain in the E-plane of a corner-reflector antenna. $G(\theta, \phi) = 4.31$ dB at $(90^\circ, 90^\circ)$.

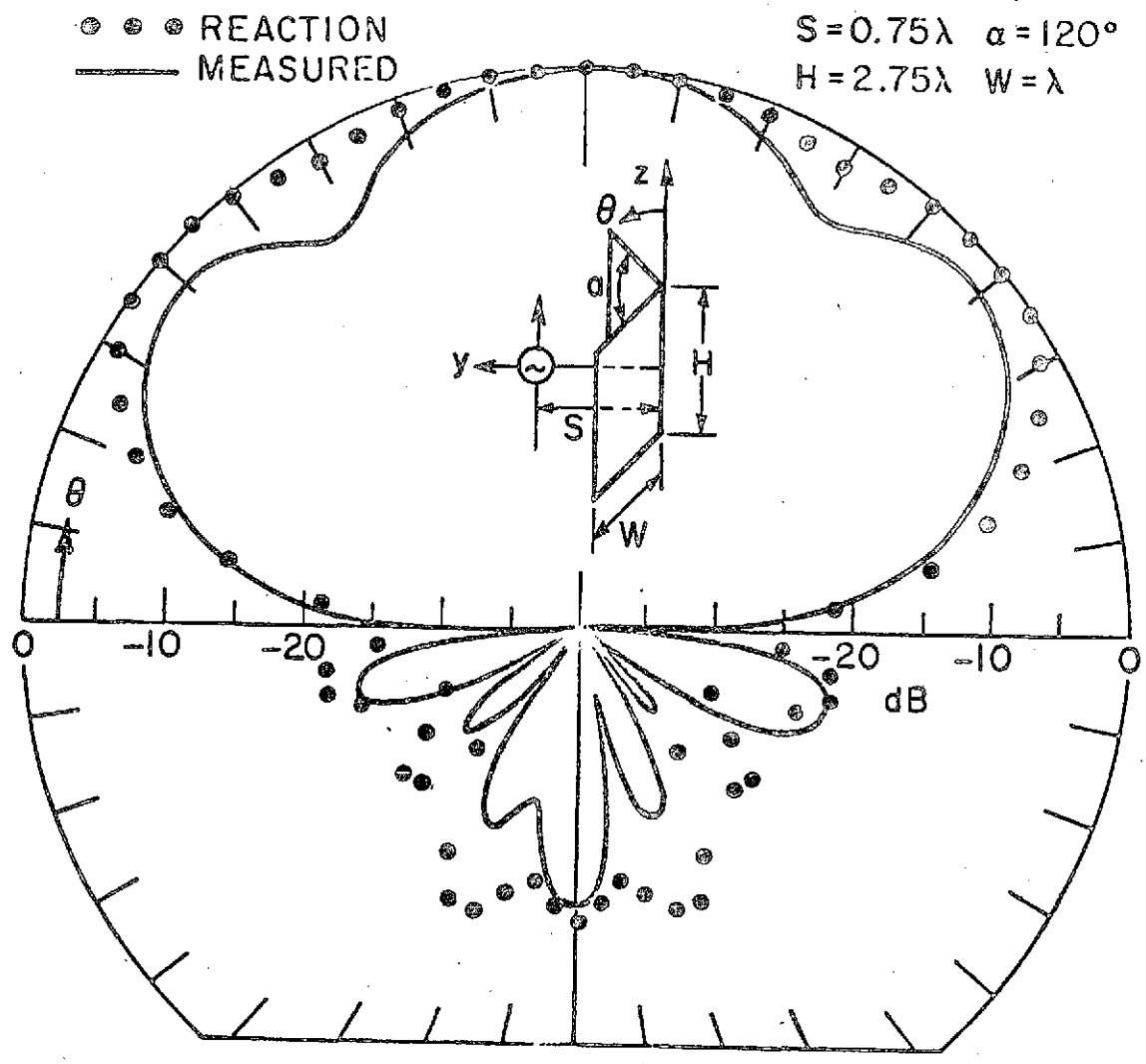


Fig. 47--Relative gain in the E-plane of a corner-reflector antenna. $G(\theta, \phi) = 4.05$ dB at $(90^\circ, 90^\circ)$.

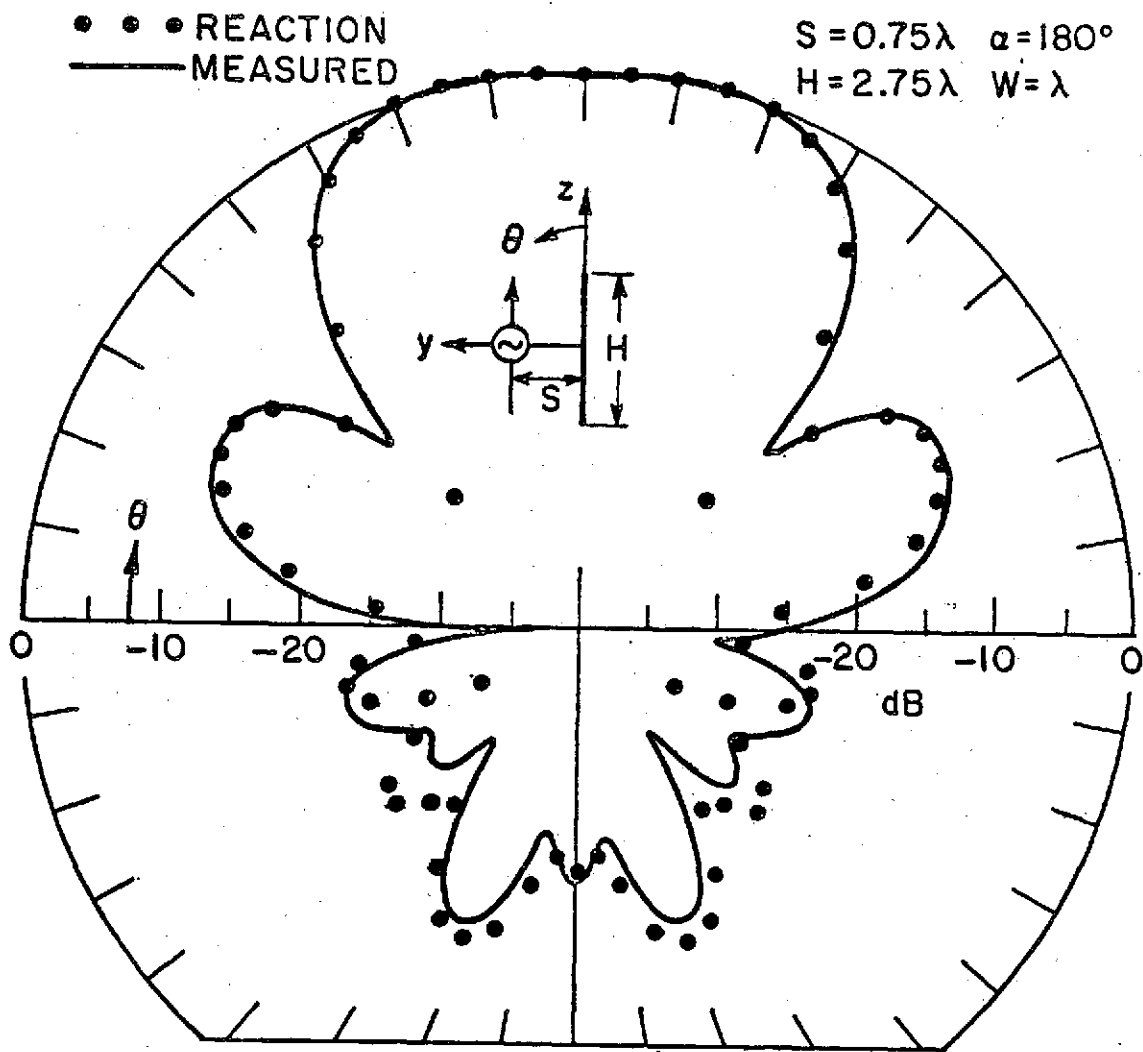


Fig. 48--Relative gain in the E-plane of a corner-reflector antenna. $G(\theta, \phi) = 7.48$ dB at $(90^\circ, 90^\circ)$.

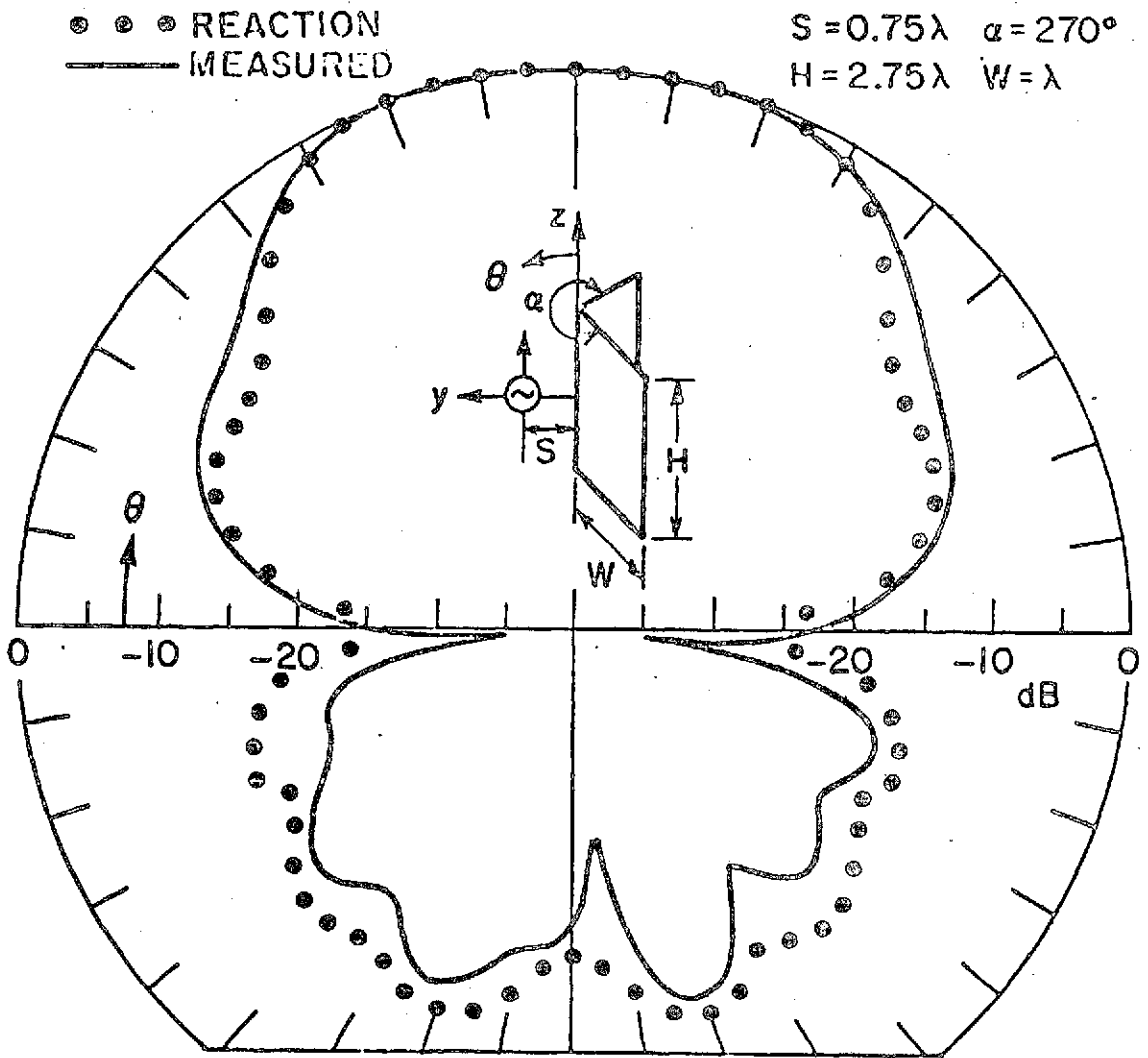


Fig. 49--Relative gain in the E-plane of a corner-reflector antenna. $G(\theta, \phi) = -1.06$ dB at $(90^\circ, 90^\circ)$.

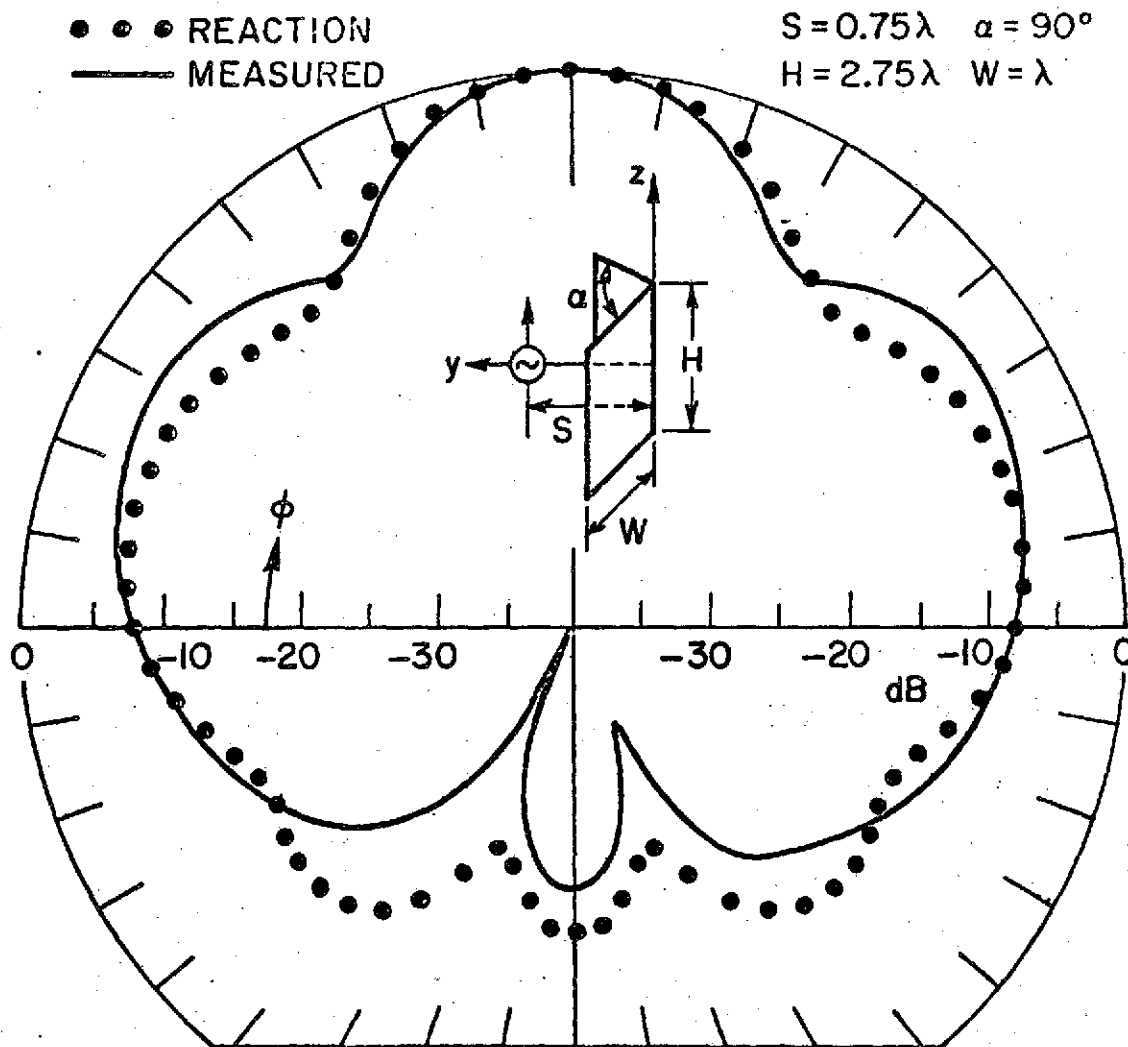


Fig. 50--Relative gain in the H-plane of a corner-
 reflector antenna. $G(\theta, \phi) = 4.31$ dB at
 $(90^\circ, 90^\circ)$.

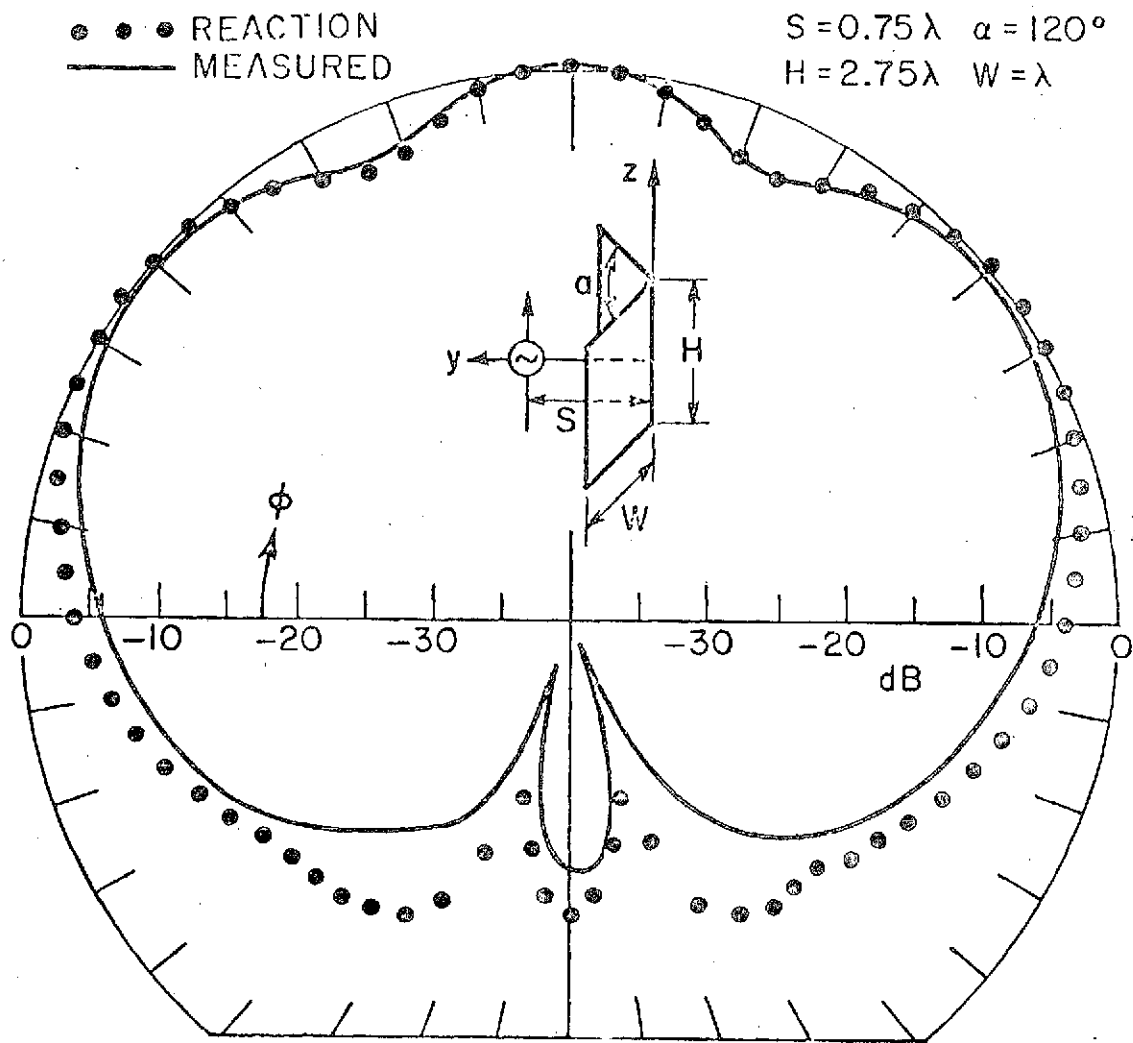


Fig. 51--Relative gain in the H-plane of a corner-reflector antenna. $G(\theta, \phi) = 4.05$ dB at $(90^\circ, 90^\circ)$.

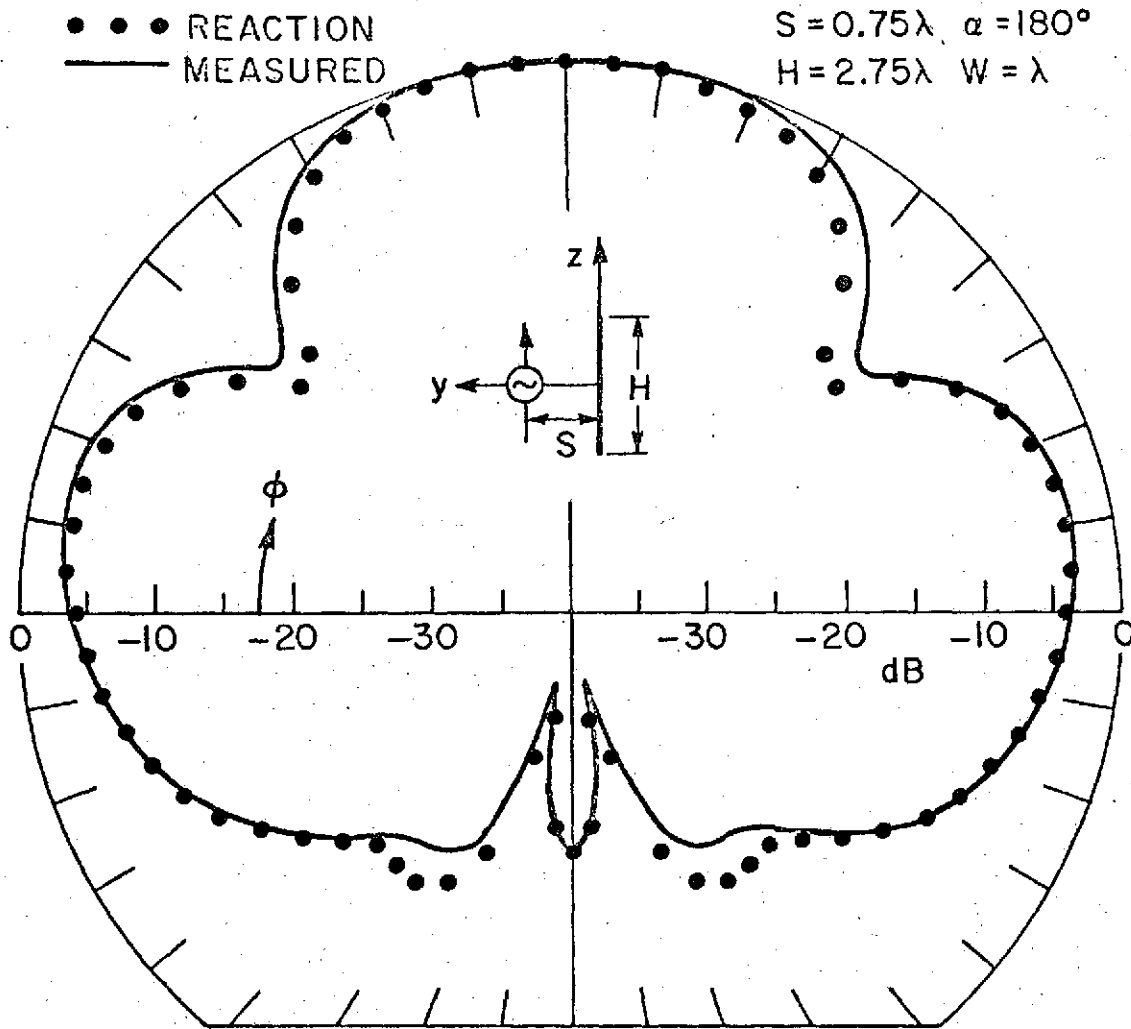


Fig. 52--Relative gain in the H-plane of a corner-reflector antenna. $G(\theta, \phi) = 7.48$ dB at $(90^\circ, 90^\circ)$.

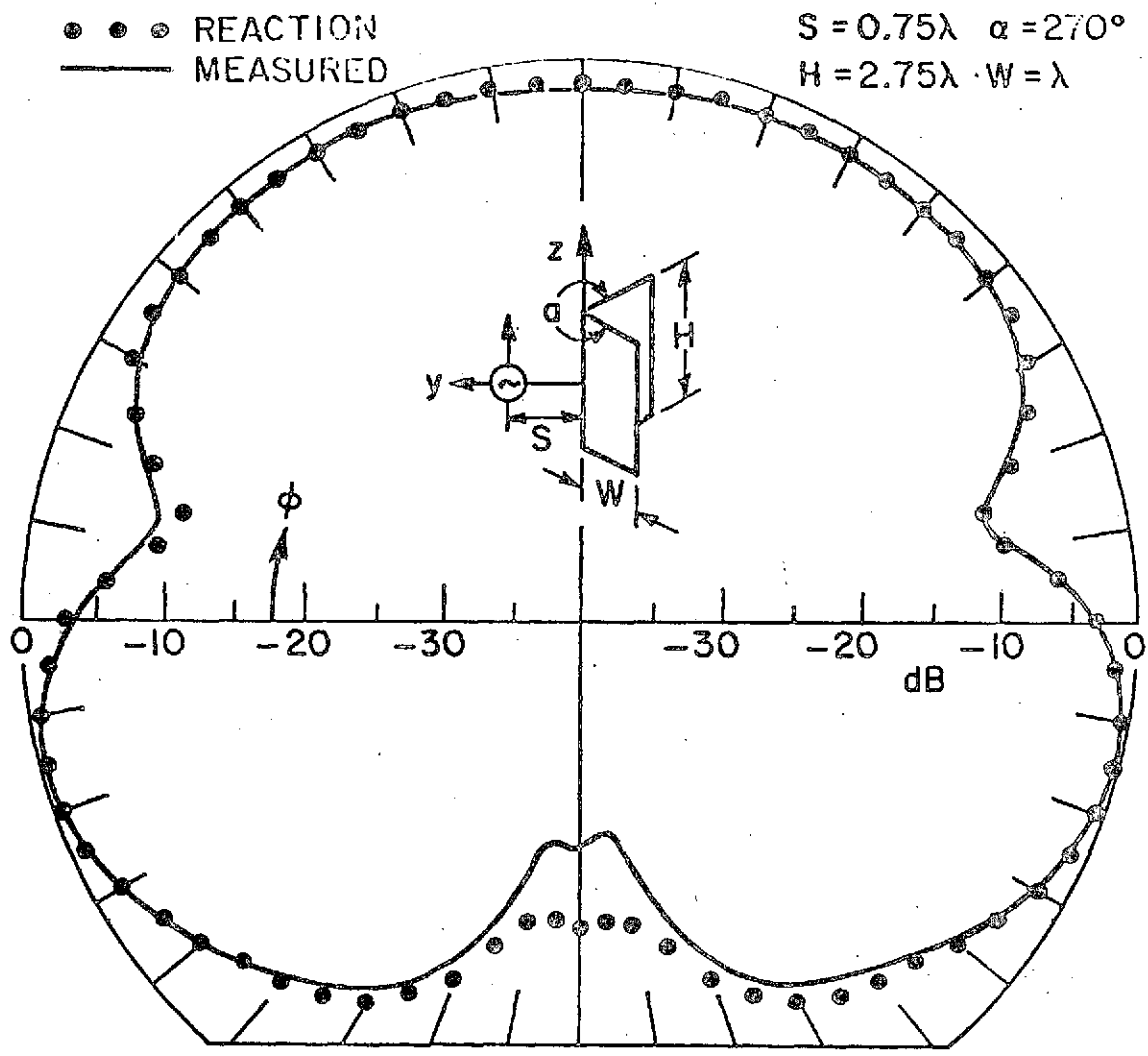


Fig. 53--Relative gain in the H-plane of a corner-reflector antenna. $G(\theta, \phi) = -1.06$ dB at $(90^\circ, 90^\circ)$.

CHAPTER IX SUMMARY AND DISCUSSIONS

The reaction concept and Galerkin's method are employed to develop an integral-equation formulation for radiation and scattering from perfectly-conducting plates, corner reflectors and dielectric-coated conducting cylinders.

For the two-dimensional problems, the contour of the cylinder is divided into segments and the surface-current density on the conducting surface is expanded with sinusoidal bases for the TE polarization and rectangular-pulse bases for the TM polarization. Reaction tests are enforced with electric test sources. This reaction-Galerkin technique yields accurate results for scattering by cylinders with as few as five segments per wavelength. Furthermore, this technique provides a symmetric impedance matrix in the matrix equation. The point-matching procedure, on the other hand, generates an unsymmetric impedance matrix and requires on the order of ten segments per wavelength to yield accurate results.

For a coated cylinder, the dielectric layer is modeled with the equivalent polarization current radiating in free space. Maxwell's equations and the boundary conditions are employed to express the polarization-current distribution in terms of the surface-current density on the conducting surface. The impedance matrix has the same size for an uncoated cylinder and a cylinder with a thin dielectric coating. It is found that the polarization-current model is more accurate than the popular surface-impedance model.

For the three-dimensional problems, a new model that involves dividing the conducting surface into cells, expanding the current distribution with subsectional bases and enforcing reaction tests with electric surface dipoles is developed and applied to the problems of radiation and scattering from perfectly-conducting rectangular plates and corner reflectors up to six square wavelengths in size. For arbitrary aspect and polarization, this sinusoidal-Galerkin technique yields good results for scattering by a one-wavelength square plate with an 18 x 18 matrix. For this same problem, the wire-grid model (and the surface-cell model with pulse bases and collocation) requires a matrix size of 60 x 60. Thus, the new surface-current model offers a substantial improvement in computer storage requirements. This model can also be applied to nonplanar surfaces provided that the general surface is approximated by a set of planar cells. In this case, the cells may have to be reduced in size to obtain a satisfactory fit. This will increase the number of cells employed for modeling, thereby limiting the application of this model for nonplanar surfaces. However, extensions can be made such that the individual cell is doubly-curved in nature, and integration techniques can

be developed for evaluating the reaction between these curved cells. With this extension, the problem of radiation and scattering from curved surfaces can be analyzed more efficiently, and bodies with surface areas up to ten square wavelengths may be analyzed. For problems involving more complicated geometry, such as antennas mounted on aircraft, a combination of planar and curved cells can be employed to model the aircraft surfaces.

REFERENCES

1. Mei, K. K. and Van Bladel, J. G., "Scattering by Perfectly-Conducting Rectangular Cylinders," IEEE Trans., Vol. AP-11, March 1963, pp. 185-192.
2. Andreasen, M. G., "Scattering from Parallel Metallic Cylinders With Arbitrary Cross Sections," IEEE Trans., Vol. AP-12, November 1964, pp. 746-754.
3. Mullin, C. R., Sandburg, R. and Velline, C. O., "A Numerical Technique for the Determination of Scattering Cross Sections of Infinite Cylinders of Arbitrary Geometrical Cross Section," IEEE Trans., Vol. AP-13, January 1965, pp. 141-149.
4. Richmond, J. H., "Scattering by an Arbitrary Array of Parallel Wires," IEEE Trans., Vol. MTT-13, July 1965, pp. 408-412.
5. Wallenberg, R. F. and Harrington, R. F., "Radiation From Apertures in Conducting Cylinders of Arbitrary Cross Section," IEEE Trans., Vol. AP-17, January 1969, pp. 56-62.
6. Shafai, L., "An Improved Integral Equation for the Numerical Solution of Two-Dimensional Diffraction Problems," Canadian Journal of Physics, Vol. 48, 1970, pp. 954-963.
7. Bennett, C. L. and Weeks, W. L., "Transient Scattering from Conducting Cylinders," IEEE Trans., Vol. AP-18, September 1970, pp. 627-633.
8. Wilton, D. R. and Mittra, Raj, "A New Numerical Approach to the Calculation of Electromagnetic Scattering Properties of Two-Dimensional Bodies of Arbitrary Cross Section," IEEE Trans., Vol. AP-20, May 1972, pp. 310-317.
9. Richmond, J. H., "An Integral-Equation Solution for TE Radiation and Scattering from Conducting Cylinders," Report 2902-7, October 1972, ElectroScience Laboratory, Department of Electrical Engineering, The Ohio State University; prepared under Grant NGL 36-008-138 for NASA, Langley Research Center, Hampton, Virginia 23364.
10. Richmond, J. H., "A Wire-Grid Model for Scattering by Conducting Bodies," IEEE Trans., Vol. AP-14, November 1966, pp. 782-786.
11. Oshiro, F. K., "Source Distribution Technique for the Solution of General Electromagnetic Scattering Problems," Proc. First GISAT Symposium, Vol. 1, Part 1, Mitre Corporation, 1965.

12. Knepp, D. L., "Numerical Analysis of Electromagnetic Radiation Properties of Smooth Conducting Bodies of Arbitrary Shape in The Presence of Known External Sources," Ph.D. Dissertation, University of Pennsylvania, 1971.
13. Rumsey, V. H., "Reaction Concept in Electromagnetic Theory," Physical Review, Vol. 94, June 15, 1954, pp. 1483-1491.
14. Richmond, J. H., "Radiation and Scattering by Thin-Wire Structures in the Complex Frequency Domain," Report 2902-10, July 1973. ElectroScience Laboratory, Department of Electrical Engineering, The Ohio State University.
15. Schelkunoff, S. A., "On Diffraction and Radiation of Electromagnetic Waves," Physical Review, Vol. 56, August 15, 1969.
16. Rhodes, D. R., "On the Theory of Scattering by Dielectric Bodies," Report 475-1, July 1953, ElectroScience Laboratory, Department of Electrical Engineering, The Ohio State University; prepared under Contract AF 18(600)-19 for Wright Air Development Center, Wright-Patterson Air Force Base, Ohio (AD-18279).
17. Harrington, R. F., Field Computation by Moment Methods, The MacMillan Company, New York, 1968, pp. 18-19.
18. Kouyoumjian, R. G., "The Calculation of the Echo Area of Perfectly Conducting Objects by the Variational Method," Ph.D. Dissertation, The Ohio State University, 1953.

APPENDIX A

ELECTRIC FIELD INDUCED IN THE THIN DIELECTRIC LAYER COATED ON A PERFECTLY-CONDUCTING POLYGON CYLINDER ILLUMINATED BY AN INCIDENT PLANE WAVE

Consider a dielectric-coated, perfectly-conducting polygon cylinder illuminated by an incident plane wave as shown below. The dielectric layer is a source-free region and has a thickness of d and a dielectric constant ϵ . The segment length of the cylinder is denoted by l . Define a coordinate system such that $\hat{z} \times \hat{t} = \hat{z}$,

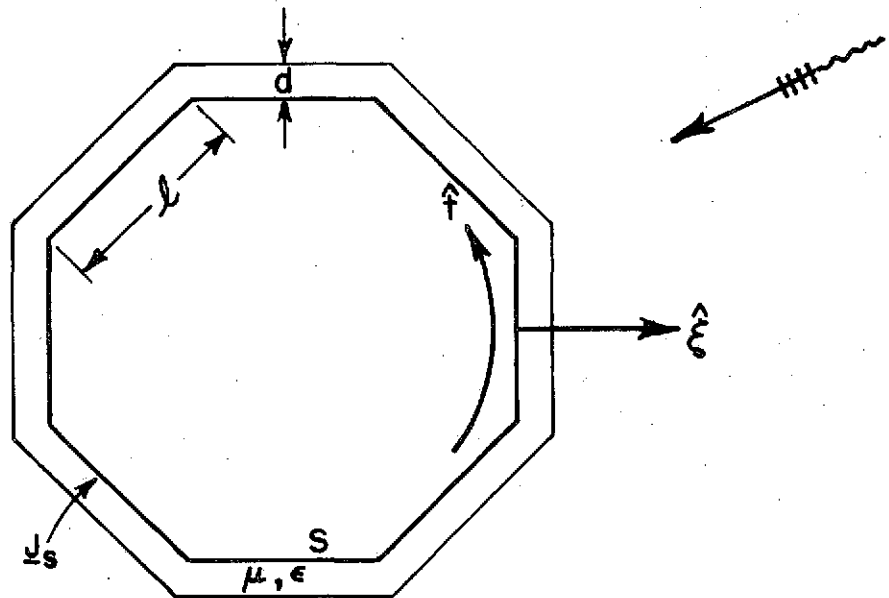


Fig. 54--Dielectric-coated, perfectly-conducting polygon cylinder illuminated by an incident plane wave.

where \hat{t} is a unit vector tangent to the conducting surface and \hat{z} is a unit vector normal to the conducting surface. The incident plane wave is either transverse-electric or transverse-magnetic with respect to \hat{z} -axis.

For a perfectly-conducting cylinder with a thin dielectric coating ($d/l \ll 1$), the magnetic field inside the dielectric layer can be expressed as follows:

$$(103) \quad \underline{H} = \underline{H}_S \cos(\beta\zeta)$$

where \underline{H}_S is the magnetic field induced on the conducting surface S and is related to the surface-current density \underline{J}_S by

$$(104) \quad \underline{H}_S = \underline{J}_S \times \hat{\zeta}.$$

Coordinate ζ measures the distance normally outward from the conducting surface and β is the transverse propagation constant in the dielectric region which can be determined from the wave equation. From Eqs. (103) and (104) and Maxwell's equations, the electric field inside the dielectric layer can be given as

$$(105) \quad \underline{E} = \frac{1}{j\omega\epsilon} \nabla \times [(\underline{J}_S \times \hat{\zeta}) \cos(\beta\zeta)].$$

For the transverse-magnetic incidence case, the surface current density has only a \hat{z} -component $\underline{J}_S = \hat{z} J_S(t)$ and $\beta = k_1 = k\sqrt{\epsilon_r}$. From Eq. (105), it can be shown that

$$(106) \quad \underline{E} = \frac{-k_1}{j\omega\epsilon} \sin(k_1\zeta) \underline{J}_S \quad (\text{TM case})$$

For transverse-electric case, the surface-current density has only a \hat{t} -component $\underline{J}_S = \hat{t} J_S(t)$ and $\beta = k_\zeta = k\sqrt{\epsilon_r - 1}$. For this case, Eq. (105) yields

$$(107) \quad \underline{E} = \frac{1}{j\omega\epsilon} [(\hat{z} \times \underline{J}_S') \cos(k_\zeta\zeta) + k_\zeta \sin(k_\zeta\zeta) \underline{J}_S].$$

If $k_\zeta\zeta \ll 1$, Eq. (107) reduces to

$$(108) \quad \underline{E} = \frac{1}{j\omega\epsilon} \cos(k_\zeta\zeta) (\hat{z} \times \underline{J}_S') \quad (\text{TE case})$$

where \underline{J}_S' is the derivative of the surface-current density.

APPENDIX B
COMPUTER PROGRAMS FOR RADIATION AND SCATTERING
FROM TM DIELECTRIC-COATED CYLINDERS

```

INCLUDE CROUTB,2902W
COMPLEX C(40,40),ZS,CJ(40)
COMPLEX EJ,EJJ,CST,EM,EJE
DIMENSION X(40),Y(40),D(40),IA(40),IB(40)
COMMON/COA/CCC,ER2,TSK2L
DATA IDM,INT/40,10/
DATA PI,TP/3.14159,6.28318/
WRITE(1,998)
998  FORMAT(5X,'LDP=?,ZS=?/')
     READ(0,-) LDP,ZS
10   CONTINUE
     WRITE(1,999)
999  FORMAT(5X,'NCASE=? 1=RECTANGULAR,2=CIRCULAR,3=STRIP/')
     READ(0,-) NCASE
     WRITE(1,997)
     READ(0,-) PHI,DPH,BSC
     GO TO (400,500,300),NCASE
300  CONTINUE
     PHI=90.
     READ(0,-) WK,NM,TSL,ER2
     TSK2L=TSL*TP*SQRT(ER2)
     CCC=(ER2-1.)/ER2*(1.-COS(TSK2L))
     WRITE(6,4) WK
     WK=WK*2.
     NP=NM+1
     DX=WK/NM
     DO 1 I=1,NP
     Y(I)=.0
     X(I)=DX*(I-1)
1    CONTINUE
     DO 2 J=1,NM
     IA(J)=J
     IB(J)=J+1
     D(J)=DX
     CJ(J)=CMPLX(2.*PI/DX,.0)
2    CONTINUE
     GO TO 600
500  CONTINUE
     PHI=.0
     PHR=PHI*PI/180.
     CPH=COS(PHR)
     SPH=SIN(PHR)
     CST=TP/(-30.*(.707,-.707))
     READ(0,-) DL,TSL,ER2,XKS
     WRITE(6,4) DL,TSL,ER2

```

```

CC      TSK2L=TSL*TP*SQRT(ER2)
        CCC=(ER2-1.)/ER2*(1.-COS(TSK2L))
CC
        NM=12+20.*DL
        IF(NM.LT.16) NM=16
        WRITE(1,-)NM
        NP=NM
        PHO=TP/NM
        BL=.5*(PI*DL/NM)/SIN(.5*PHO)
        DO 11 I=1,NM
        X(I)=TP*BL*COS(PHO*(I-1))
        Y(I)=TP*BL*SIN(PHO*(I-1))
        IA(I)=1
        IB(I)=I+1
        IF(I.EQ.NM) IB(I)=1
        D(I)=TP*BL*2.*SIN(.5*PHO)
11      CONTINUE
        GO TO 80
400     CONTINUE
997     FORMAT(5X,'PHI,DPH,BSC=?,BSC>0. **YES/ ')
        IF(LOP.EQ.2) READ(0,-) XKS,YKS
        IF(LOP.EQ.2) WRITE(6,4)XKS,YKS
        PHR=PHI*PI/180.
        CPH=COS(PHR)
        SPH=SIN(PHR)
        CST=TP/(-30.*( .707,-.707))
        READ(0,-) AX,BY,TSL,ER2
        WRITE(6,4) AX,BY,TSL,ER2
        TSK2L=TSL*TP*SQRT(ER2)
        CCC=(FR2-1.)/FR2*(1.-COS(TSK2L))
        CALL REC(AX,BY,IDM,NM,NP,X,Y,IA,IB)
        DO 260 I=1,NM
        X(I)=TP*X(I)
        Y(I)=TP*Y(I)
260     CONTINUE
        DO 45 J=1,NM
        K=IA(J)
        L=IB(J)
        D(J)=SQRT((X(L)-X(K))**2+(Y(L)-Y(K))**2)
45      CONTINUE
80      CONTINUE
        DO 22 I=1,NM
        KA=IA(I)
        KB=IB(I)
        IF(LOP.EQ.2) GO TO 33
        CALL CFF(X(KA),Y(KA),X(KB),Y(KB),D(I),CPH,SPH,ZS,EJ,EM,EJE)
        CJ(I)=EJ*CST/D(I)/D(I)
CCC
        GO TO 22

```

```

33  CONTINUE
    CALL CELS(X(KA),Y(KA),X(KB),Y(KB),XKS,YKS,D(I),INT,FJ)
    CJ(I)=EJ*TP*TP/D(I)/D(I)
    CJ(I)=CJ(I)/(-60.*PI)
CCC
    WRITE(6,4) CJ(I)
22  CONTINUE
600  CONTINUE
    ISYM=0
C
    RS=CABS(ZS)
    IF(RS.GT.0.) ISYM=1
C
CC   IF(TSL.GT.0.) ISYM=1
CC
    CALL CDANT(C,D,X,Y,ZS,IA,IB,ISYM,IDM,INT,NM,NP)
    IF(ISYM.EQ.10) GO TO 1000
    DO 3 I=1,1
    DO 3 J=1,NM
    WRITE(6,4) C(I,J)
4   FORMAT(5X,5F10.4/)
3   CONTINUE
    CALL CROUT(C,CJ,NM,IDM,ISYM,1,1)
    PH=0.0
    IF(BSC.GT.0.) PH=PHI
30  CONTINUE
    PHR=PH*PI/180.
    CPH=COS(PHR)
    SPH=SIN(PHR)
    EJJ=(.0,.0)
    DO 250 K=1,NM
    KA=IA(K)
    KB=IB(K)
    CALL CFF(X(KA),Y(KA),X(KB),Y(KB),D(K),CPH,SPH,
2ZS,FJ,FM,EJE)
    EJJ=EJJ+(EJ+EJE)*CJ(K)+EM*CJ(K)
250 CONTINUE
    IF(LOP.EQ.2) EJJ=EJJ+CEXP(CMPLX(.0,XKS*CPH+YKS*SPH+PI/4.))
    EAB=CABS(EJJ)
    FWL=2.*PI*EAB*EAB
    EWS=EWL*PI*2.
    WRITE(1,-) PH,EWL
    WRITE(6,4) PH,EWL,EAB
    PH=PH+DPH
    PHEND=360.
    IF(BSC.GT.0.) PHEND=PHI
    IF(PH.LE.PHEND) GO TO 30
1000 CONTINUE
    READ(0,-) IC
    IF(IC.EQ.0) GO TO 10
    CALL EXIT
    END

```

```

SUBROUTINE CDANT(C,D,X,Y,ZS,IA,IB,ISYM,IDM,INT,NM,NP)
COMPLEX ZS,P11,C(IDM,IDM)
DIMENSION X(IDM),Y(IDM),D(IDM),IA(IDM),IB(IDM)
DO 20 I=1,NM
DO 20 J=1,NM
20 C(I,J)=(.0,.0)
DMAX=.0
DO 25 J=1,NM
DK=D(J)
25 IF(DK.GT.DMAX) DMAX=DK
WRITE(I,-)DMAX
IF(DMAX.LT.3.) GO TO 30
ISYM=10
RETURN
30 CONTINUE
DO 200 K=1,NM
KA=IA(K)
KB=IB(K)
DK=D(K)
LL=1
IF(ISYM.EQ.0) LL=K
DO 200 L=LL,NM
LA=IA(L)
LB=IB(L)
DL=D(L)
IF(K.EQ.L) GO TO 120
IND=(LA-KA)*(LB-KA)*(LA-KB)*(LB-KB)
IF(IND.EQ.0) GO TO 80
C
CALL ZMMC(X(KA),Y(KA),X(KB),Y(KB),X(LA),Y(LA),X(LB),Y(LB),
ZS,DK,DL,INT,P11)
GO TO 168
80 CONTINUE
JM=KB
JC=KA
IND=(KB-LA)*(KB-LB)
IF(IND.NE.0) GO TO 82
JC=KB
JM=KA
82 JP=LA
IF(LB.EQ.JC) GO TO 83
JP=LB
83 CALL ZMMB(X(JM),Y(JM),X(JC),Y(JC),X(JP),Y(JP),ZS,DK,DL,INT,P11)
GO TO 168
120 CALL ZMMA(DK,ZS,P11)
168 C(K,L)=P11
200 CONTINUE
RETURN
END

```



```

SUBROUTINE ZMMA(DK,ZS,P11)
COMPLEX ZS,H0,H1,VH,G1,Y,P11
COMMON/COA/CCC,ER2,TSK2L
DATA PI/3.14159/
TP=2.*PI
ETA=120.*PI
CALL HANK(DK,H0,H1,1)
G1=VH(DK)
D=DK/TP
P11=D/(2.*TP)*G1-1./((2.*TP*TP)*(DK*H1-(.0,2.)/PI)
P11=P11*TP*ETA/D/D
Y=P11*2./ETA
CC
P11=P11+P11*CCC
CC
C
P11=P11+ZS*PI/DK
C
RETURN
END
SUBROUTINE ZMMP(X1,Y1,X2,Y2,X3,Y3,ZS,
2DK1,DK2,INT,Q11)
COMPLEX VH,ZS,Q11,Y11,CCP,G1,G2,G12,
2H10,H11,H20,H21,H120,H121,HPC,HP1,HMO,HM1
COMPLEX DQ11P,DQ11M,RKH1P,RKH1M,DQ11,DCNT
COMMON/COA/CCC,ER2,TSK2L
DATA CCP/(.0,.63662)/
DATA PI/3.14159/
RS=CABS(ZS)
CBET=(X2-X1)/DK1
SBET=(Y2-Y1)/DK1
XB=(X3-X1)*CBET+(Y3-Y1)*SBET
YB=-(X3-X1)*SBET+(Y3-Y1)*CBET
CAL=(XE-DK1)/DK2
SAL=ABS(YB/DK2)
AL=ATAN2(SAL,CAL)
CNT=15.*4.*PI*PI/DK2/DK1
DK12=DK1+DK2
IF(CAL.LT.0.) GO TO 20
IF(SAL.GT.0.04) GO TO 20
CALL HANK(DK1,H10,H11,1)
CALL HANK(DK2,H20,H21,1)
DK12=DK1+DK2
CALL HANK(DK12,H120,H121,1)
G1=VH(DK1)
G2=VH(DK2)
G12=VH(DK12)
Q11=CNT*(-CCP+DK1*(H11-G1)+DK2*(H21-G2)-DK12*(H121-G12))
CC
Q11=Q11+Q11*CCC
CC

```

```

RETURN
20 CONTINUE
INP=2*(INT/2)
IP=INP+1
JP=IP
FIT=INP
ALT=AL/2.
CALT=COS(ALT)
SALT=SIN(ALT)
RCP=DK12*CALT
RSP=(DK2-DK1)*SALT
PHC=ATAN2(RSP,RCP)
SGI=-1.
PHM=-ALT
PHP=PHC
DPHM=(PHC+ALT)/FIT
DPHP=(ALT-PHC)/FIT
Y11=(.0,.0)

C
DQ11=(.0,.0)

C
DO 200 I=1,JP
D=SGI+3.
IF(I.EQ.1.OR.I.EQ.IP) D=1.
SAP=SIN(ALT+PHP)
SAM=SIN(ALT-PHM)
ARGP=DK2*SAL/SAP
ARGM=DK1*SAL/SAM
CALL HANK(ARGP,HPO,HP1,1)
CALL HANK(ARGM,HMO,HM1,1)

C
IF(RS.LE.0.) GO TO 300
DARGP=ARGP/FIT
DARGM=ARGM/FIT
RKP=.0
RKM=.0
SGJ=-1.
DQ11P=(.0,.0)
DQ11M=(.0,.0)
RKH1P=CCP
RKH1M=CCP
DO 100 J=1,JP
C=SGJ+3.
IF(J.EQ.1.OR.J.EQ.JP) C=1.
IF(J.EQ.1) GO TO 94
CALL HANK(RKP,H10,H11,1)
CALL HANK(RKM,H20,H21,1)
RKH1P=RKP*H11
RKH1M=RKM*H21

```

```

04  CONTINUE
    DQ11P=DQ11P+RKHIP*C
    DQ11M=DQ11M+RKH1M*C
    RKP=RKP+DARGP
    RKM=RKM+DARGM
    SGJ=-SGJ
100  CONTINUE
    DQ11=DQ11+SAM*(DQ11P*DARGP*DPHP+DQ11M*DARGM*DPHM)*D
300  CONTINUE
C
    Y11=Y11+(ARGM*HM1*DPHM+ARGP*HP1*DPHP)*D
    PHM=PHM+DPHM
    PHP=PHP+DPHP
    SGI=-SGI
200  CONTINUE
    Q11=CNT*(Y11/3./SAL-CCP*AL/SAL)
CC
    Q11=Q11+Q11*CCC
CC
C
    DCNT=ZS*CMPLX(.0,-2.*PI)/(4.*DK1*DK2*SAL)
    DQ11=DQ11*DCNT/9.
    Q11=Q11+DQ11
C
    RETURN
    END
    SUBROUTINE ZMMC(X1,Y1,X2,Y2,X3,Y3,X4,Y4,ZS,
2DK1,DK2,INT,P11)
    COMPLEX P11,G3,G13,G23,G123,VH,HA0,HA1,HBO,HB1,HCO,HC1,HDO,HD1,
    COMPLEX HX,HY,DP11,DCNT
    COMPLEX HO,H1
    COMMON/COA/CCC,ER2,TSK2L
    DATA PI/3.14159/
    RS=CABS(ZS)
    CBET=(X2-X1)/DK1
    SBET=(Y2-Y1)/DK1
    XA=(X3-X1)*CBET+(Y3-Y1)*SBET
    XB=(X4-X1)*CBET+(Y4-Y1)*SBET
    YA=- (X3-X1)*SBET+(Y3-Y1)*CBET
    YB=- (X4-X1)*SBET+(Y4-Y1)*CBET
    CAL=(XB-XA)/DK2
    SAL=(YB-YA)/DK2
    CNT=15.*4.*PI*PI/DK1/DK2
    ASAL=ABS(SAL)
    IF(ASAL.GT..04) GO TO 20
    IF(YB.NE..0) GO TO 20
    DK3=ABS(XA-DK1)
C

```

```

IF(XA.LT.0.0) DK3=ABS(XB)
C
DK13=DK1+DK3
DK23=DK2+DK3
DK123=DK1+DK2+DK3
CALL HANK(DK3 ,HA0,HA1,1)
CALL HANK(DK13 ,HB0,HB1,1)
CALL HANK(DK23 ,HC0,HC1,1)
CALL HANK(DK123,HDC,HD1,1)
G3=VH(DK3)
G13=VH(DK13)
G23=VH(DK23)
G123=VH(DK123)
P11=CNF*(DK3*(G3-HA1)-DK13*(G13-HB1)-DK23*(G23-HC1)+DK123*
2(G123-HD1))
CC
P11=P11+P11*CCC
CC
RETURN
20 CONTINUE
RMIN=10000.
X=XA
Y=YA
DX=DK2*CAL/4.
DY=DK2*SAL/4.
DO 40 J=1,5
YS=.0
R=ABS(Y)
IF(R.GT.1.E-15)YS=Y*Y
XS=0.0
XAB=ABS(X-DK1)
IF(XAB.GT.1.E-15) XS=XAB*XAB
IF(X.LT.0.) R=SQRT(X*X+YS)
IF(X.GT.DK1) R=SQRT(XS+YS)
IF(R.LT.RMIN) RMIN=R
X=X+DX
Y=Y+DY
40 CONTINUE
FNT=1+(4*INT)/10
ISS=FNT*DK1/RMIN
ISS=2*(ISS/2)
IF(ISS.LT.2) ISS=2
IF(ISS.GT.20) ISS=20
FSS=ISS
ISQ=ISS+1
DS=DK1/FSS
ITT=FNT*DK2/RMIN
ITT=2*(ITT/2)
IF(ITT.LT.2) ITT=2
IF(ITT.GT.20) ITT=20

```

```

FIT=ITT
ITQ=ITT+1
DT=DK2/FIT
DX=DT*CAL
DY=DT*SAL
X=XA
Y=YA
SGJ=-1.
P11=(.0,.0)
C
DP11=(.0,.0)
C
DO 200 J=1,ITQ
D=SGJ+3.
IF(J.EQ.1.OR.J.EQ.ITQ) D=1.
XP=.0
YS=.0
YAB=ABS(Y)
IF(YAB.GT.1.E-15) YS=YAB*YAB
EZ=(.0,.0)
C
HX=(.0,.0)
HY=(.0,.0)
C
SGI=-1.
DO 100 I=1,ISQ
C=SGI+3.
IF(I.EQ.1.OR.I.EQ.ISQ) C=1.
DELX=ABS(X-XP)
DXS=.0
IF(DELX.GT.1.E-15) DXS=DELX*DELX
RK=SQRT(DXS+YS)
C
SPH=Y/RK
CPH=(X-XP)/RK
C
CALL HANK(RK,H0,H1,0)
EZ=EZ+H0*C
XP=XP+DS
SGI=-SGI
C
IF(RS.LE.0.) GO TO 100
HX=HX+H1*(-SPH)*C
HY=HY+H1*CPH*C
C
100 CONTINUE
EZ=EZ*DS/3.
P11=P11+EZ*D
C
HX=HX*DS/3.
HY=HY*DS/3.
DP11=DP11+(HX*CAL+HY*SAL)*D

```

```

C      SGJ=-SGJ
      X=X+DX
      Y=Y+DY
200  CONTINUE
      P11=P11*DT/3.
      P11=P11*CNT
CC
      P11=P11+P11*CCC
CC
C      DCNT=ZS*CMPLX(.0,-2.*PI)/(4.*DK1*DK2)
      DP11=DP11*DCNT*DT/3.
      P11=P11+DP11
C
      RETURN
      END
      SUBROUTINE HANK(X,H,H1,IO)
      COMPLEX H,H1
      DATA TSP/.63661977/
      IF(X.GT.3.)GO TO 100
      XLN=TSP*ALOG(X/2.)
      R=.0
      B1=.0
      Y=.0
      Y1=.0
      X1=X/3.
      X2=X1*X1
      IF(X1.LT..1)GO TO 60
      X4=X2*X2
      X6=X2*X4
      IF(X1.LT..3)GO TO 55
      X8=X2*X6
      X10=X2*X8
      X12=X2*X10
      R=.21E-3*X12-.39444E-2*X10+.444479E-1*X8
      Y=-.24846E-3*X12+.427916E-2*X10-.4261214E-1*X8
      B1=.1109E-4*X12-.31761E-3*X10+.443319E-2*X8
      Y1=.27873E-2*X12-.400976E-1*X10+.3123951*X8
55  B=R-.3163866*X6+1.2656208*X4
      Y=Y+.25300117*X6-.74350384*X4
      B1=B1-.3954289E-1*X6+.21093573*X4
      Y1=Y1-1.3164827*X6+2.1682709*X4
60  R=R-2.2499997*X2+1.
      Y=Y+.60559366*X2+.36746691+XLN*B
      B1=X*(B1-.56249985*X2+.5)
      Y1=(Y1+.2212091*X2-.6366198)/X+XLN*B1
      GO TO 200
100 SW=SQRT(X)

```

```

X1=3./X
X2=X1*X1
X3=X1*X2
X4=X1*X3
X5=X1*X4
X6=X1*X5
F=.79788456-.77E-6*X1-.55274E-2*X2-.9512E-4*X3+.137237E-2*X4
2-.72805E-3*X5+.14476E-3*X6
T=X-.78539816-.4166397E-1*X1-.3954E-4*X2+.262573E-2*X3
2-.54125E-3*X4-.29333E-3*X5+.13558E-3*X6
B=F*COS(T)/SW
Y=F*SIN(T)/SW
F=.79788456+.156E-5*X1+.1659667E-1*X2+.17105E-3*X3-.249511E-2*X4
2+.113653E-2*X5-.20033E-3*X6
T=X-2.3561945+.12499612*X1+.565E-4*X2-.637879E-2*X3+.74348E-3*X4
2+.79824E-3*X5-.29166E-3*X6
B1=F*COS(T)/SW
Y1=F*SIN(T)/SW
200 H=CMPLX(B,-Y)
H1=CMPLX(B1,-Y1)
RETURN
END
COMPLEX FUNCTION VH(X)
DIMENSION A(8),B(8)
COMPLEX G(51),H0,H1
DATA G/
2(.0,.0),(.19933,-.34570),(.39470,-.50952),
2(.58224,-.59927),(.75834,-.63787),(.91973,-.63707),
2(1.06356,-.60490),(.18750,-.54783),(.128982,-.47156),
2(1.36940,-.38136),(.142577,-.28219),(.145913,-.17871),
2(1.47029,-.07527),(.146070,.02420),(.143231,.11618),
2(1.38757,.19766),(.132928,.26620),(.126056,.31997),
2(1.18468,.35775),(.110497,.37897),(.102473,.38367),
2(.94712,.37250),(.87502,.34665),(.81101,.30780),
2(.75721,.25802),(.71531,.19972),(.68647,.13551),
2(.67131,.06814),(.66993,.00036),(.68187,-.06517),
2(.70622,-.12595),(.74160,-.17976),(.78628,-.22471),
2(.83821,-.25931),(.89512,-.28253),(.95464,-.29377),
2(1.01435,-.29295),(.10719,-.28043),(.112509,-.25702),
2(1.17193,-.22393),(.121075,-.18270),(.124021,-.13516),
2(1.25939,-.08335),(.126778,-.02940),(.126529,.02451),
2(1.25227,.07626),(.122947,0.12385),(.119799,.16550),
2(1.15928,.19969),(.1114997,.22523),(.106701,.24129)/
DATA PI/3.14159/
DATA A/.06233,.00404,.00101,.00054,
2.00040,.00028,.00013,.00003/
DATA B/.79788,.01256,.00179,.00067,
2.00041,.00025,.00011,.00002/
IF(X.LE..9) GO TO 200
IF(X.LT.10.) GO TO 100

```

```

VJ=.0
VY=.0
DO 10 I=1,8
K=I-1
SIGN=(-1.)**I*(-1.)
VJ=VJ+A(I)*(8./X)**(2*K+1)*SIGN
VY=VY+B(I)*(8./X)**(2*K)*SIGN
10 CONTINUE
VH=1.-CMPLX(VJ,-VY)*CEXP(CMPLX(.0,PI/4.-X))/SQRT(X)
RETURN
100 CONTINUE
Y=5.*X
J=Y+1.5
IF(J.LT.2) J=2
IF(J.GT.50) J=50
JM=J-1
JP=J+1
FJ=J
YJ=FJ-1.
Q=Y-YJ
QT=Q/2.
C=QT*(Q-1.)
D=QT*(Q+1.)
E=1.-Q**2
VH=C*G(JM)+D*G(JP)+F*G(J)
VH=CONJG(VH)
RETURN
200 CONTINUE
CALL HANK(X,H0,H1,2)
HBO=X-X**3/9.+X**5/(9.*25.)-X**7/(9.*25.*49.)
HB1=X*X/3.-X**4/45.+X**6/(63.*25.)-X**8/(81.*25.*49.)
VH=X*H0+X*(HBO*H1-HB1*H0)
RETURN
END
SUBROUTINE CFF(XA,YA,XB,YB,DK,CPH,SPH,ZS,EJ,EM,EJE)
COMPLEX ZS,FJ,EJA,EJB,F,EM,FJE,E1,E2
COMMON/CDA/CCC,ER2,TSK2L
DATA PI/3.14159/
ETA=120.*PI
CA=(XB-XA)/DK
CB=(YB-YA)/DK
A=XA*CPH+YA*SPH
B=XB*CPH+YB*SPH
EJA=CMPLX(COS(A),SIN(A))
EJB=CMPLX(COS(B),SIN(B))
C=CA*CPH+CB*SPH
S=CB*CPH-CA*SPH
F=CMPLX(.0,DK)*EJA
IF(ABS(C).GT..001) F=(EJB-EJA)/C
EJ=-30.*( .707,-.707)*F
EM=ZS*(.707,-.707)*S*F/(4.*PI)

```


CC

```
SP=1.+S/SQRT(FR2)
SM=1.-S/SQRT(FR2)
E1=CMPLX(0.,TSK2L)
E2=CMPLX(0.,-TSK2L)
IF(SP.GT.0.001) E2=(CEXP(CMPLX(.0,TSK2L*SP))-1.)/SP
IF(SM.GT.0.001) E1=(CEXP(CMPLX(.0,-TSK2L*SM))-1.)/SM
EJE=-FJ*(FR2-1.)/FR2*(E1+E2)*.5
```

CC

```
RETURN
END
SUBROUTINE CELS(X1,Y1,X2,Y2,XS,YS,DK,INT,P1)
COMPLEX HO,H1,P1
DATA PI/3.14159/
CBET=(X2-X1)/DK
SBET=(Y2-Y1)/DK
XA=(XS-X1)*CBET+(YS-Y1)*SBET
YA=-(XS-X1)*SBET+(YS-Y1)*CBET
X=XA
Y=YA
YSQ=Y**2
RMIN=ABS(Y)
IF(X.LT.0.0) RMIN=SQRT(X*X+YSQ)
IF(X.GT.DK) RMIN=SQRT((X-DK)**2+YSQ)
FNT=1+(4*INT)/10
ISS=FNT*DK/RMIN
ISS=2*(ISS/2)
IF(ISS.LT.2) ISS=2
FIT=ISS
ISQ=ISS+1
DS=DK/FIT
SGI=-1.
XP=0.
P1=(0.,0.)
DO 100 I=1,ISQ
C=SGI+3.
IF(I.EQ.1.OR.I.EQ.ISQ) C=1.
DELX=X-XP
RK=SQRT(DELX**2+YSQ)
CALL HANK(RK,HO,H1,0)
P1=P1+HO*C
SGI=-SGI
XP=XP+DS
100 CONTINUE
P1=P1*(-30.*PI)*DS/3.
RETURN
END
SUBROUTINE REC(A,B,IDM,NM,NP,X,Y,IA,IB)
DIMENSION X(IDM),Y(IDM),IA(IDM),IB(IDM)
NX=A*5.+1.5
NY=B*5.+1.5
```

```

IF(NX.LT.4)NX=4
IF(NY.LT.4)NY=4
DX=A/NX
DY=B/NY
NM=2*(NX+NY)
DO 3 J=1,NM
IA(J)=J
IB(J)=J+1
3 IF (J .EQ. NM) IB(J)=1
NP=NM
NYP=NY+1
IT=2*NY+NX+2
AT=.5*A
BT=.5*B
DO 1 I=1,NYP
II=IT-I
X(I)=AT
Y(I)=-BT+(I-1)*DY
X(II)=-X(I)
1 Y(II)=Y(I)
IT=NYP+2*(NX-2)
IS=NY+2
IE=NX+NY
DO 2 I=IS,IE
II=NM-(I-IS)
X(I)=AT-(I-IS+1)*DX
Y(I)=BT
X(II)=X(I)
2 Y(II)=-Y(I)
RETURN
END

```

APPENDIX C
COMPUTER PROGRAMS FOR RADIATION AND SCATTERING
FROM TE DIELECTRIC-COATED CYLINDERS

```

COMPLEX CQT,ZS,ZI1,ZI2,YI1,YI2,HZM,HZS,HZT
COMPLEX C(56,56),CJ(56),HJJ(56),HMM(56),VJ(56),HJJEQ(56)
DIMENSION IA(56),IB(56),I1(56),I2(56),I3(56),JA(56),JB(56)
DIMENSION MD(56,5),ND(56),X(56),Y(56),D(56),XC(56),YC(56),DC(56)
COMMON/COA/TSK,ER2,CONST
DATA IDM,INT/56,10/
DATA PI,TP,ETA/3.14159,6.28318,376.727/
2  FORMAT(1X,8F15.7)
5  FORMAT(1H0)
7  FORMAT(7F10.5)
8  FORMAT(1X,14I5)
   CQT=1.414214*ETA*CMPLX(1.,-1.)
10 READ(5,8)IWR,LOP,NM,NP
   WRITE(6,8)IWR,LOP,NM,NP
   WRITE(6,5)
   DO 50 J=1,NM
   READ(5,8)IA(J),IB(J)
50  WRITE(6,8)J,IA(J),IB(J)
   WRITE(6,5)
   CALL SORT(IA,IB,I1,I2,I3,JA,JB,MD,ND,NM,NP,N,IDM,MAX,MIN)
   IF(MIN.LT.1 .OR. MAX.GT.5)GO TO 300
   DO 55 I=1,N
55  WRITE(6,8)I,I1(I),I2(I),I3(I)
   WRITE(6,5)
   DO 60 I=1,NP
   READ(5,7)XC(I),YC(I)
   FI=I
60  WRITE(6,2)FI,XC(I),YC(I)
   WRITE(6,5)
   DO 70 JAN=1,NM
   KIM=IA(JAN)
   LIM=IB(JAN)
70  DC(JAN)=SQRT((XC(LIM)-XC(KIM))**2+(YC(LIM)-YC(KIM))**2)
   READ(5,7) TSL,ER2
   WRITE(6,2) TSL,ER2
   WRITE(6,5)
   TSK=TP*TSL
   CONST=(ER2-1.)/ER2*(COS(TSK*SQRT(ER2-1.))-1.)
80 READ(5,7)CMM,DPH,FMC,SCALE,TC
   WRITE(6,2)CMM,DPH,FMC,SCALE,TC
   WRITE(6,5)
   WAVM=300./FMC
   TPL=TP

```

```

IF(SCALF.GT.0.)TPL=TP*SCALE/WAVM
DO 90 IAN=1,NP
X(IAN)=TPL*XC(IAN)
90 Y(IAN)=TPL*YC(IAN)
DO 95 JAN=1,NM
95 D(JAN)=TPL*DC(JAN)
I12=1
ISYM=0
ZS=(.0,.0)
TK=TPL*TC
IF(CMM.GT.0.)CALL CSURF(CMM,FMC,TK,ZS)
IF(CMM.GT.0.)ISYM=1
IF(TSL.GT.0.0) ISYM=1
CALL CDANT(C,D,X,Y,ZS,IA,IB,I1,I2,I3,ISYM
B, IDM,INT,JA,JB,MD,N,ND,NM,NP)
IF(ISYM.EQ.10)GO TO 300
GO TO (110,120,130,140),LOP
110 READ(5,8)IGN
CALL VNAS(IDM,IGN,ISYM,IWR,I12,N,C,CJ,Y11)
FGN=IGN
WRITE(6,2)FGN,Y11
GO TO 200
120 READ(5,8)JSA,JSB
CALL VWAS(IA,IB,IDM,ISYM,IWR,I1,I2,I3,I12,JSA,JSB,MD,N,ND,NM
2,C,CJ,D,VJ,Y11)
FSA=JSA
FSB=JSB
WRITE(6,2)FSA,FSB,Y11
GO TO 200
130 READ(5,7)PSI,XCS,YCS
XS=TPL*XCS
YS=TPL*YCS
CALL VMLS(IA,IB,IDM,INT,ISYM,IWR,I1,I2,I3,I12,MD,N,ND,NM,
2C,CJ,D,PSI,VJ,X,Y,XS,YS,Y11,ZS)
WRITE(6,2)PSI,XCS,YCS,Y11
GO TO 200
140 READ(5,7)BSC,PHI
WRITE(6,2)BSC,PHI
200 WRITE(6,5)
IF(LOP.NE.4)G=REAL(Y11)
INC=-1
IF(LOP.EQ.4)INC=1
IPA=?
IF(LOP.EQ.4)IPA=1
IF(LOP.NE.4)BSC=-1.
NPH=360./DPH+1.5
GR=.0
DO 280 IPH=IPA,NPH
FPH=IPH-2
PH=DPH*FPH

```

```

IF(IPH.EQ.1)PH=PHI
CALL VFF(IA,IB,INC,IDM,ISYM,IWR,I1,I2,I3,I12,LOP,MD,N,ND,NM,
2C,CJ,D,EWL,G,GAIN,HJJ,HMM,HZS,HZT,PH,ECS,VJ,X,Y,XS,YS,ZS)
IF(LOP.NE.4)WRITE(6,2)PH,CAIN
IF(LOP.EQ.4)WRITE(6,2)PH,EWL,ECS
INC=-1
IF(BSC.GT.0.)INC=1
280 GR=GR+CABS(HZT)**2
WRITE(6,5)
SCS=.0174533*DPH*GR
IF(LOP.EQ.4)WRITE(6,2)SCS
GR=FTA*SCS
IF(LOP.NE.4)WRITE(6,2)GR
WRITE(6,5)
READ(5,8)JOB,LOP
IF(JOB.EQ.10)GO TO 10
IF(JOB.EQ.80)GO TO 80
IF(JOB.EQ.300)GO TO 300
GO TO(110,120,130,140),LOP
300 CONTINUE
CALL EXIT
END
SUBROUTINE SORT(IA,IB,I1,I2,I3,JA,JB,MD,ND,NM,NP,N,MAX,MIN
2,ICJ,INM)
DIMENSION IA(1),IB(1),ND(1),MD(INM,4),JSP(20)
DIMENSION I1(1),I2(1),I3(1),JA(1),JB(1)
9 FORMAT(3X,'MAX = ',I5,3X,'MIN = ',I5,3X,'N = ',I5)
I=0
DO 24 K=1,NP
NJK=0
DO 20 J=1,NM
IND=(IA(J)-K)*(IB(J)-K)
IF(IND.NE.0)GO TO 20
NJK=NJK+1
JSP(NJK)=J
20 CONTINUE
MOD=NJK-1
IF(MOD.LE.0)GO TO 24
DO 22 IMD=1,MOD
I=I+1
IF(I.GT.ICJ)GO TO 22
IPD=IMD+1
JAI=JSP(IMD)
JA(I)=JAI
JBI=JSP(IPD)
JB(I)=JBI
I1(I)=IA(JAI)
IF(IA(JAI).EQ.K)I1(I)=IB(JAI)
I2(I)=K
I3(I)=IA(JBI)
IF(IA(JBI).EQ.K)I3(I)=IB(JBI)
22 CONTINUE

```

```

24 CONTINUE
   N=I
   DO 30 J=1,NM
     ND(J)=0
     DO 30 K=1,4
30   MD(J,K)=0
     III=N
     IF(N.GT.ICJ)III=ICJ
     DO 40 I=1,III
       J=JA(I)
       DO 38 L=1,2
         ND(J)=ND(J)+1
         K=1
         M=0
32   MJK=MD(J,K)
       IF(MJK.NE.0)GO TO 34
       M=1
       MD(J,K)=I
34   K=K+1
       IF(K.GT.4)GO TO 38
       IF(M.EQ.0)GO TO 32
38   J=JB(I)
40 CONTINUE
     MIN=100
     MAX=0
     DO 46 J=1,NM
       NDJ=ND(J)
       IF(NDJ.GT.MAX)MAX=NDJ
46   IF(NDJ.LT.MIN)MIN=NDJ
       IF(MAX.GT.4 .OR. MIN.LT.1 .OR. N.GT.ICJ)WRITE(6,9)MAX,MIN,N
       RETURN
     END
     SUBROUTINE CDANT(C,D,X,Y,ZS,IA,IB,I1,I2,I3,ISYM
2, IDM,INT,JA,JB,MD,N,ND,NM,NP)
     COMPLEX ZS,P11,P12,P21,P22,Q11,Q12,Q21,Q22,P(2,2),Q(2,2)
     COMPLEX C(IDM,IDM)
     DIMENSION X(1),Y(1),D(1),IA(1),IB(1),JA(1),JB(1)
     DIMENSION I1(1),I2(1),I3(1),MD(IDM,4),ND(1)
2   FORMAT(3X,'DMAX = ',E10.3,3X,'DMIN = ',E10.3)
     DO 20 I=1,N
       DO 20 J=1,N
20  C(I,J)=(.0,.0)
       DMAX=.0
       DMIN=100.
       DO 25 J=1,NM
         K=IA(J)
         L=IB(J)
         D(J)=SQRT((X(L)-X(K))**2+(Y(L)-Y(K))**2)
         IF(D(J).GT.DMAX)DMAX=D(J)
25  IF(D(J).LT.DMIN)DMIN=D(J)
       DRAT=DMIN/DMAX
       IF(DMAX.LT.3. .AND. DRAT.GT..01)GO TO 30
       N=0
       WRITE(6,2)DMAX,DMIN

```

```

RETURN
30 DO 200 K=1,NM
   NDK=ND(K)
   KA=IA(K)
   KB=IB(K)
   DK=D(K)
   DO 200 L=1,NM
   NDL=ND(L)
   LA=IA(L)
   LB=IB(L)
   DL=D(L)
   NIL=0
   DO 200 II=1,NDK
   I=MD(K,II)
   FI=1.
   IF(KB.EQ.I2(I))GO TO 36
   IF(KB.EQ.I1(I))FI=-1.
   IS=1
   GO TO 40
36 IF(KA.EQ.I3(I))FI=-1.
   IS=2
40 DO 200 JJ=1,NDL
   J=MD(L,JJ)
   IF(ISYM.NE.0)GO TO 42
   IF(I.GT.J)GO TO 200
42 FJ=1.
   IF(LB.EQ.I2(J))GO TO 46
   IF(LB.EQ.I1(J))FJ=-1.
   JS=1
   GO TO 50
46 IF(LA.EQ.I3(J))FJ=-1.
   JS=2
50 IF(NIL.NE.0)GO TO 168
   NIL=1
   IF(K.EQ.L)GO TO 120
   IND=(LA-KA)*(LB-KA)*(LA-KB)*(LB-KB)
   IF(IND.EQ.0)GO TO 80
C   SEGMENTS K AND L SHARE NO POINTS
   CALL ZMM3(X(KA),Y(KA),X(KB),Y(KB),X(LA),Y(LA),X(LB),Y(LB),ZS,
2DK,DL,INT,P(1,1),P(1,2),P(2,1),P(2,2))
   GO TO 168
C   SEGMENTS K AND L SHARE ONE POINT (THEY INTERSECT)
80 KG=3
   JM=KB
   JC=KA
   KF=-1
   IND=(KB-LA)*(KB-LB)
   IF(IND.NE.0)GO TO 82
   JC=KB

```

```

KF=1
JM=KA
KG=0
82 LG=3
JP=LA
LF=-1
IF(LB.EQ.JC)GO TO 83
JP=LB
LF=1
LG=0
83 SGN=KF*LF
CALL ZMM2(X(JM),Y(JM),X(JC),Y(JC),X(JP),Y(JP),ZS,DK,DL,
2INT,Q(1,1),Q(1,2),Q(2,1),Q(2,2))
DO 98 KK=1,2
KP=IABS(KK-KG)
DO 98 LL=1,2
LP=IABS(LL-LG)
98 P(KP,LP)=SGN*Q(KK,LL)
GO TO 168
C K=L (SELF REACTION OF SEGMENT K)
120 CALL ZMM1(DK,ZS,P(1,1),P(1,2))
P(2,1)=P(1,2)
P(2,2)=P(1,1)
168 C(I,J)=C(I,J)+FI*FJ*P(IS,JS)
200 CONTINUE
RETURN
END
SUBROUTINE ZMM1(DK,ZS,P11,P12)
COMPLEX ZS,HO,H1,P11,P12
C
COMMON/COA/TSK,ER2,CONST
C
DATA PI/3.14159/
CDK=COS(DK)
SDK=SIN(DK)
CALL HANK(DK,HO,H1,2)
SDKS=SDK**2
CDKS=CDK**2
P11 =-2.*H1*CDK+HO*SDK+2.*(0,1.)*(1.+CDKS)/PI/DK
P12 =-HO*CDK*SDK+H1*(1.+CDKS)-4.*(0,1.)*CDK/PI/DK
P11=15.*DK*P11/SDKS*(1.+CONST)
P12=15.*DK*P12/SDKS*(1.+CONST)
C
TDK=2.*DK
CTDK=COS(TDK)
STDK=SIN(TDK)
CCT=SIN(TSK*SQRT(ER2-1.))/SQRT(ER2-1.)
P11=P11+CCT*(ER2-1.)/ER2*(0,7.5)*(TDK+STDK)/SDKS
P12=P12-(CCT*(ER2-1.)/ER2*(0,7.5))*
2(CDK*(TDK+STDK)+SDK*(1.-CTDK))/SDKS

```


C

```

RS=CABS(ZS)
IF(RS.LE.0.)GO TO 100
CST=16.*PI*SDKS
TDK=2.*DK
CTDK=COS(TDK)
STDK=SIN(TDK)
P11=P11+ZS*(TDK-STDK)/CST
P12 =P12 +ZS*((1.-CTDK)*SDK+(STDK-TDK)*CDK)/CST
100 RETURN
END
SUBROUTINE ZMM2(X1,Y1,X2,Y2,X3,Y3,ZS
2,DK1,DK2,INT,Q11,Q12,Q21,Q22)
COMPLEX HO,H1,HHO,HH1,SHO,SH1,Q11,Q12,Q21,Q22
COMPLEX DHHO,DHH1,DHO,DH1,DSHO,DSH1
COMPLEX S11,S12,S21,S22,T11,T12,T21,T22,Y11,Y12,Y21,Y22
COMPLEX DT11,DT12,DT21,DT22,DY11,DY12,DY21,DY22
COMPLEX ZS,RKH1, SX1, SX2, CCP, FUN, CQT

COMPLEX CX1,CX2,DS11,DS12,DS21,DS22
COMPLEX DP11,DP12,DP21,DP22,P11,P12,P21,P22
COMMON/COA/TSK,ER2,CONST

DATA CCP,PI/(.0,.63662),3.14159/
SDK1=SIN(DK1)
SDK2=SIN(DK2)
CDK1=COS(DK1)
CDK2=COS(DK2)
CBET=(X2-X1)/DK1
SBET=(Y2-Y1)/DK1
XB=(X3-X1)*CBET+(Y3-Y1)*SBET
YB=-(X3-X1)*SBET+(Y3-Y1)*CBET
CAL=(XB-DK1)/DK2
SAL=ABS(YB/DK2)
CALL HANK(DK2,HHO,HH1,2)
DHHO=DK2*HHO
DHH1=DK2*HH1
C1S2=CDK1*SDK2
C1C2=CDK1*CDK2
IF(CAL.LT.0.)GO TO 20
IF(SAL.GT..04)GO TO 20
CNT=-15.*CAL/SDK1/SDK2
CALL HANK(DK1,HO,H1,2)
DHO=DK1*HO
DH1=DK1*H1
DKS=DK1+DK2
CALL HANK(DKS,SHO,SH1,2)
DSHO=DKS*SHO
DSH1=DKS*SH1
Q11=CN*(CDK1*DSH1-C1S2*DHO-C1C2*DH1-DHH1+CCP*CDK2)
Q12=CN*(CDK2*DHH1-SDK2*DHHO-CCP+CDK1*DH1+C1S2*DSHO-C1C2*DSH1)
Q21=CN*(SDK2*DHO-DSH1+CDK2*DH1+CDK1*DHH1-CCP*C1C2)
Q22=CN*(C1S2*DHHO-C1C2*DHH1+CCP*CDK1-DH1-SDK2*DSHO+CDK2*DSH1)

```

```

Q11=Q11*(1.+CONST)
Q12=Q12*(1.+CONST)
Q21=Q21*(1.+CONST)
Q22=Q22*(1.+CONST)
RETURN
20 S11=-DHH1+CCP*CDK2
S12=-SDK2*DHH0+CDK2*DHH1-CCP
S21=(DHH1-CCP*CDK2)*CDK1
S22=(SDK2*DHH0-CDK2*DHH1+CCP)*CDK1
C
DS11=DHH0+CCP*SDK2
DS12=-CDK2*DHH0-SDK2*DHH1
DS21=CDK1*(-DS11)
DS22=CDK1*(-DS12)
C
DKS1=DK1**2
AL=ATAN2(SAL,CAL)
RMIN=DK1
IF(CAL.GE.0.)GO TO 30
RMIN=DK1*SAL
DCR=-DK1*CAL
IF(DK2.LT.DCR)RMIN=SQRT(DKS1+2.*DK1*DK2*CAL+DK2*DK2)
30 FNT=1+(4*INT)/10
INP=FNT*DK2/RMIN
INP=2*(INP/2)
IF(INP.LT.2)INP=2
IP=INP+1
DT=DK2/INP
TK=.0
SX1=(.0,.0)
SX2=(.0,.0)
C
CX1=(.0,.0)
CX2=(.0,.0)
C
SGI=-1.
DO 90 I=1,IP
D=SGI+3.
IF(I.EQ.1 .OR. I.EQ.IP)D=1.
TKS=TK*TK
RK=SQRT(DKS1+2.*DK1*TK*CAL+TKS)
CALL HANK(RK,H0,H1,0)
S1=SIN(DK2-TK)
S2=SIN(TK)
SX1=SX1+S1*H0*D
SX2=SX2+S2*H0*D
C
C1=-COS(DK2-TK)
C2=COS(TK)
CX1=CX1+C1*H0*D
CX2=CX2+C2*H0*D

```

C

```
90 SGI=-SGI
TK=TK+DT
SX1=SX1*DT/3.
SX2=SX2*DT/3.
S21=S21-SX1
S22=S22-SX2
S12=S12+CDK1*SX2
S11=S11+CDK1*SX1
```

C

```
CX1=CX1*DT/3.
CX2=CX2*DT/3.
DS11=DS11+CDK1*CX1
DS12=DS12+CDK1*CX2
DS21=DS21-CX1
DS22=DS22-CX2
```

C

```
INP=2*(INT/2)
IP=INP+1
JP=IP
T11=(.0,.0)
T12=(.0,.0)
T21=(.0,.0)
T22=(.0,.0)
COT=(.0,.0)
RS=CABS(ZS)
Y11=(.0,.0)
Y12=(.0,.0)
Y21=(.0,.0)
Y22=(.0,.0)
```

C

```
P11=(.0,.0)
P12=(.0,.0)
P21=(.0,.0)
P22=(.0,.0)
```

C

```
B=.0
IF(AL.LT..05)GO TO 210
ALT=AL/2.
CALT=COS(ALT)
SALT=SIN(ALT)
RCP=(DK1+DK2)*CALT
RSP=(DK2-DK1)*SALT
PHC=ATAN2(RSP,RCP)
SGI=-1.
PH=-ALT
DPH=AL/INP
DO 200 I=1,IP
D=SGI+3.
IF(I.FQ.1 .OR. I.EQ.IP)D=1.
SAP=SIN(ALT+PH)
SAM=SIN(ALT-PH)
```

```
IF(PH.LE.PHC)RMAX=DK1*SAL/SAM
IF(PH.GT.PHC)RMAX=DK2*SAL/SAP
DRK=RMAX/INP
RK=.0
SGJ=-1.
DT11=(.0,.0)
DT12=(.0,.0)
DT21=(.0,.0)
DT22=(.0,.0)
DY11=(.0,.0)
DY12=(.0,.0)
DY21=(.0,.0)
DY22=(.0,.0)
```

C

```
DP11=(.0,.0)
DP12=(.0,.0)
DP21=(.0,.0)
DP22=(.0,.0)
```

C

```
RKH1=CCP
DO 100 J=1,JP
C=SGJ+3.
IF(J.EQ.1 .OR. J.EQ.JP)C=1.
IF(J.EQ.1)GO TO 94
CALL HANK(RK,H0,H1,1)
RKH1=RK*H1
```

94

```
CONTINUE
SK=RK*SAM/SAL
TK=RK*SAP/SAL
C1=COS(SK)
C2=COS(DK1-SK)
S1=SIN(DK2-TK)
S2=SIN(TK)
FUN=C*RKH1
DY11=DY11-FUN*C1*S1
DY12=DY12-FUN*C1*S2
DY21=DY21+FUN*C2*S1
DY22=DY22+FUN*C2*S2
```

C

```
S1P=-COS(DK2-TK)
S2P=COS(TK)
DP11=DP11-FUN*S1P*C1
DP12=DP12-FUN*S2P*C1
DP21=DP21+FUN*S1P*C2
DP22=DP22+FUN*S2P*C2
```

C

```
SGJ=-SGJ
RK=RK+DRK
IF(RS.LE.0.)GO TO 100
SS1=SIN(SK)
SS2=SIN(DK1-SK)
```

```

DT11=DT11+FUN*SS1*S1
DT12=DT12+FUN*SS1*S2
DT21=DT21+FUN*SS2*S1
DT22=DT22+FUN*SS2*S2
100 CONTINUE
B=SAP*DRK*D
Y11=Y11+B*DY11
Y12=Y12+B*DY12
Y21=Y21+B*DY21
Y22=Y22+B*DY22
C
P11=P11+B*DP11
P12=P12+B*DP12
P21=P21+B*DP21
P22=P22+B*DP22
C
PH=PH+DPH
SGI=-SGI
IF(RS.LE.0.)GO TO 200
T11=T11+B*DT11
T12=T12+B*DT12
T21=T21+B*DT21
T22=T22+B*DT22
200 CONTINUE
B=DPH/9.
IF(RS.GT.0.)CQT=(.0,1.)*ZS*DPH/(72.*PI*SDK1*SDK2*SAL)
210 CNT=-15./SDK1/SDK2
Q11=CNT*(CAL*(1.+CONST)*S11+B*Y11)+CQT*T11
Q12=CNT*(CAL*(1.+CONST)*S12+B*Y12)+CQT*T12
Q21=CNT*(CAL*(1.+CONST)*S21+B*Y21)+CQT*T21
Q22=CNT*(CAL*(1.+CONST)*S22+B*Y22)+CQT*T22
C
CCT=SIN(TSK*SQRT(ER2-1.))/SQRT(ER2-1.)
Q11=Q11-CNT*CCT*(ER2-1.)/ER2*(DS11*SAL-B*P11*CAL/SAL)
Q12=Q12-CNT*CCT*(ER2-1.)/ER2*(DS12*SAL-B*P12*CAL/SAL)
Q21=Q21-CNT*CCT*(ER2-1.)/ER2*(DS21*SAL-B*P21*CAL/SAL)
Q22=Q22-CNT*CCT*(ER2-1.)/ER2*(DS22*SAL-B*P22*CAL/SAL)
C
RETURN
END
SUBROUTINE ZMM3(X1,Y1,X2,Y2,X3,Y3,X4,Y4,ZS,
2DK1,DK2,INT,P11,P12,P21,P22)
COMPLEX HHA,HHB,ZS,HZ1,HZ2,CQT,ET1,ET2,H0,H1
COMPLEX P11,P12,P21,P22,S11,S12,S21,S22,T11,T12,T21,T22
C
COMPLEX EQ1,EQ2,Q11,Q12,Q21,Q22
COMMON/COA/TSK,ER2,CONST
C
DIMENSION CC1(21),SS1(21),CC2(21),SS2(21)
DATA ETA,PI/376.727,3.14159/
S11=(.0,.0)
S12=(.0,.0)
S21=(.0,.0)

```

```
S22=(.0,.0)
T11=(.0,.0)
T12=(.0,.0)
T21=(.0,.0)
T22=(.0,.0)
```

C

```
Q11=(.0,.0)
Q12=(.0,.0)
Q21=(.0,.0)
Q22=(.0,.0)
```

C

```
CBET=(X2-X1)/DK1
SBET=(Y2-Y1)/DK1
XA=(X3-X1)*CBET+(Y3-Y1)*SBET
XB=(X4-X1)*CBET+(Y4-Y1)*SBET
YA=-X3-X1)*SBET+(Y3-Y1)*CBET
YB=-X4-X1)*SBET+(Y4-Y1)*CBET
CAL=(XB-XA)/DK2
SAL=(YB-YA)/DK2
RMIN=10000.
X=XA
Y=YA
DX=DK2*CAL/4.
DY=DK2*SAL/4.
DO 40 J=1,5
YS=.0
R=ABS(Y)
IF(R.GT.1.E-15)YS=Y*Y
XS=.0
XAB=ABS(X-DK1)
IF(XAB.GT.1.E-15)XS=XAB*XAB
IF(X.LT.0.)R=SQRT(X*X+YS)
IF(X.GT.DK1)R=SQRT(XS+YS)
IF(R.LT.RMIN)RMIN=R
X=X+DX
40 Y=Y+DY
FNT=1+(4*INT)/10
ISS=FNT*DK1/RMIN
ISS=2*(ISS/2)
IF(ISS.LT.2)ISS=2
IF(ISS.GT.20)ISS=20
FSS=ISS
ISQ=ISS+1
DS=DK1/FSS
ITT=FNT*DK2/RMIN
ITT=2*(ITT/2)
IF(ITT.LT.2)ITT=2
IF(ITT.GT.20)ITT=20
FTT=ITT
ITQ=ITT+1
DT=DK2/FTT
XP=.0
```

```

SGN=-1.
RS=CABS(ZS)
JUMP=0
ASAL=ABS(SAL)
IF(RS.LE.0..AND.ASAL.LT..04)JUMP=1
IF(JUMP.EQ.1)GO TO 60
DO 50 I=1,ISQ
C=SGN+3.
IF(I.EQ.1 .OR. I.EQ.ISQ)C=1.
CC1(I)=C*COS(DK1-XP)
SSI(I)=C*SIN(DK1-XP)
CC2(I)=C*COS(XP)
SS2(I)=C*SIN(XP)
SGN=-SGN
50 XP=XP+DS
60 DX=DT*CAL
DY=DT*SAL
X=XA
Y=YA
TK=.0
SGJ=-1.
CDK1=COS(DK1)
DO 200 J=1,ITQ
D=SGJ+3.
IF(J.EQ.1 .OR. J.EQ.ITQ)D=1.
CT1=D*SIN(DK2-TK)
CT2=D*SIN(TK)
C
CTP1=-D*COS(DK2-TK)
C
CTP2=D*COS(TK)

XP=.0
YS=.0
YAB=ABS(Y)
IF(YAB.GT.1.E-15)YS=YAB*YAB
ET1=(.0,.0)
ET2=(.0,.0)
HZ1=(.0,.0)
HZ2=(.0,.0)
RKA=SQRT(X*X+YS)
RKB=SQRT((X-DK1)**2+YS)
SPH=YAB/RKA+YAB/RKB
IF(SPH.LT..04 .OR. JUMP.EQ.1)GO TO 110
DO 100 I=1,ISQ
DELX=ABS(X-XP)
DXS=.0
IF(DELX.GT.1.E-15)DXS=DELX*DELX
RK=SQRT(DXS+YS)
SPH=Y/RK
C1=CC1(I)
S1=SSI(I)
C2=CC2(I)
S2=SS2(I)

```

```

CALL HANK(RK,H0,H1,1)
ET1=ET1-C1*SPH*H1
ET2=ET2+C2*SPH*H1
XP=XP+DS
IF(RS.LE.0.)GO TO 100
HZ1=HZ1+S1*H1*SPH
HZ2=HZ2+S2*H1*SPH
100 CONTINUE
110 CALL HANK(RKA,HHA,H1,0)
CALL HANK(RKB,H0,H1,0)
C
EQ1=ET1*CAL*DS/3.-SAL*(CDK1*HHA-H0)
EQ2=ET2*CAL*DS/3.-SAL*(CDK1*H0-HHA)
Q11=Q11+CTP1*EQ1
Q12=Q12+CTP2*EQ1
Q21=Q21+CTP1*EQ2
Q22=Q22+CTP2*EQ2
C
ET1=ET1*SAL*DS/3.+CAL*(CDK1*HHA-H0)
ET2=ET2*SAL*DS/3.+CAL*(CDK1*H0-HHA)
S11=S11+CT1*ET1
S12=S12+CT2*ET1
S21=S21+CT1*ET2
S22=S22+CT2*ET2
SGJ=-SGJ
TK=TK+DT
X=X+DX
Y=Y+DY
IF(RS.LE.0.)GO TO 200
T11=T11+CT1*HZ1
T12=T12+CT2*HZ1
T21=T21+CT1*HZ2
T22=T22+CT2*HZ2
200 CONTINUE
SDK1=SIN(DK1)
SDK2=SIN(DK2)
CST=-ETA*DT/(24.*PI*SDK1*SDK2)
CQT=(.0,1.)*DS*DT*ZS/(72.*PI*SDK1*SDK2)
P11=CST*(1.+CONST)*S11+CQT*T11
P12=CST*(1.+CONST)*S12+CQT*T12
P21=CST*(1.+CONST)*S21+CQT*T21
P22=CST*(1.+CONST)*S22+CQT*T22
C
CC
CCT=SIN(TSK*SQRT(ER2-1.))/SQRT(ER2-1.)
CCT=CCT*(ER2-1.)/ER2
P11=P11-CCT*Q11*CST
P12=P12-CCT*Q12*CST
P21=P21-CCT*Q21*CST
P22=P22-CCT*Q22*CST
C

```



```

RETURN
END
SUBROUTINE HANK(X,H,H1,IO)
COMPLEX H,H1
DATA TSP/.63661977/
IF(X.GT.3.)GO TO 100
XLN=TSP*ALOG(X/2.)
B=.0
B1=.0
Y=.0
Y1=.0
X1=X/3.
X2=X1*X1
IF(X1.LT..1)GO TO 60
X4=X2*X2
X6=X2*X4
IF(X1.LT..3)GO TO 55
X8=X2*X6
X10=X2*X8
X12=X2*X10
B=.21E-3*X12-.39444E-2*X10+.444479E-1*X8
Y=-.24846E-3*X12+.427916E-2*X10-.4261214E-1*X8
B1=.1109E-4*X12-.31761E-3*X10+.443319E-2*X8
Y1=.27873E-2*X12-.400976E-1*X10+.3123951*X8
55 B=B-.3163866*X6+1.2656208*X4
Y=Y+.25300117*X6-.74350384*X4
B1=B1-.3954289E-1*X6+.21093573*X4
Y1=Y1-1.3164827*X6+2.1682709*X4
60 B=B-2.2499997*X2+1.
Y=Y+.60559366*X2+.36746691+XLN*B
B1=X*(B1-.56249985*X2+.5)
Y1=(Y1+.2212091*X2-.6366198)/X+XLN*B1
GO TO 200
100 SW=SQRT(X)
X1=3./X
X2=X1*X1
X3=X1*X2
X4=X1*X3
X5=X1*X4
X6=X1*X5
F=.79788456-.77E-6*X1-.55274E-2*X2-.9512E-4*X3+.137237E-2*X4
2-.72805E-3*X5+.14476E-3*X6
T=X-.78539816-.4166397E-1*X1-.3954E-4*X2+.262573E-2*X3
2-.54125E-3*X4-.29333E-3*X5+.13558E-3*X6
B=F*COS(T)/SW
Y=F*SIN(T)/SW
F=.79788456+.156E-5*X1+.1659667E-1*X2+.17105E-3*X3-.249511E-2*X4
2+.113653E-2*X5-.20033E-3*X6
T=X-2.3561945+.12499612*X1+.565E-4*X2-.637879E-2*X3+.74348E-3*X4
2+.79824E-3*X5-.29166E-3*X6
B1=F*COS(T)/SW
Y1=F*SIN(T)/SW

```

```

200 H=CMPLX(B,-Y)
    H1=CMPLX(B1,-Y1)
    RETURN
    END
    SUBROUTINE CROUT(C,S,ICC,ISYM,IWR,I12,N)
    COMPLEX C(ICC,ICC),S(1)
    COMPLEX F,P,SS,T
2   FORMAT(1X,1I5,1F10.3,1F15.7,1F10.0)
5   FORMAT(1H0)
    IF(I12.NE.1)GO TO 22
    IF(N.EQ.1)S(1)=S(1)/C(1,1)
    IF(N.EQ.1)GO TO 100
    IF(ISYM.NE.0)GO TO 8
    DO 6 I=1,N
    DO 6 J=1,N
6   C(J,I)=C(I,J)
8   F=C(1,1)
    DO 10 L=2,N
10  C(1,L)=C(1,L)/F
    DO 20 L=2,N
    LLL=L-1
    DO 20 I=L,N
    F=C(I,L)
    DO 11 K=1,LLL
11  F=F-C(I,K)*C(K,L)
    C(I,L)=F
    IF(L.EQ.1)GO TO 20
    P=C(L,L)
    IF(ISYM.EQ.0)GO TO 15
    F=C(L,I)
    DO 12 K=1,LLL
12  F=F-C(L,K)*C(K,I)
    C(L,I)=F/P
    GO TO 20
15  F=C(I,L)
    C(L,I)=F/P
20  CONTINUE
22  DO 30 L=1,N
    P=C(L,L)
    T=S(L)
    IF(L.EQ.1)GO TO 30
    LLL=L-1
    DO 25 K=1,LLL
25  T=T-C(L,K)*S(K)
30  S(L)=T/P
    DO 38 L=2,N
    I=N-L+1
    II=I+1
    T=S(I)
    DO 35 K=II,N
35  T=T-C(I,K)*S(K)

```

```

38  S(I)=T
    IF(IWR.LE.0) GO TO 100
    CNOR=.0
    DO 40 I=1,N
    SA=CABS(S(I))
40  IF(SA.GT.CNOR)CNOR=SA
    IF(CNOR.LE.0.)CNOR=1.
    DO 44 I=1,N
    SS=S(I)
    SA=CABS(SS)
    SNOR=SA/CNOR
    PH=.0
    IF(SA.GT.0.)PH=57.29578*ATAN2(AIMAG(SS),REAL(SS))
44  WRITE(6,2)I,SNOR,SA,PH
    WRITE(6,5)
100 RETURN
    END
    SUBROUTINE VNAS(IDM,IGN,ISYM,IWR,I12,N,C,CJ,Y11)
    COMPLEX C(IDM,IDM),CJ(1),Y11
    DO 20 I=1,N
20  CJ(I)=(.0,.0)
    CJ(IGN)=(1.,0.)
    CALL CROUT(C,CJ,IDM,ISYM,IWR,I12,N)
    I12=2
    Y11=CJ(IGN)
    RETURN
    END
    SUBROUTINE VWAS(IA,IB,IDM,ISYM,IWR,I1,I2,I3,I12,JSA,JSB,MD,N,ND
2,NM,C,CJ,D,VJ,Y11)
    COMPLEX C(IDM,IDM),CJ(1),VJ(1),Y11
    DIMENSION IA(1),IB(1),I1(1),I2(1),I3(1),MD(IDM,4),ND(1),D(1)
    AK=.0
    DO 20 K=JSA,JSB
20  AK=AK+D(K)
    DO 30 I=1,N
30  VJ(I)=(.0,.0)
    IF(JSB.GT.JSA)GO TO 200
    K=JSA
    DK=D(K)
    V=(1.-COS(DK))/(AK*SIN(DK))
    KA=IA(K)
    KB=IB(K)
    NDK=ND(K)
    DO 140 II=1,NDK
    I=MD(K,II)
    FI=1.
    IF(KB.EQ.I2(II))GO TO 136
    IF(KB.EQ.I1(II))FI=-1.
    GO TO 140
136 IF(KA.EQ.I3(II))FI=-1.
140 VJ(I)=VJ(I)+FI*V

```

```

      GO TO 280
200  KA=IA(JSA)
      KB=IB(JSA)
      LA=IA(JSA+1)
      LB=IB(JSA+1)
      IND=(LA-KB)*(LB-KB)
      IF(IND.EQ.0)GO TO 210
      KA=IB(JSA)
      KB=IA(JSA)
210  DO 250 K=JSA,JSB
      DK=D(K)
      V=(1.-COS(DK))/(AK*SIN(DK))
      NDK=ND(K)
      DO 240 II=1,NDK
      I=MD(K,II)
      FI=1.
      IF(KB.EQ.I2(II))GO TO 236
      IF(KB.EQ.I1(II))FI=-1.
      GO TO 240
236  IF(KA.EQ.I3(II))FI=-1.
240  VJ(II)=VJ(II)+FI*V
      IF(K.EQ.JSB)GO TO 250
      LA=IA(K+1)
      LB=IB(K+1)
      KA=KB
      KB=LA
      IF(LA.EQ.KA)KB=LB
250  CONTINUE
280  DO 300 I=1,N
300  CJ(I)=VJ(I)
      CALL CROUT(C,CJ,IDM,ISYM,IWR,I12,N)
      I12=2
      Y11=(.0,.0)
      DO 400 I=1,N
400  Y11=Y11+VJ(I)*CJ(I)
      RETURN
      END
      SUBROUTINE VMLS(IA,IB,IDM,INT,ISYM,IWR,I1,I2,I3,I12,MD,N,ND,NM,
2C,CJ,D,PSI,VJ,X,Y,XS,YS,Y11,ZS)
      COMPLEX C(IDM,IDM),CJ(1),VJ(1),Y11,P1,P2,Q1,Q2,ZS
      DIMENSION IA(1),IB(1),I1(1),I2(1),I3(1)
      DIMENSION MD(IDM,4),ND(1),X(1),Y(1),D(1)
      DATA ETA,TP/376.727,6.28318/
      DO 100 I=1,N
      VJ(I)=(.0,.0)
100  CJ(I)=(.0,.0)
      DO 240 K=1,NM
      KA=IA(K)
      KB=IB(K)
      CALL CMLS(PSI,X(KA),Y(KA),X(KB),Y(KB),XS,YS,D(K),INT,P1,P2,Q1,Q2
      Q1=ZS*Q1
      Q2=ZS*Q2
      NDK=ND(K)

```

```

DO 240 II=1,NDK
I=MD(K,II)
FI=1.
IF(KB.EQ.I2(II)) GO TO 236
IF(KB.EQ.I1(II)) FI=-1.
CJ(II)=CJ(II)+FI*P1
VJ(II)=VJ(II)+FI*(P1+Q1)
GO TO 240
236 IF(KA.EQ.I3(II)) FI=-1.
CJ(II)=CJ(II)+FI*P2
VJ(II)=VJ(II)+FI*(P2+Q2)
240 CONTINUE
CALL CROUT(C,CJ,IDM,ISYM,IWR,I12,N)
I12=2
Y11=CMPLX(TP/(4.*ETA),0.)
DO 300 I=1,N
300 Y11=Y11+CJ(I)*VJ(I)
RETURN
END
SUBROUTINE CMLS(PSI,X1,Y1,X2,Y2,XS,YS,DK,INT,P1,P2,Q1,Q2)
COMPLX CST,H0,H1,P1,P2,Q1,Q2
DATA ETA/376.727/
DKH=DK/25.
D1=SQRT((XS-X1)**2+(YS-Y1)**2)
D2=SQRT((XS-X2)**2+(YS-Y2)**2)
P2=(.0,.0)
P1=CMPLX(.5*PSI/360.,0.)
Q1=(.0,.0)
Q2=(.0,.0)
IF(D1.LT.DKH)GO TO 200
P1=(.0,.0)
P2=CMPLX(.5*PSI/360.,0.)
IF(D2.LT.DKH)GO TO 200
SDK=SIN(DK)
P1=(.0,.0)
P2=(.0,.0)
CBET=(X2-X1)/DK
SBET=(Y2-Y1)/DK
XA=(XS-X1)*CBET+(YS-Y1)*SBET
YA=-(XS-X1)*SBET+(YS-Y1)*CBET
X=XA
Y=YA
YSQ=Y**2
RMIN=ABS(Y)
IF(X.LT.0.)RMIN=SQRT(X*X+YSQ)
IF(X.GT.DK)RMIN=SQRT((X-DK)**2+YSQ)
FNT=1+(4*INT)/10
ISS=FNT*DK/RMIN
IF(ISS.LT.2)ISS=2
DS=DK/ISS
XP=DS/2.

```

```

DO 100 I=1,ISS
DELX=X-XP
RK=SQRT(DELX**2+YSQ)
SPH=Y/RK
S1=SIN(DK-XP)
S2=SIN(XP)
CALL HANK(RK,H0,H1,2)
P1=P1+S1*H1*SPH
P2=P2+S2*H1*SPH
Q1=Q1+S1*H0
Q2=Q2+S2*H0
100 XP=XP+DS
CST=(.0,1.)*DS/(4.*SDK)
P1=CST*P1
P2=CST*P2
CNT=-DS/(4.*ETA*SDK)
Q1=CNT*Q1
Q2=CNT*Q2
200 RETURN
END

```

```

SUBROUTINE VFF(IA,IB,INC,IDM,ISYM,IWR,I1,I2,I3,I12,LOP,MD,N,ND,NM
2C,CJ,D,EWL,C,GAIN,HJJ,HMM,HZS,HZT,PH,ECS,VJ,X,Y,XS,YS,ZS)
COMPLEX CQT,DQT,HJ1,HJ2,HM1,HM2,HZM,HZS,HZT,ZS
COMPLEX CJ(1),HJJ(1),HMM(1),C(IDM,IDM),VJ(1)
COMPLEX HJ1J,HJ2J,HJJEQ(40)
DIMENSION IA(1),IB(1),I1(1),I2(1),I3(1),MD(IDM,4)
DIMENSION ND(1),X(1),Y(1),D(1)
COMPLEX CONPH
COMMON/COB/CONPH
COMMON/COA/TSK,ER2,CONST
DATA ETA,TP/376.727,6.28318/
CQT=1.414214*ETA*CMPLX(1.,-1.)
IF(ISYM.NE.0)DQT=CQT*CONJG(ZS)/ZS
ECS=.0
PHR=.0174533*PH
CPH=COS(PHR)
SPH=SIN(PHR)
DO 232 I=1,N
HJJEQ(I)=(.0,.0)
HJJ(I)=(.0,.0)
232 HMM(I)=(.0,.0)
DO 250 K=1,NM
KA=IA(K)
KB=IB(K)
CALL CFF(X(KA),Y(KA),X(KB),Y(KB),D(K)
2,CPH,SPH,ZS,HJ1,HJ2,HM1,HM2,HJ1J,HJ2J)
NDK=ND(K)
DO 250 II=1,NDK
I=MD(K,II)
F1=1.

```

```

IF(KB.EQ.12(1))GO TO 236
IF(KB.EQ.11(1))FI=-1.
HJJ(1)=HJJ(1)+FI*HJ1
HMM(1)=HMM(1)+FI*HM1
HJJEQ(1)=HJJEQ(1)+FI*HJ1J
GO TO 250
236 IF(KA.EQ.13(1))FI=-1.
HJJ(1)=HJJ(1)+FI*HJ2
HMM(1)=HMM(1)+FI*HM2
HJJEQ(1)=HJJEQ(1)+FI*HJ2J
250 CONTINUE
IF(INC.LE.0)GO TO 270
DO 260 I=1,N
CJ(I)=CQT*HJJ(I)
VJ(I)=CJ(I)
260 IF(ISYM.NE.0)VJ(I)=VJ(I)-DQT*HMM(I)
CALL CRDUT(C,CJ,IDM,ISYM,IWR,I12,N)
I12=2
DO 265 I=1,N
265 ECS=ECS+REAL(VJ(I)*CONJG(CJ(I)))
FCS=ECS/ETA
270 HZS=(.0,.0)
DO 360 I=1,N
360 HZS=HZS+CJ(I)*(HJJ(I)+HMM(I))+CJ(I)*(CONPH*HJJ(I)+HJJEQ(I))
HAB=CABS(HZS)
IF(LOP.FQ.4)FWL=TP*HAB*HAB
HZT=HZS
IF(LOP.NE.3)GO TO 400
PSI=XS*CPH+YS*SPH
HZM=CMPLX(COS(PSI),SIN(PSI))
HZM=-(.1,.1)*HZM/(2.*1.414214*ETA)
HZT=HZS+HZM
400 HAB=CABS(HZT)
IF(LOP.LT.4)GAIN=TP*ETA*HAB*HAB/G
RETURN
END
SUBROUTINE CFF(XA,YA,XB,YB,DK,CPH,SPH,ZS,HJ1,HJ2,HM1,HM2,
2HJ1J,HJ2J)
COMPLEX EJA,EJB,CST,ZS,HJ1,HJ2,HM1,HM2
COMPLEX E1,E2,CSTJ,PHASE,FB1,FB2,HJ1J,HJ2J
COMPLEX CONPH
COMMON/COB/CONPH
COMMON/COA/TSK,ER2,CONST
DATA ETA,PI/376.727,3.14159/
CA=(XB-XA)/DK
CB=(YB-YA)/DK
G=CA*CPH+CB*SPH
P=CB*CPH-CA*SPH
GK=P**2
A=XA*CPH+YA*SPH
B=XB*CPH+YB*SPH

```

```

EJA=CMPLX(COS(A),SIN(A))
EJB=CMPLX(COS(B),SIN(B))
SDK=SIN(DK)
CDK=COS(DK)
IF(GK.LT..001)GO TO 250
CST=CMPLX(1.,1.)/(4.*PI*SDK*1.414214*GK)
HM1=CST*(EJA*CMPLX(CDK,G*SDK)-EJB)
HM2=CST*(EJB*CMPLX(CDK,-G*SDK)-EJA)
GO TO 300
250 CST=CMPLX(-1.,1.)/(8.*PI)*1.414214*SDK
IF(G.LT.0.)GO TO 280
HM1=CST*(DK*EJB-SDK*EJA)
HM2=CST*(SDK*EJB-DK*EJA)
GO TO 300
280 HM1=CST*(SDK*EJA-DK*EJB)
HM2=CST*(DK*EJA-SDK*EJB)
300 HJ1=P*HM1
HJ2=P*HM2
HM1=-ZS*HM1/ETA
HM2=-ZS*HM2/ETA
CC
D=TSK/2./PI
E1=CMPLX(.5*D,.0)
E2=CMPLX(-.5*D,.0)
SP=2.*PI*(SQRT(ER2-1.)+P)
SM=2.*PI*(SQRT(ER2-1.)-P)
SSP=SIN(SP*D)
CSP=COS(SP*D)
SSM=SIN(SM*D)
CSM=COS(SM*D)
IF(SP.GT.0.001)E2=(.0,-.5)*(CMPLX(CSP,-SSP)-1.)/SP
IF(SM.GT.0.001)E1=(.0,-.5)*(CMPLX(CSM,SSM)-1.)/SM
PHASE=E1-E2
CONPH=(.0,1.)*(ER2-1.)/ER2*(-E1-E2)
IF(GK.GT.0.001)GO TO 500
FB1=.5*(DK*EJA+SDK*EJB)*PHASE
FB2=.5*(DK*EJB+SDK*EJA)*PHASE
GO TO 400
500 CONTINUE
FB1=PHASE*(CMPLX(.0,G)*EJB+CMPLX(SDK,-G*CDK)*EJA)
FB2=PHASE*(CMPLX(.0,G)*EJA-CMPLX(SDK,G*CDK)*EJB)
400 CONTINUE
CSTJ=CMPLX(1.,1.)/(4.*PI*SDK*1.414214)
IF(GK.GT..001)
2CSTJ=CMPLX(1.,1.)/(4.*PI*SDK*1.414214*GK)
OO=1.
HJ1J=OO*CSTJ*(ER2-1.)/ER2*G*(-FB1)
HJ2J=OO*CSTJ*(ER2-1.)/ER2*G*(-FB2)

```


CC

```
RETURN
END
SUBROUTINE CSURF(CMM,FMC,TK,ZS)
COMPLEX ETA,R,ZS,ETBT
DATA E,ETA0,TP,U/R.85433E-12,376.727,6.28318,12.5664E-7/
ALPH=SQRT(TP*FMC*U*CMM/2.)*1.E6
SQT=SQRT(TP*FMC*U/(2.*CMM))
ETA=CMPLX(SQT,SQT)
TAT=2.*TK*SQRT(CMM/(2.*E*TP*FMC))
ZS=ETA
IF(TAT.GT.60.)GO TO 100
ETAT=EXP(-TAT)
ETBT=CMPLX(COS(TAT),-SIN(TAT))
R=ETAT*ETBT*(ETA0-ETA)/(ETA0+ETA)
ZS=ETA*(1.+R)/(1.-R)
100 RETURN
END
```

APPENDIX D
COMPUTER PROGRAMS FOR RADIATION AND SCATTERING
FROM PERFECTLY-CONDUCTING PLATES

```

DIMENSION C(31),NN(40),MM(40)
COMPLEX Z(40,40),Z11,Z12,ZSS,ZIJ
COMPLEX VA,VB,VC,VD,VTA,VTB,VPA,VPB,EST
COMPLEX VT(40),VP(40),ET(40),EP(40)
IDM=40
PI=3.141592
TP=2.*PI
RFAD(5,98)ZKL,TK,NS,NMAX,NW
98 FORMAT(2F10.4,3I10)
333 CONTINUE
ZL=ZKL/PI
TK=TK*TP
NZ=NW
CALL SIMWC(NMAX,C)
NP=NS-1
NZS=NZ-1
MODES=NW*NZS
MODET=2*MODES
AL=ZL*2./NZ
HL=AL/NS
DWL=ZL/NZ
DDW=DWL/(NMAX-1)
DO 11 K=1,NW
DO 11 L=1,NZS
Z12=(0.0,0.0)
NI=K+(L-1)*NW
DO 30 II=1,1
Y1=DDW*(II-1)*TP
Y2=Y1
Y3=Y1
DO 30 JJ=1,NMAX
DT=ATAN2(DWL,1.414)/(NMAX-1)
CC=C(JJ)
TH=DT*(JJ-1)
DV=1.414*DWL/(NMAX-1)
V=DV*(JJ-1)+(K-2)*0.707*DWL
YA=V*TP*1.414
IF(K.EQ.1.AND.L.LE.3) YA=TAN(TH)*TP*1.414
YB=YA
YC=YA
Z11=(0.0,0.0)
DO 10 I=1,NP

```

```

ZI=-AL*0.5+HL*I
FI=COS(PI*ZI/AL)
Z1=(-ZL*0.5+(I-1)*HL)*TP
Z2=Z1+HL*TP
Z3=Z2+HL*TP
DO 10 J=1,NP
ZJ=-AL*0.5+HL*J
FJ=COS(ZJ*PI/AL)
ZA=(-ZL*0.5+(J-1)*HL)*TP+(L-1)*ZL*TP/NZ
ZB=ZA+HL*TP
ZC=ZB+HL*TP
ZSS=Z1J(TK,TK,TK,Y1,Y2,Y3,Z1,Z2,Z3,.0,.0,.0,YA,YB,YC,ZA,ZB,ZC)
2*FI*FJ
Z11=Z11+ZSS
10 CONTINUE
CL=K*DWL-1.414*V
IF(V.LT.(K-1)*0.707*DWL) CL=1.414*V-(K-2)*DWL
IF(K.NE.1) Z12=Z12+Z11*CC*DV*CL
IF(K.EQ.1.AND.L.GT.3) Z12=Z12+Z11*CC*DV*CL
IF(K.EQ.1.AND.L.LE.3) Z12=Z12+Z11*CC*DT*(DWL-1.414*TAN(TH))/
2(COS(TH)*COS(TH))
30 CONTINUE
CK=2.
IF(K.EQ.1.AND.L.LE.3) CK=4.
Z(1,N1)=Z12*CK*0.707/3./((DWL*DWL)
11 CONTINUE
DO 40 M=1,NZS
DO 40 N=1,NW
I=N+(M-1)*NW
MM(I)=M-1
NN(I)=N-1
40 CONTINUE
DO 1 I=1,MODES
DO 1 J=1,MODES
N1=IABS(MM(J)-MM(I))
N2=IABS(NN(J)-NN(I))
DO 2 M=1,NZS
DO 2 N=1,NW
NI=N+(M-1)*NW
IF(N1.FQ.M-1.AND.N2.EQ.N-1) GO TO 3
2 CONTINUE
3 CONTINUE
Z(I,J)=Z(1,N1)
1 CONTINUE
DO 33 I=1,MODES
DO 33 J=1,MODES
II=I+MODES
JJ=J+MODES
33 Z(II,JJ)=Z(I,J)
C THIS PART FOR CROSS-COUPLING

```

```

NMAX=3
DDW=DWL/(NMAX-1)
CALL SIMWC(NMAX,C)
DO 22 K=1,NW
DO 22 L=1,NZS
NI=K+(L-1)*NW
DO 22 M=1,NW
DO 22 N=1,NZS
NJ=M+(N-1)*NW+MODES
Z12=(0.0,0.0)
DO 31 II=1,NMAX
CI=C(II)
X1=TK
X2=TK
X3=TK
Y1=DDW*(II-1)*TP+(K-1)*DWL*TP
Y2=Y1
Y3=Y1
DO 31 JJ=1,NMAX
CJ=C(JJ)
XA=0.0
XB=0.0
XC=0.0
ZA=TP*(ZL-DDW*(JJ-1)-(M-1)*DWL)
ZB=ZA
ZC=ZA
Z11=(0.0,0.0)
DO 32 I=1,NP
ZI=-0.5*AL+HL*I
FI=COS(ZI*PI/AL)
Z1=(I-1)*HL*TP+(L-1)*TP*ZL/NZ
Z2=Z1+HL*TP
Z3=Z2+HL*TP
DO 32 J=1,NP
ZJ=-0.5*AL+HL*J
FJ=COS(ZJ*PI/AL)
YA=(J-1)*HL*TP+(N-1)*TP*ZL/NZ
YB=YA+HL*TP
YC=YB+HL*TP
ZSS=ZIJ(X1,X2,X3,Y1,Y2,Y3,Z1,Z2,Z3,XA,XB,XC,YA,YB,YC,ZA,ZB,ZC)
2*FI*FJ
Z11=ZSS+Z11
32 CONTINUE
Z12=Z12+Z11*CI*CJ
31 CONTINUE
Z(NI,NJ)=Z12*DDW*DDW/(DWL*DWL)/(3.**2)
WRITE(6,99) NI,NJ,Z(NI,NJ)
99 FORMAT(2I10,2F10.4)
22 CONTINUE

```

C THIS PART FIND THE VOLTAGES

```
NMAX=15
CALL SIMWC(NMAX,C)
DDW=DWL/(NMAX-1)
THI=90.
PHI=0.0
100 CONTINUE
CTHI=COS(THI*PI/180.)
STHI=SIN(THI*PI/180.)
CPHI=COS(PHI*PI/180.)
SPHI=SIN(PHI*PI/180.)
DO 51 K=1,NW
DO 51 L=1,NZS
NI=K+(L-1)*NW
NJ=NI+MODES
VT(NI)=(0.0,0.0)
VA=(0.0,0.0)
VC=(0.0,0.0)
DO 52 II=1,NMAX
CI=C(II)
X1=0.
X2=0.
Y1=DDW*(II-1)*TP+(K-1)*DWL*TP
Y2=Y1
ZA=TP*(ZL-DDW*(II-1)-(L-1)*DWL)
ZB=ZA
VD=(0.0,0.0)
VB=(0.0,0.0)
DO 53 I=1,NP
ZI=-0.5*AL+HL*I
FI=COS(ZI*PI/AL)
Z1=(I-1)*HL*TP+(L-1)*TP*ZL/NZ
Z2=Z1+HL*TP
YA=(I-1)*HL*TP+(K-1)*TP*ZL/NZ
YB=YA+HL*TP
CALL ZFFD(X1,Y1,Z1,X2,Y2,Z2,HL*TP,CTHI,STHI,CPHI,SPHI,VTA,VPA)
CALL ZFFD(X1,YA,ZA,X2,YB,ZB,HL*TP,CTHI,STHI,CPHI,SPHI,VTB,VPB)
VB=VB+VTA*FI
VD=VD+VTB*FI
53 CONTINUE
VC=VC+VD*DDW*CI
VA=VA+VB*DDW*CI
52 CONTINUE
ET(NI)=VA/3./DWL
ET(NJ)=VC/3./DWL
VT(NI)=ET(NI)/CMPLX(0.0,-60.*PI)
VT(NJ)=ET(NJ)/CMPLX(0.0,-60.*PI)
51 CONTINUE
IF (PHI .EQ. 0.0) CALL CROUT(Z,VT,MODET,IDM,0,1,1)
IF (PHI .EQ. 45.) CALL CROUT(Z,VT,MODET,IDM,0,1,2)
EST=(0.0,0.0)
DO 123 I=1,MODET
EST=EST+ET(I)*VT(I)
```

```

123 CONTINUE
  ESTA=CABS(EST)
  ESTP=ATAN2(AIMAG(EST),REAL(EST))*180./PI
  SIG=4.*PI*ESTA*FSTA
  WRITE(6,124) ZL,SIG,ESTA,ESTP
124 FORMAT(5X,4F10.4)
  PHI=PHI+45.0
  IF (PHI .LE. 45.0) GO TO 100
  ZKL=ZKL+0.4
  END
  COMPLEX FUNCTION ZMN(DL,HL,SL)
  REAL L,LE,LL
  B=6.2831853
  D=DL
  L=HL
  LE=HL
  HC=SL
  BLE=B*LE
  H=ABS(HC)-L
  LL=LE
  HPL=H+LL
  HP2L=H+2.0*LL
  HP3L=H+3.0*LL
  HML=H-LL
  SBL=SIN(BLE)
  CBL=COS(BLE)
  SBH=SIN(B*H)
  CBH=COS(B*H)
  SBHML=SIN(B*HML)
  CBHML=COS(B*HML)
  SBHPL=SIN(B*HPL)
  CBHPL=COS(B*HPL)
  SBHP2L=SIN(B*HP2L)
  CBHP2L=COS(B*HP2L)
  SBHP3L=SIN(B*HP3L)
  CBHP3L=COS(B*HP3L)
  TEMP=SQRT(D*D+H*H)+H
  V1=B*D*D/TEMP
  U1=B*TEMP
  TEMP=SQRT(D*D+HML*HML)+HML
  U0=B*TEMP
  V0=B*D*D/TEMP
  TEMP=SQRT(D*D+HPL*HPL)+HPL
  U3=B*TEMP
  V3=B*D*D/TEMP
  TEMP=SQRT(D*D+HP2L*HP2L)+HP2L
  U2=B*D*D/TEMP
  V2=B*TEMP
  TEMP=SQRT(D*D+HP3L*HP3L)+HP3L
  U4=B*D*D/TEMP
  V4=B*TEMP
  CALL SICI (SIU0,CIU0,U0)
  CALL SICI (SIU1,CIU1,U1)
  CALL SICI (SIV2,CIV2,V2)

```

```

CALL SICI (SIV4,CIV4,V4)
CALL SICI (SIU3,CIU3,U3)
IF (D.LE.0.0) GO TO 80
CALL SICI (SIV1,CIV1,V1)
CALL SICI (SIV0,CIV0,V0)
CALL SICI (SIV3,CIV3,V3)
CALL SICI (SIU2,CIU2,U2)
CALL SICI (SIU4,CIU4,U4)
R=15.0*(CBHML*(CIU0+CIV0-CIU1-CIV1)-SBHML*(-SIU0+SIV0+SIU1-SIV1)+C
2BHPL*(2.*CIV3+2.*CIU3-CIU2-CIV2-CIU1-CIV1)+SBHPL*(-SIV3+SIU3+SIU2-
3SIV2-SIU1+SIV1+SIU3-SIV3)+CBHP3L*(-CIU2-CIV2+CIU4+CIV4)+SBHP3L*(SI
4U2-SIV2-SIU4+SIV4)+2.*CBL*CBH*(-CIV1-CIU1+CIV3+CIU3)+2.*CBL*SBH*(
5SIV1-SIU1-SIV3+SIU3)+2.*CBL*CBHP2L*(CIV3+CIU3-CIU2-CIV2)+2.*CBL*SB
6HP2L*(-SIV3+SIU3+SIU2-SIV2))
X=15.0*(CBHML*(-SIU0-SIV0+SIU1+SIV1)-SBHML*(-CIU0+CIV0+CIU1-CIV1)+
2CBHPL*(-2.*SIV3-2.*SIU3+SIU2+SIV2+SIU1+SIV1)+SBHPL*(-2.*CIV3+2.*C
3IU3+CIU2-CIV2-CIU1+CIV1)+CBHP3L*(SIU2+SIV2-SIU4-SIV4)+SBHP3L*(CIU2
4-CIV2-CIU4+CIV4)+2.*CBL*CBH*(SIV1+SIU1-SIV3-SIU3)+2.*CBL*SBH*(CIV
5I-CIU1-CIV3+CIU3)+2.*CBL*CBHP2L*(-SIV3-SIU3+SIU2+SIV2)+2.*CBL*SBHP
62L*(-CIV3+CIU3+CIU2-CIV2))
GO TO 90
80 CONTINUE
R=15.0*(CBHML*(CIU0-CIU1+ALOG(H/HML))+SBHML*(SIU0-SIU1)+SBHPL*
2(2.*SIU3-SIV2-SIU1)+CBHPL*(2.*CIU3-CIV2-CIU1+ALOG(HP2L/HPL))+
3ALOG(H/HPL))+CBHP3L*(CIV4-CIV2+ALOG(HP2L/HP3L))+SBHP3L*(SIV4-SIV2
4)+2.*CBL*CBH*(CIU3-CIU1+ALOG(H/HPL))+2.*CBL*SBH*(SIU3-SIU1)+
52.*CBL*CBHP2L*(CIU3-CIV2+ALOG(HP2L/HPL))+2.*CBL*SBHP2L*(SIU3-
6SIV2))
X=15.0*(CBHML*(SIU1-SIU0)+SBHML*(CIU0-CIU1+ALOG(HML/H))+CBHPL*
2(SIV2+SIU1-2.*SIU3)+SBHPL*(2.*CIU3-CIV2-CIU1+ALOG(HPL/HP2L))+
3ALOG(HPL/H))+CBHP3L*(SIV2-SIV4)+SBHP3L*(CIV4-CIV2+ALOG(HP3L/HP2L)
4)+2.*CBL*CBH*(SIU1-SIU3)+2.*CBL*SBH*(CIU3-CIU1+ALOG(HPL/H))+2.*CB
5L*CBHP2L*(SIV2-SIU3)+2.*CBL*SBHP2L*(CIU3-CIV2+ALOG(HPL/HP2L)))
90 ZMN=CMPLX(R,X)/(SBL*SBL)
RETURN
END
SUBROUTINE SICI(SI,CI,X)
Z=ARS(X)
IF(Z-4.0)1,1,4
1 Y=(4.0-Z)*(4.0+Z)
SI=-1.570797E0
IF(Z)3,2,3
2 CI=-1.0E38
RETURN
3 SI=X*(((1.753141E-9*Y+1.568988E-7)*Y+1.374168E-5)*Y+6.929889E-4)
2*Y+1.964882E-2)*Y+4.395509E-1+SI/X)
CI=((15.772156E-1+ALOG(Z))/Z-Z*(((1.386985E-10*Y+1.584996E-8)*Y
2+1.725752E-6)*Y+1.185999E-4)*Y+4.990920E-3)*Y+1.315308E-1))*Z
RETURN

```

```

4 SI=SIN(Z)
  Y=COS(Z)
  Z=4.0/Z
  U=(((((((4.048069E-3*Z-2.279143E-2)*Z+5.515070E-2)*Z-7.261642E-2)
2*Z+4.987716E-2)*Z-3.332519E-3)*Z-2.314617E-2)*Z-1.134958E-5)*Z
3+6.250011E-2)*Z+2.583989E-10
  V=((((((-5.108699E-3*Z+2.819179E-2)*Z-6.537283E-2)*Z
2+7.902034E-2)*Z-4.400416E-2)*Z-7.945556E-3)*Z+2.601293E-2)*Z
3-3.764000E-4)*Z-3.122418E-2)*Z-6.646441E-7)*Z+2.500000E-1
  CI=Z*(SI*V-Y*U)
  SI=-Z*(SI*U+Y*V)
  IF(X)5,6,6
5 SI=-3.141593E0-SI
6 RETURN
  END
  SUBROUTINE CROUT(C,S,N,IDM,ISYM,IWR,I12)
  COMPLEX C(IDM,IDM),S(IDM)
  COMPLEX F,P,SS,T
2  FORMAT(1X,1I5,1F10.3,1F15.7,1F10.0)
5  FORMAT(1H0)
  IF(I12.NE.1)GO TO 22
  IF(N.EQ.1)S(1)=S(1)/C(1,1)
  IF(N.EQ.1)GO TO 100
  IF(ISYM.NE.0)GO TO 8
  DO 6 I=1,N
  DO 6 J=1,N
  C(J,1)=C(I,J)
6  CONTINUE
8  CONTINUE
  F=C(1,1)
  DO 10 L=2,N
10 C(I,L)=C(I,L)/F
  DO 20 L=2,N
  LLL=L-1
  DO 20 I=L,N
  F=C(I,L)
  DO 11 K=1,LLL
11 F=F-C(I,K)*C(K,L)
  C(I,L)=F
  IF(L.EQ.1)GO TO 20
  P=C(L,L)
  IF(ISYM.EQ.0)GO TO 15
  F=C(L,1)
  DO 12 K=1,LLL
12 F=F-C(L,K)*C(K,1)
  C(L,1)=F/P
  GO TO 20
15 F=C(I,L)
  C(L,1)=F/P
20 CONTINUE
22 CONTINUE

```



```

DO 30 L=1,N
P=C(L,L)
T=S(L)
IF(L.EQ.1)GO TO 30
LLL=L-1
DO 25 K=1,LLL
25 T=T-C(L,K)*S(K)
30 S(L)=T/P
DO 38 L=2,N
I=N-L+1
II=I+1
T=S(I)
DO 35 K=II,N
35 T=T-C(I,K)*S(K)
38 S(I)=T
IF(IWR.LE.0) GO TO 100
CNDR=.0
DO 40 I=1,N
SA=CABS(S(I))
IF(SA.GT.CNDR)CNDR=SA
40 CONTINUE
IF(CNDR.LE.0.)CNDR=1.
DO 44 I=1,N
SS=S(I)
SA=CABS(SS)
SNDR=SA/CNDR
PH=.0
IF(SA.GT.0.)PH=57.29578*ATAN2(AIMAG(SS),REAL(SS))
WRITE(6,2)I,SNDR,SA,PH
44 CONTINUE
WRITE(6,5)
100 CONTINUE
RETURN
END
COMPLEX FUNCTION ZIJ(X1,X2,X3,Y1,Y2,Y3,Z1,Z2,Z3,XA,XB,XC,YA,YB,YC,
2ZA,ZB,ZC)
COMPLEX P11,P12,P21,P22
COMPLEX Q11,Q12,Q21,Q22
COMPLEX S11,S12,S21,S22
COMPLEX R11,R12,R21,R22
AK=0.005*2.0*3.141592
INT=0
D12=SQRT((X1-X2)*(X1-X2)+(Y1-Y2)*(Y1-Y2)+(Z1-Z2)*(Z1-Z2))
D23=SQRT((X2-X3)*(X2-X3)+(Y2-Y3)*(Y2-Y3)+(Z2-Z3)*(Z2-Z3))
DAB=SQRT((XA-XB)*(XA-XB)+(YA-YB)*(YA-YB)+(ZA-ZB)*(ZA-ZB))
DCB=SQRT((XC-XB)*(XC-XB)+(YC-YB)*(YC-YB)+(ZC-ZB)*(ZC-ZB))
CD12=COS(D12)
SD12=SIN(D12)
CD23=COS(D23)
SD23=SIN(D23)
CDAB=COS(DAB)
SDAB=SIN(DAB)

```

```

CDCB=COS(DCB)
SDCB=SIN(DCB)
CALL ZGS(X1,Y1,Z1,X2,Y2,Z2,XA,YA,ZA,XB,YB,ZB,AK,D12,CD12,SD12,
2DAB,SDAB,INT,P11,P12,P21,P22)
CALL ZGS(X1,Y1,Z1,X2,Y2,Z2,XB,YB,ZB,XC,YC,ZC,AK,D12,CD12,SD12,
2DCB,SDCB,INT,Q11,Q12,Q21,Q22)
CALL ZGS(X2,Y2,Z2,X3,Y3,Z3,XA,YA,ZA,XB,YB,ZB,AK,D23,CD23,SD23,
2DAB,SDAB,INT,R11,R12,R21,R22)
CALL ZGS(X2,Y2,Z2,X3,Y3,Z3,XB,YB,ZB,XC,YC,ZC,AK,D23,CD23,SD23,
2DCB,SDCB,INT,S11,S12,S21,S22)
ZIJ=P22+Q21+R12+S11
RETURN
END
SUBROUTINE SIMWC(NMAX,C)
DIMENSION C(31)
DO 1 N=1,NMAX
XNN=FLOAT(N)
NN=N/2
TT=XNN/2.
DIF=TT-FLOAT(NN)
NC=2
IF(DIF.EQ.0.) NC=4
IF(N.EQ.1.OR.N.EQ.NMAX) NC=1
C(N)=NC
1 CONTINUE
RETURN
END
SUBROUTINE ZFFD(XA,YA,ZA,XB,YB,ZB,D,CTH,STH,CPH,SPH,ET,EP)
COMPLEX ET,EP,ES,EJA,EJB
XAB=XB-XA
YAB=YB-YA
ZAB=ZB-ZA
CA=XAB/D
CB=YAB/D
CG=ZAB/D
G=(CA*CPH+CB*SPH)*STH+CG*CTH
GK=1.-G*G
ET=(0.0,0.0)
EP=(0.0,0.0)
IF(GK.LT.0.001) GO TO 200
B=XB*STH*CPH+YB*STH*SPH+ZB*CTH
EJB=CMPLX(COS(B),SIN(B))
SKD=SIN(D)
CKD=COS(D)
CGD=COS(G*D)
ES=60.0*(.0,1.)*EJB*(CKD-CGD)/SKD/GK
T=(CA*CPH+CB*SPH)*CTH-CG*STH
P=-CA*SPH+CB*CPH
ET=ES*T
EP=ES*P
200 CONTINUE
RETURN
END

```

```

SUBROUTINE ZGS(XA,YA,ZA,XB,YB,ZB,X1,Y1,Z1,X2,Y2,Z2,AK,
2DS,CDS,SDS,DT,SDT,INT,P11,P12,P21,P22)
COMPLEX CST,EJ1,EJ2,EJA,EJB,ER1,ER2,ET1,ET2,P11,P12,P21,P22,GAM
COMPLEX SGDS,SGDT
DATA ETA,GAM,PI/376.727,(.0,1.),3.14159/
CA=(X2-X1)/DT
CB=(Y2-Y1)/DT
CG=(Z2-Z1)/DT
CAS=(XB-XA)/DS
CBS=(YB-YA)/DS
CGS=(ZB-ZA)/DS
CC=CA*CAS+CB*CBS+CG*CGS
IF(ABS(CC).GT.0.997)GO TO 200
SZ=(X1-XA)*CAS+(Y1-YA)*CBS+(Z1-ZA)*CGS
IF(INT.EQ.0)GO TO 300
CGDS=CDS
SGDS=CMPLX(.0,SDS)
SGDT=CMPLX(.0,SDT)
INS=2*(INT/2)
IF(INS.LT.2)INS=2
IP=INS+1
DELT=DT/INS
T=.0
DSZ=CC*DELT
P11=(.0,.0)
P12=(.0,.0)
P21=(.0,.0)
P22=(.0,.0)
AKS=AK*AK
SGN=-1.
DO 100 IN=1,IP
ZZ1=SZ
ZZ2=SZ-DS
XXZ=X1+T*CA-XA-SZ*CAS
YYZ=Y1+T*CB-YA-SZ*CBS
ZZZ=Z1+T*CG-ZA-SZ*CGS
PS=XXZ**2+YYZ**2+ZZZ**2
R1=SQRT(RS+ZZ1**2)
EJA=CMPLX(COS(R1),-SIN(R1))
EJ1=EJA/R1
R2=SQRT(RS+ZZ2**2)
EJB=CMPLX(COS(R2),-SIN(R2))
EJ2=EJB/R2
ER1=EJA*SGDS+ZZ1*EJ1*CGDS-ZZ2*EJ2
ER2=-EJB*SGDS+ZZ2*EJ2*CGDS-ZZ1*EJ1
FAC=.0
IF(RS.GT.AKS)FAC=(CA*XXZ+CB*YYZ+CG*ZZZ)/RS
ET1=CC*(EJ2-EJ1*CGDS)+FAC*ER1
ET2=CC*(EJ1-EJ2*CGDS)+FAC*ER2
C=3.+SGN
IF(IN.EQ.1 .OR. IN.EQ.IP)C=1.

```

```

C1=C*SIN(DT-T)
C2=C*SIN(T)
P11=P11+ET1*C1
P12=P12+ET1*C2
P21=P21+ET2*C1
P22=P22+ET2*C2
T=T+DELT
SZ=SZ+DSZ
100 SGN=-SGN
CST=-(.0,1.)*ETA*DELT/(12.*PI*SGDS*SGDT)
P11=CST*P11
P12=CST*P12
P21=CST*P21
P22=CST*P22
RETURN
200 SZ1=(X1-XA)*CAS+(Y1-YA)*CBS+(Z1-ZA)*CGS
RH1=SQRT((X1-XA-SZ1*CAS)**2+(Y1-YA-SZ1*CBS)**2+(Z1-ZA-SZ1*CGS)**2)
SZ2=SZ1+DT*CC
RH2=SQRT((X2-XA-SZ2*CAS)**2+(Y2-YA-SZ2*CBS)**2+(Z2-ZA-SZ2*CGS)**2)
DDK=(RH1+RH2)/2.
IF(DDK.LT.AK)DDK=AK
CALL ZGMM(.0,DS,SZ1,SZ2,DDK,CDS,SDS,SDT,1.,P11,P12,P21,P22)
RETURN
300 SS=SQRT(1.-CC*CC)
CAD=(CGS*CB-CBS*CG)/SS
CBD=(CAS*CG-CGS*CA)/SS
CGD=(CBS*CA-CAS*CB)/SS
DK=(X1-XA)*CAD+(Y1-YA)*CBD+(Z1-ZA)*CGD
DK=ABS(DK)
IF(DK.LT.AK)DK=AK
XZ=XA+SZ*CAS
YZ=YA+SZ*CBS
ZZ=ZA+SZ*CGS
XP1=X1-DK*CAD
YP1=Y1-DK*CBD
ZP1=Z1-DK*CGD
CAP=CBS*CCD-CGS*CBD
CBP=CGS*CAD-CAS*CGD
CGP=CAS*CBD-CBS*CAD
P1=CAP*(XP1-XZ)+CBP*(YP1-YZ)+CGP*(ZP1-ZZ)
T1=P1/SS
S1=T1*CC-SZ
CALL ZGMM(S1,S1+DS,T1,T1+DT,DK,CDS,SDS,SDT,CC,P11,P12,P21,P22)
RETURN
END
SUBROUTINE EXPJ(V1,V2,W12)
COMPLEX EC,E15,S,T,UC,VC,V1,V2,W12,Z
DIMENSION V(21),W(21),D(16),E(16)
DATA V/ 0.22284667E 00,
20.11889321E 01,0.29927363E 01,0.57751436E 01,0.98374674E 01,
20.15982874E 02,0.93307812E-01,0.49269174E 00,0.12155954E 01,
20.22699495E 01,0.36676227E 01,0.54253366E 01,0.75659162E 01,
20.10120228E 02,0.13130282E 02,0.16654408E 02,0.20776479E 02,
20.25623894E 02,0.31407519E 02,0.38530683E 02,0.48026086E 02/

```

```

DATA W/ 0.45896460E 00,
20.41700083E 00,0.11337338E 00,0.10399197E-01,0.26101720E-03,
20.89854791E-06,0.21823487E 00,0.34221017E 00,0.26302758E 00,
20.12642582E 00,0.40206865E-01,0.85638778E-02,0.12124361E-02,
20.11167440E-03,0.64599267E-05,0.22263169E-06,0.42274304E-08,
20.39218973E-10,0.14565152E-12,0.14830270E-15,0.16005949E-19/
DATA D/ 0.22495842E 02,
2 0.74411568E 02,-0.41431576E 03,-0.78754339E 02, 0.11254744E 02,
2 0.16021761E 03,-0.23862195E 03,-0.50094687E 03,-0.68487854E 02,
2 0.12254778E 02,-0.10161976E 02,-0.47219591E 01, 0.79729681E 01,
2-0.21069574E 02, 0.22046490E 01, 0.89728244E 01/
DATA E/ 0.21102107E 02,
2-0.37959787E 03,-0.97489220E 02, 0.12900672E 03, 0.17949226E 02,
2-0.12910931E 03,-0.55705574E 03, 0.13524801E 02, 0.14696721E 03,
2 0.17949528E 02,-0.32981014E 00, 0.31028836E 02, 0.81657657E 01,
2 0.22236961E 02, 0.39124892E 02, 0.81636799E 01/

```

```
Z=VI
```

```
DO 100 JIM=1,2
```

```
X=REAL(Z)
```

```
Y=AIMAG(Z)
```

```
E15=(.0,.0)
```

```
AB=CABS(Z)
```

```
IF(AB.EQ.0.)GO TO 90
```

```
IF(X.GE.0. .AND. AB.GT.10.)GO TO 80
```

```
YA=ABS(Y)
```

```
IF(X.LE.0. .AND. YA.GT.10.)GO TO 80
```

```
IF(YA-X.GE.17.5.OR.YA.GE.6.5.OR.X+YA.GE.5.5.OR.X.GE.3.)GO TO 20
```

```
IF(X.LE.-9.)GO TO 40
```

```
IF(YA-X.GE.2.5)GO TO 50
```

```
IF(X+YA.GE.1.5)GO TO 30
```

```
10 N=6.+3.*AB
```

```
F15=1./(N-1.)-Z/N**2
```

```
15 N=N-1
```

```
E15=1./(N-1.)-Z*E15/N
```

```
IF(N.GE.3)GO TO 15
```

```
E15=Z*E15-CMPLX(.577216+ALOG(AB),ATAN2(Y,X))
```

```
GO TO 90
```

```
20 J1=1
```

```
J2=6
```

```
GO TO 31
```

```
30 J1=7
```

```
J2=21
```

```
31 S=(.0,.0)
```

```
YS=Y*Y
```

```
DO 32 I=J1,J2
```

```
X1=V(I)+X
```

```
CF=W(I)/(X1*X1+YS)
```

```
32 S=S+CMPLX(X1*CF,-YA*CF)
```

```
GO TO 54
```

```
40 T3=X*X-Y*Y
```

```
T4=2.*X*YA
```

```
T5=X*T3-YA*T4
```

```
T6=X*T4+YA*T3
```

```

UC=CMPLX(D(11)+D(12)*X+D(13)*T3+T5-E(12)*YA-E(13)*T4,
2      F(11)+F(12)*X+F(13)*T3+T6+D(12)*YA+D(13)*T4)
VC=CMPLX(D(14)+D(15)*X+D(16)*T3+T5-E(15)*YA-F(16)*T4,
2      F(14)+F(15)*X+F(16)*T3+T6+D(15)*YA+D(16)*T4)
GO TO 52
50  T3=X*X-Y*Y
    T4=2.*X*YA
    T5=X*T3-YA*T4
    T6=X*T4+YA*T3
    T7=X*T5-YA*T6
    T8=X*T6+YA*T5
    T9=X*T7-YA*T8
    T10=X*T8+YA*T7
    UC=CMPLX(D(1)+D(2)*X+D(3)*T3+D(4)*T5+D(5)*T7+T9-(E(2)*YA+E(3)*T4
2+F(4)*T6+E(5)*T8),E(1)+E(2)*X+E(3)*T3+E(4)*T5+E(5)*T7+T10+
3(D(2)*YA+D(3)*T4+D(4)*T6+D(5)*T8))
    VC=CMPLX(D(6)+D(7)*X+D(8)*T3+D(9)*T5+D(10)*T7+T9-(E(7)*YA+E(8)*T4
2+F(9)*T6+E(10)*T8),E(6)+E(7)*X+E(8)*T3+E(9)*T5+E(10)*T7+T10+
3(D(7)*YA+D(8)*T4+D(9)*T6+D(10)*T8))
52  EC=UC/VC
    S=EC/CMPLX(X,YA)
54  EX=EXP(-X)
    T=EX*CMPLX(COS(YA),-SIN(YA))
    E15=S*T
56  IF(Y.LT.0.)E15=CONJG(E15)
    GO TO 90
80  E15=.409319/(Z+.193044)+.421831/(Z+1.02666)+.147126/(Z+2.56788)+
2.206335E-1/(Z+4.90035)+.107401E-2/(Z+8.18215)+.158654E-4/(Z+
312.7342)+.317031E-7/(Z+19.3957)
    E15=E15*CEXP(-Z)
90  IF(JIM.FG.1)W12=E15
100 Z=V2
    Z=V2/V1
    TH=ATAN2(AIMAG(Z),REAL(Z))-ATAN2(AIMAG(V2),REAL(V2))
2+ATAN2(AIMAG(V1),REAL(V1))
    AB=ABS(TH)
    IF(AB.LT.1.)TH=.0
    IF(TH.GT.1.)TH=6.2831853
    IF(TH.LT.-1.)TH=-6.2831853
    W12=W12-E15+CMPLX(.0,TH)
    RETURN
    END
SUBROUTINE ZGMM(S1,S2,T1,T2,D,CGDS,SGD1,SGD2,CPS1,P11,P12,P21,P22)
COMPLEX E(2,2),F(2,2),GAM,P11,P12,P21,P22
COMPLEX EB,EC,EK,EL,EKL,EGZI,ES1,ES2,ET1,ET2,FXPA,EXPB
COMPLEX FGZ(2,2),GM(2),GP(2)
COMPLEX EXA(2),FXB(2)
DATA ETA,GAM,PI/376.727,(.0,1.),3.14159/
DSQ=D*D
SGDS=SGD1
IF(S2.LT.S1)SGDS=-SGD1

```

```

SGDT=SGD2
IF(T2.LT.T1)SGDT=-SGD2
IF(ABS(CPSI).GT.0.997)GO TO 110
ES1=CEXP(GAM*S1)
ES2=CEXP(GAM*S2)
ET1=CEXP(GAM*T1)
ET2=CEXP(GAM*T2)
C=D/SQRT(1.-CPSI*CPSI)
B=C*CPSI
EB=CEXP(GAM*CMPLX(.0,B))
EC=CEXP(GAM*CMPLX(.0,C))
DO 10 K=1,2
DO 10 L=1,2
10 F(K,L)=(.0,.0)
EK=EB
DO 50 K=1,2
FK=(-1)**K
FL=EC
DO 40 L=1,2
FL=(-1)**L
EKL=EK*EL
XX=FK*B+FL*C
SI=S1
DO 30 I=1,2
R1=SQRT(DSQ+SI*SI+T1*T1-2.*SI*T1*CPSI)
R2=SQRT(DSQ+SI*SI+T2*T2-2.*SI*T2*CPSI)
CALL EXPJ(GAM*CMPLX(R1+FK*SI+FL*T1,-XX),
2 GAM*CMPLX(R2+FK*SI+FL*T2,-XX),EXA(I))
CALL EXPJ(GAM*CMPLX(R1+FK*SI+FL*T1,XX),
2 GAM*CMPLX(R2+FK*SI+FL*T2,XX),EXB(I))
IF(K.EQ.2 .OR. L.EQ.2)GO TO 30
ZC=SI*CPSI
EGZI=CEXP(GAM*ZC)
CALL EXPJ(GAM*(R1+ZC-T1),GAM*(R2+ZC-T2),EXPB)
CALL EXPJ(GAM*(R1-ZC+T1),GAM*(R2-ZC+T2),EXPA)
F(I,1)=2.*SGDS*(.0,1.)*EXPA/EGZI
F(I,2)=2.*SGDS*(.0,1.)*EXPB*EGZI
30 SI=S2
E(K,L)=E(K,L)+(EXA(2)-EXA(1))*EKL+(EXB(2)-EXB(1))/EKL
40 EL=1./EC
50 EK=1./EB
CST=-FTA/(16.*PI*SGDS*SGDT)
P11=CST*(( F(1,1)+E(2,2)*ES2-E(1,2)/ES2)*ET2
A +(-F(1,2)-E(2,1)*ES2+E(1,1)/ES2)/ET2)
P12=CST*((-F(1,1)-E(2,2)*ES2+E(1,2)/ES2)*ET1
B +( F(1,2)+E(2,1)*ES2-E(1,1)/ES2)/ET1)
P21=CST*((-F(2,1)-E(2,2)*ES1+E(1,2)/ES1)*ET2
C +( F(2,2)+E(2,1)*ES1-E(1,1)/ES1)/ET2)
P22=CST*(( F(2,1)+E(2,2)*ES1-E(1,2)/ES1)*ET1
D +(-F(2,2)-E(2,1)*ES1+E(1,1)/ES1)/ET1)
RETURN

```

```

110 IF(CPS1.LT.0.)GO TO 120
    TA=T1
    TB=T2
    GO TO 130
120 TA=-T1
    TB=-T2
    SGT=-SGDT
130 SI=S1
    DO 150 I=1,2
        IJ=TA
        DO 140 J=1,2
            ZIJ=TJ-SI
            R=SQRT(DSQ+ZIJ*ZIJ)
            W=R+ZIJ
            IF(ZIJ.LT.0.)W=DSQ/(R-ZIJ)
            V=R-ZIJ
            IF(ZIJ.GT.0.)V=DSQ/(R+ZIJ)
            IF(J.EQ.1)V1=V
            IF(J.EQ.1)W1=W
            EGZ(I,J)=CFXP(GAM*ZIJ)
140 TJ=TB
    CALL FXPJ(GAM*V1,GAM*V,GP(1))
    CALL FXPJ(GAM*W1,GAM*W,GM(I))
150 SI=S2
    CST=ETA/(8.*PI*SGDS*SGDT)
    P11=CST*(GM(2)*EGZ(2,2)+GP(2)/EGZ(2,2)
    2-CGDS*(GM(1)*EGZ(1,2)+GP(1)/EGZ(1,2)))
    P12=CST*(-GM(2)*EGZ(2,1)-GP(2)/EGZ(2,1)
    2+CGDS*(GM(1)*EGZ(1,1)+GP(1)/EGZ(1,1)))
    P21=CST*(GM(1)*EGZ(1,2)+GP(1)/EGZ(1,2)
    2-CGDS*(GM(2)*EGZ(2,2)+GP(2)/EGZ(2,2)))
    P22=CST*(-GM(1)*EGZ(1,1)-GP(1)/EGZ(1,1)
    2+CGDS*(GM(2)*EGZ(2,1)+GP(2)/EGZ(2,1)))
    RETURN
    END

```